COMPARISON OF HIGH ENERGY LASER EXPECTED DWELL TIMES AND PROBABILITY OF KILL FOR MISSION PLANNING SCENARIOS IN ACTUAL AND STANDARD ATMOSPHERES

THESIS

Jarred L. Burley, Captain, USAF
AFIT/APPLPHY/ENP/12-M02

DEPARTMENT OF THE AIR FORCE
AIR UNIVERSITY

AIR FORCE INSTITUTE OF TECHNOLOGY

Wright-Patterson Air Force Base, Ohio

AFIT/APPLPHY/ENP/12-M02

COMPARISON OF HIGH ENERGY LASER EXPECTED DWELL TIMES AND PROBABILITY OF KILL FOR MISSION PLANNING SCENARIOS IN ACTUAL AND STANDARD ATMOSPHERES

THESIS

Presented to the Faculty

Department of Engineering Physics

Graduate School of Engineering and Management

Air Force Institute of Technology

Air University

Air Education and Training Command

in Partial Fulfillment of the Requirements for the

Degree of Master of Science in Applied Physics

Jarred L. Burley, BS

Captain, USAF

March 2012

AFIT/APPLPHY/ENP/12-M02

COMPARISON OF HIGH ENERGY LASER EXPECTED DWELL TIMES AND PROBABILITY OF KILL FOR MISSION PLANNING SCENARIOS IN ACTUAL AND STANDARD ATMOSPHERES

Jarred L. Burley, BS
Captain, USAF

Approved:

Steven T. Fiorino, PhD (Chairman)	Date
Salvatore J. Cusumano, PhD (Member)	Date
Richard J. Bartell (Member)	Date

Abstract

The directed energy modeling and simulation (M&S) community can make important direct contributions to the joint warfighting community by providing the capability to estimate expected performance on high energy laser systems in relevant engagement scenarios accounting for variability in system performance arising from spatial, spectral, and temporal variations in operating conditions. The Air Force Institute of Technology Center for Directed Energy's High Energy Laser Tactical Decision Aid (HELTDA) is a one-on-one engagement level model that functions as a near-term mission planning tool. The HELTDA allows observation of vertical profiles of atmospheric effects for standard, climatological, ground observation-based, and numerical weather model-based atmospheres. These atmospheric profiles are used to enable the wavelength-dependent forward and off-axis scattering characteristics and absorption effects on electromagnetic energy delivered at any wavelength from 0.4 μm to 8.6 m to be evaluated by the operator prior to weapon engagement. The use of correlated probabilistic climatological data for over 573 land sites worldwide and a $1^\circ \times 1^\circ$ grid over all ocean locations allows for probabilistic analysis of effect and confidence level estimation.

In the current study, the 1976 U.S. Standard Atmosphere, a 50th percentile climatological profile, a ground observation based profile, and 48, 24, and 12 hour Global Forecast System (GFS) numerical weather model forecast derived profiles are compared to actual sounding data and characterized for temperature, dew point, relative humidity, wind speed, and wind direction predictive performance. Additionally, predictive HEL engagement performance is analyzed for relevant engagement scenarios for multiple wavelengths in an effort to quantify HELTDA's mission impact. Clear

operational optimization is demonstrated by employing GFS forecast predictions for HEL engagements in nearly all cases. Ground observation based profiles demonstrate increased aggregate predictive capability of meteorological parameters compared with climatology but fail to better predict dwell times for the 1.045 μm wavelength. At the water absorbing 1.31525 μm wavelength, dwell times for ground observation based profiles correlate to increased predictive capability revealing a wavelength dependence attributed to the multivariate nature of HEL energy propagation. Specific cases are analyzed and demonstrate the dwell time optimization and tactical advantages possible with altitude, heading, and flight profile modifications. Overall, the results indicate that in a majority of cases, existing conditions may be exploited for an operational advantage in the employment of directed energy weapons if correctly anticipated and analyzed.

Acknowledgements

I owe a debt of gratitude to my advisor, Dr. Steven Fiorino. Thank you for your instruction and your patience. Your wit and your optimism made this entire experience a memorable one and it truly was a pleasure working with you. I would also like to thank Rick Bartell and Dr. Salvatore Cusumano. Your expertise and guidance was critical to this research.

Thank you to the entire AFIT/CDE staff and faculty for your support and encouragement. I am indebted to Dan Grahn for just about every piece of code used and to Michelle Via for constantly answering my random questions.

Finally, I would like to thank my incredible wife and family for your constant encouragement, your endless support, and for your love. I am truly blessed to come home to you each and every day. I thank God for this opportunity, but know that none of it would have been possible had He not given me you!

Jarred L. Burley

Table of Contents

Page

List of Figures

Figure Page

List of Tables

Table Page

COMPARISON OF HIGH ENERGY LASER EXPECTED DWELL TIMES AND PROBABILITY OF KILL FOR MISSION PLANNING SCENARIOS IN ACTUAL AND STANDARD ATMOSPHERES

I. Introduction

Problem Significance

As laser technology has progressed the Department of Defense (DOD) has invested significantly in the development of high-energy laser (HEL) and high power microwave weapon research. Currently, no fielded HEL weapon systems exist, yet there are many programs working towards both tactical and strategic weapons. There exists a clear distinction between these types of systems as current strategic systems are envisioned to operate at relatively high altitudes at long ranges while a tactical system will most certainly operate in the troposphere at relatively short ranges, and more specifically through the Earth's boundary layer (the lowest 1-2 km of the atmosphere). This is a significant distinction as the atmospheric effects on energy propagation vary significantly at these altitudes.

Currently the Airborne Laser Test Bed (ALTB), a chemical oxygen-iodine laser (COIL) originally designed to defeat ballistic missiles in boost phase, is the prime example of a program intended to operate above the effects of the boundary layer [25]. At present, an atmospheric decision aid (ADA) for understanding the effectiveness already exists for a high altitude environment [16]. Conversely, the Electric Laser on a Large Aircraft (ELLA) program, which seeks to integrate the Defense Advanced Research Projects Agency's (DARPA) High Energy Liquid Laser Area Defense System

(HELLADS) laser onto a B-1 aircraft for demonstration of tactical engagements, remains at the forefront of aircraft-based tactical laser engagement programs. The goal of the HELLADS program is to produce a kilowatt class laser with an order of magnitude reduction in weight compared to existing technology [22]. If successful, the HEL weapon footprint will be significantly reduced and tactical engagements will be a realizable possibility. At present an operationally-oriented mission planning decision aid for HEL tactical engagements does not exist.

In an effort to provide the warfighter planning capabilities for potential directed energy weapons the Air Force Institute of Technology (AFIT) Center for Directed Energy (CDE) has developed a novel high energy laser tactical decision aid (HELTDA) for mission planning and preparation. The HELTDA provides the capability to characterize the lower troposphere in order to maximize the effectiveness of tactical HEL weapon systems such as ELLA. By characterizing the weather and atmosphere via physically-based simulated engagements, the warfighter would be able to input specific weather characteristics such as visibility, wind speed, and wind direction to optimize the effectiveness of using tactical laser weapons in any given environment for mission planning, weapon engagements, and tests in and through the boundary layer [6]. Furthermore, in the absence of specific current atmospheric conditions, a HELTDA would be able to provide an accurate estimate of probable engagement conditions parameters for a given location and time providing the warfighter with a probabilistic method for optimizing tactical HEL engagements.

Past studies have demonstrated the need for a decision aid for low altitude HEL operations [32]. While there exists a myriad of possible atmospheric and weather conditions, seasonal and time-of-day effects are in themselves significant enough to warrant the development and use of a HELTDA. However, no quantitative analysis of a HELTDA's mission impact has been conducted at present. This research effort

develops an impact analysis for HELTDA implementation.

Introduction to High Energy Lasers and Earth's Atmosphere

The first laser was developed in 1960 and since its inception the laser has been referred to as a solution in search of a problem [30]. Today, the laser is a technology that impacts almost all aspects of modern life; from medicine to entertainment. Since the laser's early beginnings, scientists and politicians alike have considered the potential of harnessing the laser's power to field a directed energy weapon. Vast amounts of time, energy, and money have been invested in developing this holy grail of weapons systems.

Some of the potential advantages of these weapons include the ability to initiate engagement of multiple targets nearly instantaneously as lasers propagate at the speed of light. Additionally, these systems would have deep *magazines* which means their ability to fire is limited only by their capacity to recharge and cool themselves. Since laser weapon systems expend only energy, the cost per shot comes singly from the cost of powering the device and the logistical footprint may be minimized compared to many conventional weapons. Furthermore, HEL weapons provide potential for almost surgical precision, greatly minimizing the potential for collateral damage in many engagement scenarios [17].

Conversely, there are clear disadvantages as well. In a vacuum, a laser's electromagnetic energy theoretically travels unattenuated through space from platform to target. However, when traveling through the Earth's atmosphere the energy is attenuated due to several different factors including scattering, absorption, thermal blooming, optical turbulence, etc., [20, 32, 17]. These factors can be categorized as linear and nonlinear processes. Linear processes are those in which the laser beam does not modify the characteristics of the atmosphere; for example, scattering caused

by molecules, aerosols, rain drops, or other particles. Nonlinear processes such as thermal blooming, a defocussing of the beam caused by heating of the beam path due to absorption, are directly caused by the laser beam itself [17]. The combination of these processes serves to reduce the intensity of the laser at the target. The density of the Earth's atmosphere tends to decay exponentially with height; therefore the atmosphere's effect on vertical propagation of a laser is typically more complicated than horizontal propagation for practical considerations [32]. Consequently, it is of critical importance to clearly define the atmospheric regions in which HEL systems are intended to operate, as seen in Figure 1, as system performance can vary greatly with altitude. However, even within these atmospheric regions, particularly the boundary layer,environmental factors can vary significantly and dramatically impact HEL operations.

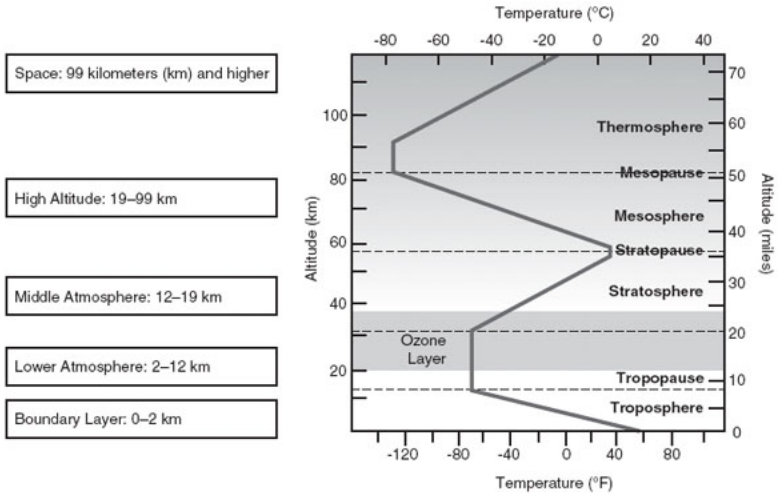

Figure 1. Structure of the atmosphere [17].

All of the United States' military branches invest in directed weapon programs operating in or through the boundary layer of the atmosphere [17]. Two systems of particular interest to the United States Air Force include the tactically oriented ELLA

system (preceded by the Advanced Tactical Laser (ATL)) and its strategic counterpart the ALTB. While many similarities exist in these airborne systems, the atmospheric environments in which they are designed to be employed are significantly different. ELLA is designed for tactical air-to-ground engagements which by necessity must propagate through the densest portions of the boundary layer. The atmospheric path of any directed energy weapon must be accurately characterized to fully understand the weapons potential impact and effectiveness, yet much of the present research focuses on ALTB and applies to the middle and upper atmosphere which is less stressing at the ranges of concern for tactical engagements. A HELTDA designed for low-altitude boundary layer engagements is critical to effectively and efficiently utilize an airborne tactical laser system.

Problem Statement

Currently no mission planning tool exists for tactical laser engagements and therefore there is no way to optimize weapon system performance. The current prototype HELTDA developed by AFIT/CDE is based on the engineering performance code called the High Energy Laser End-to-End Operational Simulation (HELEEOS) which incorporates scaling laws tied to respected wave optics code for laser propagation and may provide a solution [8]. HELEEOS's unique application of probabilistic atmospheric databases and correlated vertical profiles provides a probability of effect (P_e) output that enables the user to evaluate the uncertainty associated with the modeled engagement. The end result is a probability of kill (P_k) estimation as well as the confidence associated with this calculation [9].

The purpose of this research is to cross compare simulated low-altitude high energy laser weapon system performance for a wide range of atmospheric conditions to simulated performance data correlated with standard atmospheric profiles as well

as with collected observations through the use of AFIT/CDE's HELTDA. Laser propagation through the Earth's boundary layer is extremely variable and dependent on multiple atmospheric parameters. The intent is to show that an operational advantage can be obtained by incorporating climatological observations, current observations, and/or forecast data and leveraging the probabilistic nature of HELTDA predictions for probability of kill (P_k) as compared to results obtained using standard atmospheric conditions to predict performance.

Research Goals

The goal of this research is to demonstrate the tactical advantage gained by utilizing the HELTDA in relevant engagement scenarios by analyzing atmospheric characterization methods as they are applied to mission planning. First and foremost, relevant engagement scenarios must be defined. Any scenario used to evaluate system performance must be realistic, operationally relevant, and accepted by the user. There is currently no end user as the systems to be evaluated are in the midst of the research and development process. Therefore, it is imperative that potential users, operators, and interested parties be identified. The combined inputs of these individuals and organizations must be analyzed to construct generalized engagement scenarios which provide useful and relevant data. Analysis of time of day and seasonal variations will produce relative performance comparisons and confidence intervals for various atmospheres, thus enabling the analysis required to show the potential to reduce required dwell time and gain a tactical advantage. Through a complete understanding of the operational environment, engagements can be better prioritized, scheduled, and planned to maximize effect and reduce costs.

Organizational Overview

Chapter 2 follows and is a thorough literature review of the relevant topics necessary for a basic understanding of HEL propagation through the boundary layer with respect to weapons systems. This chapter also contains a more detailed description of the HELTDA and the calculations and analysis contained therein. Chapter 3 details the test methodology of the research effort for HELTDA data collection and analysis. Multiple data sets are identified and described in detail along with the manner in which they are employed. Relevant engagement scenarios development and justification are also presented in Chapter 3. Chapter 4 presents the results and the analysis effort to increase operational performance. Meteorological parameters for multiple atmospheres are analyzed against in-situ measurements and relative performance is accessed. HEL performance data are presented for identified engagement scenarios and mission planning optimization is discussed. Chapter 5 presents final conclusions and recommendations for future work and application.

II. Literature Review

Chapter Overview

The purpose of Chapter 2 is to provide a theoretical foundation on the subject of atmospheric laser propagation and present a comprehensive literature review of past research efforts directly related to the development and use of a HELTDA. Included is an overview and history of the HELTDA software utilized in this study.

Current Directed Energy Systems

The United States' military services each have unique missions and responsibilities which dictate equipment requirements. Consequently, as technology development has progressed in relation to directed energy systems, numerous programs have been initiated to meet each service's specific needs. While many of the fielded and proposed systems are similar, each has its own unique characteristics and specifications to consider.

United States Army.

The U.S. Army's primary battlefield environment is over land and its systems of interest tend to focus on defeating rockets, artillery, mortars, cruise missiles, short range ballistic missiles, unmanned aerial vehicles (UAV), improvised explosive devices, and man-portable air defense missiles. Current and recent systems include the Mobile Tactical High Energy Laser (MTHEL), Skyguard, Zeus, and the High Energy Laser Rocket Artillery Mortar vehicle (HELRAM). MTHEL is a legacy program designed to defeat artillery, rocket, and missile threats. Skyguard, an aircraft defense system designed to protect against man portable air defense systems, has a legacy in MTHEL.

Zeus is a laser ordnance-neutralizing system integrated onto a Humvee and HELRAM is a truck-mounted HEL designed to defeat the RAM threat [17].

United States Navy.

The U.S. Navy's primary battlefield environment includes the world's oceans and waterways as well as littoral areas. Primary concerns include protection by defeating air-sea cruise missiles, cigarette boats, UAVs, rockets, floating mines, helicopters, and fixed wing aircraft [17]. Currently, in the development phase, the Free Electron Laser promises to produce a megawatt class laser weapon by 2018, but politics and budget cuts threaten to shut the program down [31, 5]. If successful, the scalable and tunable weapon would be extremely versatile. The potential for integrating such weaponized HELs into Navy ships is high due to the power sources available on many of the larger vessels. Currently, the Maritime Laser Demonstration, developed by Northrop Grumman, has shown that a solid state laser (SSL) is capable of being integrated into a ship's existing systems with the purpose of disabling small boats [2].

United States Air Force.

The U.S. Air Force is responsible for operating in all airspace around the world. Areas of concern include aircraft protection, aircraft weaponization and tactical engagements, ballistic missile defense, and personnel protection. The Air Force Research Laboratory (AFRL) has developed the Personnel Halting and Stimulation Response man-portable laser weapon which is a nonlethal deterrent for protecting troops and controlling crowds by illuminating threatening individual's eyes. Another nonlethal system of interest is the Active Denial System (ADS). This system uses focused millimeter-wave beams to produce an intolerable heating sensation on the skin of the target individual [19]. At this time, while fully developed, there is no

indication that this system has ever been used operationally.

In the realm of missile defense, the Air Force has been responsible for managing the Airborne Laser System (ABL) depicted in Figure 2. A descendant of the Airborne Laser Lab (ALL), the ABL was designed to carry a high energy chemical oxygen-iodine laser (COIL) and shoot down enemy ballistic missiles during boost phase while operating at altitudes above the boundary layer. The system was successfully tested against a missile in 2010, but the system was determined to be more effective as a science and technology test bed for laser research and development [25].

Figure 2. Airborne laser weapon systems. On the left, the ALTB. Photo credit: USAF Photo by Jim Shryne. On the right, the ATL. Photo credit: USAF.

Regarding tactical applications of HEL weapons, the Air Force Special Operations Command (AFSOC) pursued the ATL,s a modified C-130 aircraft with an integrated COIL laser designed to support special operations engagements. Successful engagements were demonstrated in 2009 yet this system has not undergone further testing or development and is not operational [4]. The Air Force is currently actively pursing the tactical program ELLA, with the intent to integrate the DARPA HELLADS laser into a B-1. The Air Force is clearly focused on tactical engagements in and through the boundary layer of the atmosphere. This thesis focuses on the tactical employment of an air based HEL system and the tactical advantages of utilizing a mission planning tool that accounts for atmospheric conditions.

HELTDA Overview

The current prototype HELTDA is based on the High Energy Laser End-to-End Operational Simulation (HELEEOS) (engineering performance code) that supports dynamic HEL engagements in which the target, platform, and optical relays can move vertically and horizontally on any heading in a three-dimensional engagement [8]. Atmospheric effects are modeled through the use of self-contained, correlated, and probabilistic atmospheric databases. This enables the creation of correlated vertical profiles of temperature, pressure, water vapor content, optical turbulence, and atmospheric particulates and hydrometeors as they relate to line-by-line layer extinction coefficient magnitude at wavelengths from the UV to the RF. The seasonal, diurnal, and geographical spatial and temporal variations in these parameters are organized into probability density functions (PDF) which enable the realistic probable outcome analysis of probability of effect (P_e). The end result is a probability of kill (P_k) estimation as well as the confidence associated with this calculation [9]. This parametric one-on-one-engagement-level model incorporates scaling laws tied to a respected wave optics code and all significant degradation effects to include thermal blooming due to molecular and aerosol absorption, scattering extinction, and optical turbulence. Figure 3 depicts the HELTDA user interface.

Earth's Atmosphere

The Earth's atmosphere is a highly dynamic medium in which ground air, and sea based systems must all operate. The atmosphere is divided into several different regions as seen in Figure 1 which are usually distinguished by temperature lapse rate. Temperature variation in each layer is primarily due to the absorptive nature of atmospheric constituents native to each region. When considering laser weapon propagation, the most significant regions are the stratosphere and troposphere as 99%

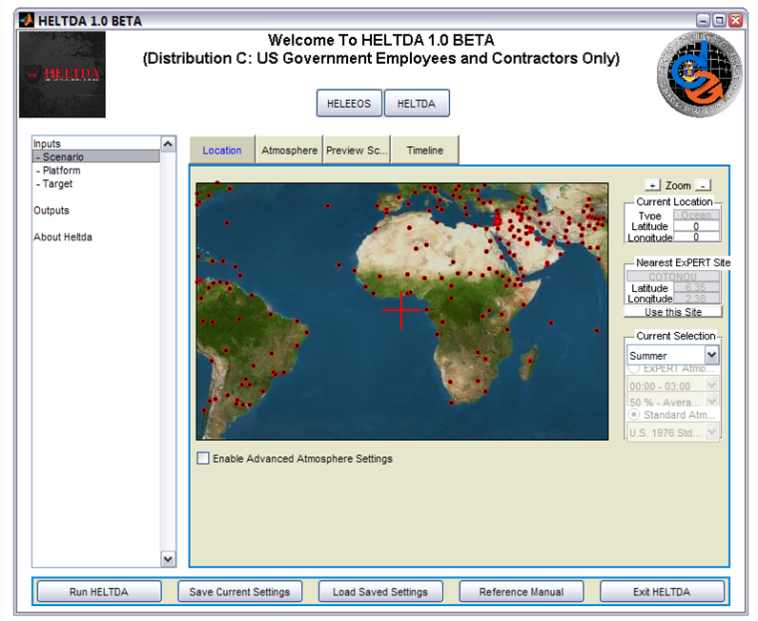

Figure 3. AFIT/CDE HELTDA Prototype home screen.

of air, and thus the attenuating effects, are found within these layers [19].

The atmospheric boundary layer, or boundary layer for short, is the portion of the Earth's atmosphere most affected by the Earth's surface and is the lowest portion of the troposphere [24]. The thickness of the layer varies significantly. It is usually on the order of 1-2 km thick [32], but according to Jacobson, the boundary layer depth can vary from 0.5 to 3 km thick [15]. The temperatures within the boundary layer vary significantly in comparison to the free troposphere and are affected by the specific heats of soil and air as well as energy transfer processes such as conduction, radiation, mechanical turbulence, thermal turbulence, and advection [15]. Temperature variations within different portions of the boundary layer are illustrated in Figure 4. The free atmosphere above the boundary layer is a quasi static/stable portion of the atmosphere which experiences negligible effects due to the surface of the Earth. At the top of the boundary layer resides a temperature inversion which can vary in vertical location and intensity depending on a multitude of factors, but is generally caused by the rapid solar heating of the Earth's surface which increases the

vertical extent of the boundary layer. This is often referred to as the capping inversion as buoyant air parcels are unable to penetrate and are trapped in the boundary layer.

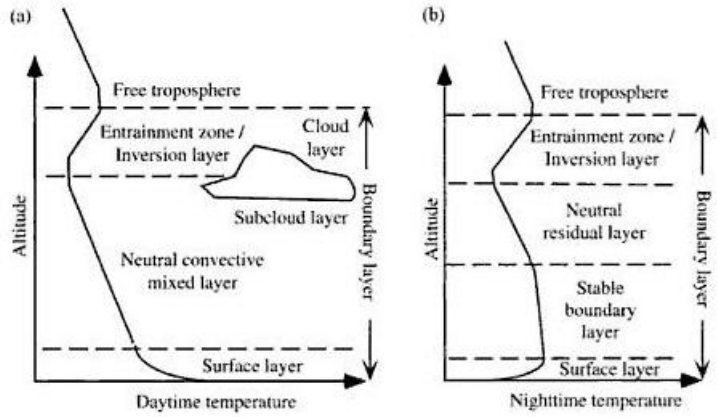

Figure 4. Variation of temperature with height during the (a) day and (b) night in the atmospheric boundary layer over land under a high pressure system [15].

The most significant distinctions between the boundary layer and the free atmosphere above is the nature of the particle content and the variability of atmospheric parameters, especially in unstable conditions. Due to the capping inversion, particulates, including pollutants and moisture, are trapped in the lower part of the troposphere along with turbulence which creates a well mixed layer. The water vapor mixing ratio, potential temperature, and the aerosol/pollutant number concentration are nearly constant in the boundary layer as seen in Figure 5 [19]. As a result, the temperature dry and moist adiabatic lapse rates, as derived from the first law of thermodynamics and the ideal gas law, can be used to describe temperature and dew point within the boundary layer. These are characterized by

$$\left(\frac{dT}{dz}\right)_{\text{dry}} = \frac{-g}{c_p} \approx -9.8\frac{K}{\text{km}} \tag{1}$$

$$\left(\frac{dT_d}{dz}\right) = \frac{-g}{\epsilon \text{l}_v}\frac{{T_d}^2}{T} \approx -1.8\frac{K}{\text{km}} \tag{2}$$

$$\left(\frac{dT}{dz}\right)_{\text{moist}} = \frac{-g}{c_p}\frac{1+l_v\frac{w_s}{\text{RT}}}{1+{l_v}^2\frac{w_s}{c_pR_vT^2}} \tag{3}$$

where g is Earth's gravitational acceleration, c_p is the specific heat of dry air, ϵ is the ratio of the gas constant for dry air to the gas constant for water vapor, l_v is the latent heat of vaporization, w_s is the mixing ratio for saturated air, and R is the gas constant. The pressure lapse rate is derived from the hydrostatic equation and yields an equation for pressure as a function of height that takes the form

$$P = P_b\left[\frac{T_b}{T_b + L_bH}\right]^{\left[\frac{g_oM}{\text{RL}_b}\right]} \tag{4}$$

where P_b is the static pressure (1013.25 mb at sea level), T_b is the standard temperature (288.15 K at sea level), L_b is the standard lapse rate (-0.065 K/m at sea level), H_b is the thickness of the layer, and M is the molar mass of Earth's air [18]. It is within this boundary layer that the most common diurnal and seasonal effects on temperature, pressure, water vapor content, optical turbulence, and atmospheric particulates and hydrometeors are observed [32]. As a result, while the atmosphere may be well mixed locally, the atmospheric conditions in the boundary layer vary greatly with location and time.

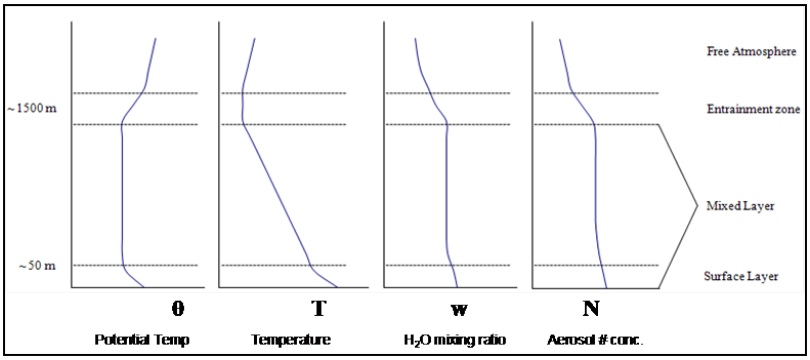

Figure 5. Variation of potential temperature, temperature, vapor mixing ratio, and aerosol concentration with height [19].

The atmosphere is composed primarily of nitrogen, oxygen, argon, and trace gases. Water vapor can comprise up to 4% by volume. Interestingly, nitrogen, oxygen, argon and carbon dioxide maintain their relative mixing ratios at near constant values throughout the lowest 80 km of the atmosphere while other trace gases vary widely with altitude. These trace gases play a significant role in the radiative transfer process through scattering, absorption, and reemission. Likewise, aerosols are most often found in greatest concentrations in the boundary layer and their variability also plays a large role in the radiative transfer of a laser weapon [19].

Existing ADA models have the potential to ignore the effects of boundary layer conditions as this portion of the atmosphere does not normally fall within their domain. The multitude of possible attenuating effects due to propagation through the boundary layer can have a drastic impact on tactical HEL engagements.

HELTDA utilizes the Environmental Reference Table (ExPERT) database to define atmospheric conditions. This joint effort, between the AFRL's Air Vehicles and Space Vehicles Directorates and the Air Force Combat Climatology Center, contains climatological values for land, ocean, and upper air at multiple sites worldwide [23]. For 573 land sites, monthly and hourly percentile data, duration data, and yearly minimum and maximum values are available for altimeter setting, dew point temperature, absolute humidity, temperature, wind speed, and wind speed with gusts at the surface. Also available is the percent frequency of occurrence for significant weather phenomena and the probabilities of when particular combinations of temperature and relative humidity occur. For upper air and ocean locations hourly observations are not available. However, data are available from balloon launches, ship data, and weather satellites at non regular intervals. This provides a basis for mean and standard deviations for climatological values. Percentiles for these regions are subsequently based on normal or gamma distributions [9].

Since multiple probabilistic and independent atmospheric variables are utilized throughout the HELTDA model, correlation between variables in the ExPERT database is essential to ensure physically realizable instances of the atmosphere. The HELTDA utilizes PDF information in the form of nine different percentiles for relative humidity: 1, 5, 10, 20, 50, 80, 90, 95, 99 for summer and winter seasons where the summer season is defined by July values and the winter season is defined by January values. This is true for all locations, yet the temperature and relative humidity are only correlated for the 573 land sites. The model assumes that the atmospheric boundary layer can be effectively characterized by default according to surface parameters. This assumption of a well mixed boundary layer with a homogeneous potential temperature, moisture, pollutant/aerosol, and wind speed profile is consistent with standard models as shown in Figure 5, Stull, and others [24]. Based on Stull's fair weather boundary layer characterization, the boundary layer height in HELTDA is set to the lowest 1,524 m and characterized by surface site values [9]. According to Fiorino et al., ''relative humidity is critically important in the growth and scattering effects of aerosols'' and ''when properly coupled with temperature, can yield correlated values of all other moisture parameters [9].'' Consequently, HELTDA uses relative humidity as the key parameter in determining how percentile values are converted for HEL propagation calculations. For boundary layer calculations, relative humidity is used to determine aerosol size distribution, scattering, and absorption, and is coupled to a temperature to produce absolute humidity for molecular absorption calculations. For calculations above the boundary layer, relative humidity is not present in the ExPERT database and must be derived from temperature and dew point. Additionally, data for each variable in this region are independent from each other due to the compilation of data from numerous collection methods. Calculations are based on the 50th percentile values of temperature and dew point and an exponentially varying number density for

aerosols. More details can be obtained in Fiorino et al. [9]. For the purposes of this paper, 50% refers to the 50th percentile when used in reference to climatology data.

For aerosol effects, the HELTDA incorporates the Global Aerosol Data Set (GADS) to describe atmospheric aerosols and constituents. In GADS aerosols are described by 10 main aerosol components which exist in mixtures and combinations. Typical components are often water soluble, water-insoluble, soot, sea salt, and minerals. The database has a resolution of $5°\times5°$ in latitude and longitude which allows for the determination of radiative properties and mass concentrations of mixed aerosols at each $5°\times 5°$ grid point [9].

Attenuation

Extinction or attenuation is the gradual loss of intensity of any type of flux when traveling through a surface or medium. In the context of laser operations in the Earth's atmosphere, extinction refers to the loss of intensity of a laser beam as it is scattered, absorbed, and transmitted. Extinction can be caused by multiple factors including air constituent molecules and atoms, cloud droplets, aerosols, and other weather phenomena. It is linearly proportional to both the intensity of the radiation as well as the number or density of particles it encounters.

Typically, extinction is quantified through the use of an extinction coefficient β_e measured in units of inverse length. Since extinction is an effect of both scattering and absorption, β_e can be described as a combination of an absorption coefficient and a scattering coefficient

$$\beta_e = \beta_a + \beta_s \tag{5}$$

where β_a is the absorption coefficient and β_s is the scattering coefficient.

Absorption.

Absorption is typically described as the transfer of energy from radiation to heat or chemical energy. Often times, the absorption of photons results in an increase in internal energy as evidenced by increases in thermal energy [20]. This is accomplished through multiple quantum interactions in which photons induce changes in rotational, vibrational or electronic energy levels and subsequent kinetic interactions or collisions move the medium towards thermodynamic equilibrium. This in turn changes the local index of refraction, thus affecting the optical path length the laser must travel. The constituents responsible for this energy transition are atmospheric atoms and molecules as well as pollutants and aerosols. The unique quantum properties of each constituent and the line broadening effects inherent in quantum theory as well as those due to pressure and temperature, collectively lead to absorption occurring in unique spectral windows. The absorption of several atmospheric constituents can be seen in Figure 6 where areas of low transmittance are termed absorption windows.

Scattering.

Scattering is defined as a redirection of radiation out of the path of propagation due to interactions with particulates. Furthermore, it is possible for radiation to be scattered from outside the original path of propagation and into the path of propagation. In general, the size of the scattering particle is the largest determinant in scattering intensity. Particles that are large in comparison to the incident wavelength act as strong scatters while particles small in comparison to wavelength act as relatively weak scatters. Consequently, to successfully address scattering, a size parameter is defined by

$$x = \frac{2\Pi r}{\lambda} \tag{6}$$

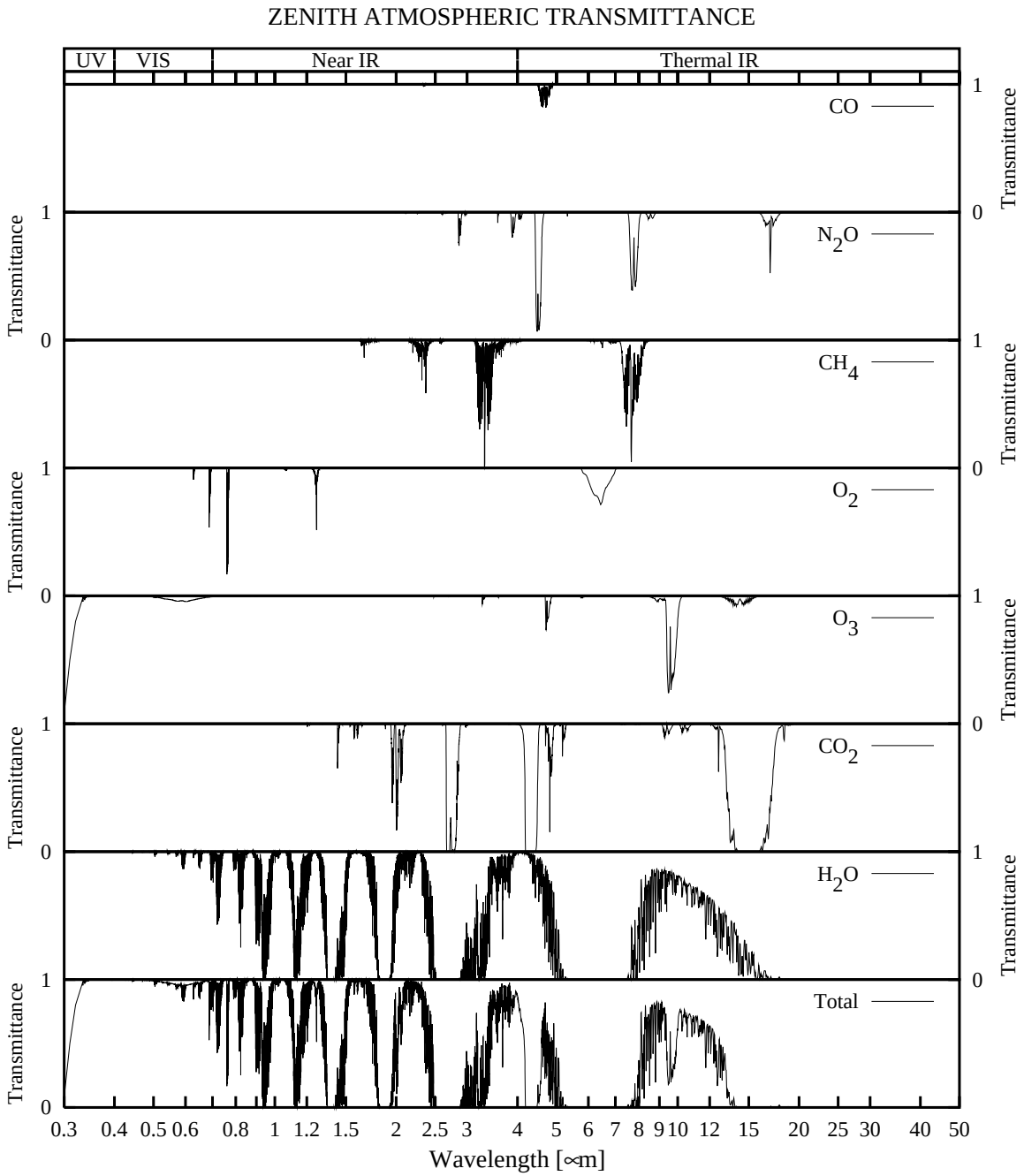

Figure 6. Mid-latitude summer atmospheric transmittance of common atmospheric constituents for an Earth to space vertical path [20].

where λ is the wavelength and r is the radius of a spherical particle [20]. The methods for which scattering is modeled vary depending on particulate size and incident wavelength as see in Figure 7. Models for non-spherical shapes do exist but are far more complex and computationally expensive.

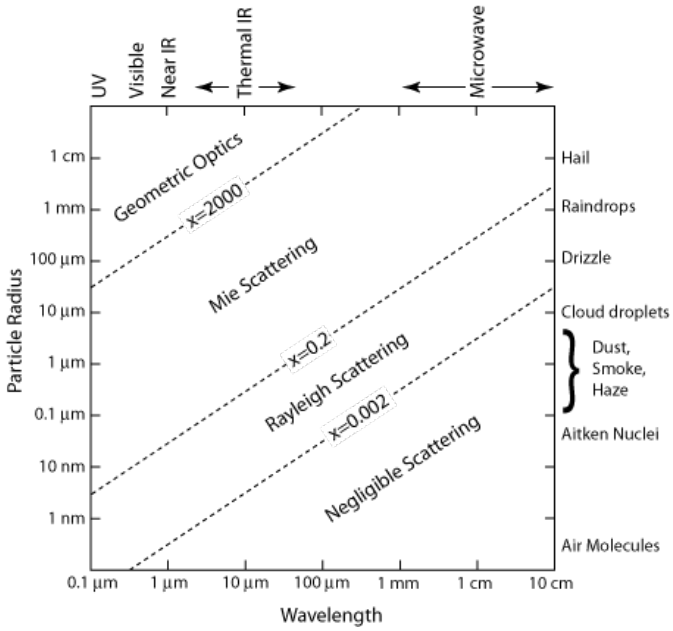

Figure 7. Relationship between particle size, radiation wavelength, and scattering behavior for atmospheric particles. Dashed lines represent rough boundaries between scattering regimes [20].

The HELTDA assumes Mie scattering and models the effects through the use of the Wiscombe Mie scattering module. The extinction, absorption, and scattering coefficients for aerosols are all calculated assuming dry environmental conditions and then altered for relative humidity conditions using

$$\beta_{e,s,a}(\lambda) = \int_{\mathrm{r1}}^{\mathrm{r2}} Q_{e,s,a}(m,\lambda,r)\pi r^2 \frac{dN(r)}{r\ln(10)d(\log r)}dr \tag{7}$$

where Q is the extinction efficiency, r is the aerosol radius, and N is the total particle

density per unit volume normalized to 1. Since humidity causes aerosol particle growth, the modal radius and refractive index for each aerosol species is allowed to vary with relative humidity and the extinction, absorption, and scattering coefficients are recalculated [9]. The humidity-altered index of refraction is given by

$$n = n_w + (n_0 - n_w) \left[\frac{r_0}{r\,(a_w)} \right]^3 \tag{8}$$

where n_w is the refractive index for liquid water, n_0 is the refractive index for the dry particles, r_0 is the radius of the dry particles, and $r(a_w)$ is the radius of the particle at a the specified relative humidity [9].

Molecular extinction in the atmosphere is primarily attributed to water vapor and carbon-dioxide (CO_2). To obtain the water vapor density, or absolute humidity, HELTDA utilizes the relative humidity and the correlated temperature and pressure in the boundary layer and temperature, pressure, and dew point above the boundary layer. CO_2 number density is derived based on pressure and the assumption that atmospheric composition is homogeneous in the region of interest [9].

Thermal Blooming.

In addition to reducing the intensity of a HEL along a specified path, absorption also causes heating of the air molecules within the beam path. This is generally true for all laser propagation but has significant impacts when considering high energy weapons due to the focused nature of the beam. The absorption of the air molecules results in density changes due to heating which alter the index of refraction and thus the intensity distribution within the beam. Known as thermal blooming, this loss mechanism has the effect of changing the beam structure and shape. A Gaussian shaped beam will often take on a crescent shape when thermal blooming is in effect as seen in Figure 8. The thermal blooming distortion number, N_D provides a quantitative

description of magnitude of effect and is defined by

$$N_D = \frac{-4\sqrt{2}kP}{\rho_0 C_p} \int_{\text{Path}} F(z) \frac{\alpha(z)T(z)n_T(z)}{V_{\text{wind}}(z)D(z)} dz \tag{9}$$

where z is the total distance along the slant path R, $n_T = dn/dT = (n_0 - 1)/T$, $\alpha(z)$ is the absorption coefficient, V_{wind} is the effective wind speed perpendicular to the beam, P is the laser power, k is the wavenumber, and $T(z)$ is the transmission at range z. $F(z)$ is the weighting function

$$F(z) = \frac{1}{\sqrt{1 + \left(\frac{1.25\lambda \mathrm{R}}{D^2}\right)^2 \left(\frac{z/R}{1-z/R}\right)^2}} \tag{10}$$

where D is the primary aperture diameter. $F(z)$ is often included to compensate for the fact that absorption near the aperture causes more significant distortion than that near the target. In general, when $N_D > 25$ thermal blooming is considered to be a significant degrading effect [19]. This typically occurs for higher powers and longer ranges. In high altitude situations, it is seldom of any concern, but for low level tactical situations, it can be of great significance. Echeverria showed that there is a trade-off between thermal blooming effects and scattering effects. At higher relative humidity levels, scattering plays a greater role in total attenuation. As scattering decreases, the total energy absorbed increases and thus thermal blooming increases. Consequently, there is a trade-off between scattering and thermal blooming which optimizes a given HEL system performance [6].

Atmospheric Turbulence.

Turbulence refers to an unsteady movement of a medium and when applied to laser propagation refers to an unsteady chaotic movement of air. It is the result of

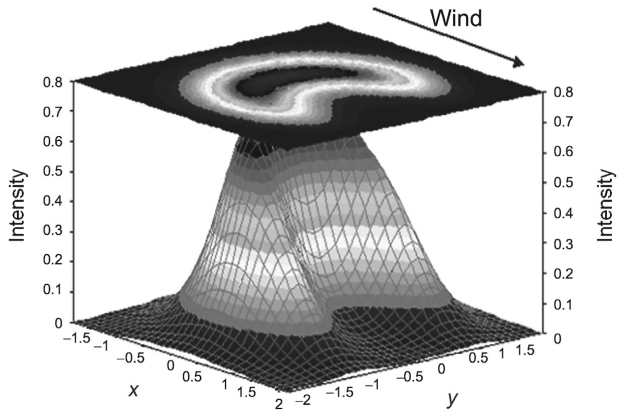

Figure 8. Thermal blooming creates an intensity pattern with a crescent shape turned into the direction of the wind [19].

vertical temperature differences, wind shear, and the effects of lager scale disturbances. Mechanical turbulence occurs when winds travel over protruding surfaces and create eddies, or wave-like motions. Thermal turbulence occurs when solar radiative heating leads to thermals which in turn create eddies. Atmospheric motions are often defined by the combination of many different scales of horizontal motion and boundary layer turbulence typically refers to scales of less than 2 km [15]. At these scale lengths, the life span of turbulent eddies are so short that they are extremely difficult to model quantitatively. This is a direct result of the nonlinear nature of turbulent fluid dynamics. For example, using the Navier-Stokes equations of motion, the buoyant nature of cumulus clouds is usually only predictable for at most a half hour while for eddies of order 100 m the time scale drops to a minute. For scales of 1 cm to 1 mm the time scale is on the order of seconds. Due to the difficulty associated with deterministic solutions, statistical descriptions of turbulence have been developed and employed to accurately describe the net effect of many small scale motions. The result of atmospheric turbulence at the boundary layer scale is the production of temperature gradients which result in variations of the atmosphere's index of refraction as a result of changes in atmospheric density. The optical path length that the light travels over relatively short paths varies, consequently leading to phase changes and difference in

intensity at the receiver or target. Optical turbulence referenced in literature usually refers to boundary layer atmospheric turbulence as it applies to visible and near-IR propagation [19]. Atmospheric turbulence has been the subject of study for centuries, but it is only within the last sixty years that significant progress has been made in understanding this phenomenon. The full statistical description of the theory of atmospheric turbulence is beyond the scope of this chapter; a basic understanding of the theory is presented as it applies to laser propagation.

When statistically characterizing small scale turbulence some assumptions are generally made. Primary among these are that the turbulence is isotropic, homogeneous, and ergodic meaning that it is independent of direction, independent of location, and that all accessible states are equally probable over a long period of time [33].

Temperature variation accounts for the majority of refractive index variations for visible and near-IR radiation. The temperature effect is empirically captured by

$$n(T) - 1 = [n(15^{\circ}\mathrm{C}) - 1] \left[\frac{1.059}{1 + \left(0.00366^{\circ}\mathrm{C}^{-1}\right) T} \right] \tag{11}$$

where n is the index of refraction and T is the temperature in Celcius. In the range of 360 to 3000 nm water vapor, CO_2, and wavelength affect the index of refraction in addition to temperature. Typically, this dependence is calculated by

$$(n-1) \times 10^{-6} = M_1(\lambda)\frac{P}{T} + 4.615(M_2(\lambda) - M_1(\lambda))\chi \tag{12}$$

where P is pressure, λ is wavelength and

$$M_1(\lambda) = 23.7134 + \frac{6838.397}{130 - \bar{\nu}^2} + \frac{45.473}{38.9 - \bar{\nu}^2} \tag{13}$$

$$M_2(\lambda) = 64.8731 + 0.58058\bar{\nu}^2 - 0.007115\bar{\nu}^4 + 0.0008851\bar{\nu}^8 \tag{14}$$

and

$$\bar{\nu}^2 = \frac{1}{\lambda}. \tag{15}$$

The structure function refers to the ergodic mean square difference in the index of refraction at points separated by distance r and is given by

$$D_n\left(\overline{r_1}, \overline{r_2}\right) = D_n(r) = \left\langle \left| n\left(r_1\right) - n\left(r_1 + r\right) \right|^2 \right\rangle. \tag{16}$$

Kolmogorov established a structure function in terms of the index of refraction structure constant, ${C_n}^2$, which measures the strength of atmospheric turbulence given by

$$D_n(r) = \begin{cases} {C_n}^2 r^{2/3} & l_0 < r < L_0 \\ {C_n}^2 {l_0}^{-4/3} r^{2/3} & r_0 < l_0 \end{cases} \tag{17}$$

where l_0 and L_0 define the inertial subrange. This is often defined as having an inner scale of 0.1 to 10 mm and an outer scale of 10 mm to 100 m [19]. This is the defined subrange over which a statistical treatment applies and where turbulent flow transitions back to laminar flow [33]. Using this result, the effect on phase can be represented by

$$D_\phi(r) = 2.91 k^2 r^{5/3} \int {C_n}^2 \mathrm{dz} \tag{18}$$

which is dependent of the path integrated ${C_n}^2$ over the entire path, where k is the angular wavenumber.

When considering laser weapon systems, ${C_n}^2$ is typically the parameter of interest to characterize optical turbulence. Typical values for weak and strong turbulence are less than $10^{-17}$and greater than 10^{-13} respectively. ${C_n}^2$ is altitude dependent as optical turbulence is typically greatest at the Earth's surface and decreases with altitude. It is important to note that this is a general trend and temperature or atmospheric density differences can cause significant changes. Vertical profiles of ${C_n}^2$ are measured

worldwide through the use of fine wire thermosonde measurements of the temperature structure constant (${C_T}^2$) coupled with pressure, temperature, humidity, and wind speed measurements. Neglecting water vapor effects allows for the calculation of C_n^2 by

$$ {C_n}^2 = {C_T}^2 \left[79 \times 10^{-6} * \frac{P}{T^2} \right]^2 \tag{19} $$

where pressure has units of hectopascals and temperature is in Kelvin.

A number of standard ${C_n}^2$ profiles have been developed to characterize these vertical profiles. Some of the most common models currently used for describing ${C_n}^2$ values are the Hufnagel-Valley 5/7 (HV 5/7), Critical Laser Enhancing Atmospheric Research (CLEAR 1), and Greenwood models. HELTDA also contains the capability to use the Starfire Optical Range (SOR) Special, Climatological, and Tunick ${C_n}^2$ profiles. The SOR Special is unique to Kirtland AFB, NM and is therefore only applicable in similar environments. The Tunick profile applies to continental surface layers between 0 and 100 meters and is often not applicable for laser engagement scenarios [10]. The climatological profile incorporates data obtained from the Master Database for Optical Turbulence Research in Support of Airborne Laser. These measurements are derived from thermosonde vertical profiles from the surface to 30 km above sea level made primarily at night due to the solar heating effects on the fine-wire probes [9]. Utilizing Equation 19, the index of refraction structure constant is obtained. Currently HELTDA only provides climatological optical turbulence data for desert and mid-latitude sites. This is due to the fact that the Master Database for Optical Turbulence contains data for Middle East locations such as Saudi Arabia, Qatar, and Bahrain as well as the mid-latitude site of Osan, South Korea. An example comparison between climatological, HV 5/7, and thermosonde measured profiles at Vandenberg AFB can be seen in Figure 9. Note the smooth nature of the models in comparison to actual conditions.

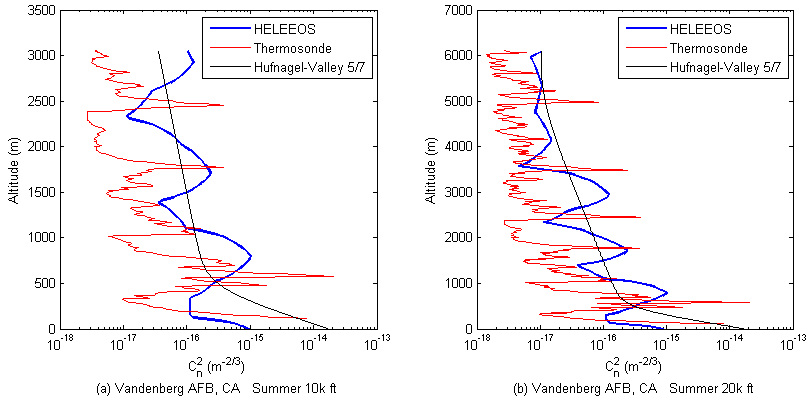

Figure 9. Comparison of HELEEOS climatological, HV 5/7, and thermosonde C_n2 profiles for (a) Vandenberg AFB, CA from surface to 10,000 ft and (b) Vandenberg AFB, CA from surface 20,000 ft. The surface to 10,000 ft is a subsection of the surface to 20,000 ft data. [33].

Gravely demonstrated that the ${C_n}^2$ distributions were log-normal distributions [14]. Consequently, HELTDA uses climatologically representative log-normal distributions curves derived from the Maser Database for Optical Turbulence to probabilistically characterize optical turbulence. A user defined relative humidity percentile as well as a turbulence percentile of interest allow the model to extract probabilistic and correlated optical turbulence values. Wisdom showed that these optical turbulence profiles match within the 80% confidence bounds with actual values measured by thermosonde [33].

The most widely accepted optical turbulence profiles by the DOD are the HV 5/7 and the Clear 1 profiles. The Clear 1 profile is only valid above 1,300 m above mean sea level (MSL). For laser engagements involving altitudes below this level, HV 5/7 is the standard optical turbulence profile.

When addressing laser system performance, the path integrated value of ${C_n}^2$ is of primary interest; thus vertical profiles are significant in determining system performance. Additionally, the location and magnitude of turbulence within the path length can significantly affect performance. Significant turbulence located near the aperture has a greater cumulative effect over the propagation path as compared

to significant turbulence located near the target. Both result in a loss of spatial coherence, but the former is far more significant. Figure 10 demonstrates the effects of optical turbulence on energy propagation. Any loss in beam energy can dramatically impact the irradiance and fluence on target and thus the overall system lethality. The use of adaptive optics to reduce wavefront error at the receiver due to atmospheric distortions can significantly improve performance. Adaptive optics systems are not considered in this research.

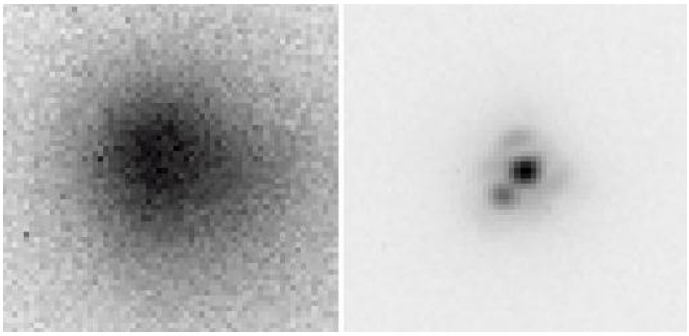

Figure 10. Optical turbulence effects. Left image is an object viewed through optical turbulence. Right image is the same object seen through an adaptive optics (AO) system [6].

Atmospheric Modeling

Standard atmospheres were born out of the need for a standard set of values in the early days of ballistic missile system design and have become industry standard for predicting atmospheric effects. However, they do not represent the atmospheric conditions most likely to be encountered in realistic engagement scenarios. In fact, the 1976 U.S. Standard Atmosphere is defined as an idealized steady state representation of the Earth's atmosphere from the surface to 1000 km over a full solar cycle. As defined by the World Meteorological Organization (WMO), it is a "hypothetical vertical distribution of atmospheric pressure, temperature, and density which, by international agreement, is representative of year-round mid latitude conditions [18]." It is important

to note that heights below 20 geopotential km do not necessarily represent an average of all available data. Assumptions include dry air, homogeneous mixing at low levels leading to constant molecular weight, and treatment as an ideal gas. Additionally, the composition of the atmosphere must be assumed. While many of the assumptions lead to values that correspond well with average values, the correlation of these values is not an accurate representation of observed atmospheric conditions. Despite this fact, standard atmospheres have been used extensively in aviation to define a standard set of conditions and reference for comparisons. Consequently, models and simulations constructed for the aviation community have followed suit and defined atmospheres in the same manner. While this proves to be a useful tool in academics, it does not translate well to an accurate representation of actual meteorological conditions encountered by an operator and severely hampers the planning process for events that are highly sensitive to atmospheric variations.

Apart from the 1976 U.S. Standard Atmosphere, there are many other atmospheric models that have been defined for various purposes. Each represents the spatially and temporally averaged atmosphere as a function of altitude at some resolution. While perhaps not as well known or universally accepted, each one contains its own set of assumptions and is designed to be valid for certain specific parameters. Common standard atmospheres are those defined for specific regions to include mid-latitude, tropical, maritime, polar, and desert regions. The use of this information for planning purposes is a good *first look*, but for realistic engagement preparation, deviations in real world conditions from such a broad spectrum product can lead to significant risk and potential costly results.

HELTDA has the capability to use both climatologically defined atmospheres as well as several different standard atmospheres. Typical standard atmospheres include the 1976 U.S. Standard Atmosphere and the 1976 U.S. Standard Dry Atmosphere.

Other defined standard atmospheres include a polar north, mid-latitude north, tropical, mid-latitude south, polar south, desert, and vacuum atmospheres.

Additional Research

HELEEOS has been utilized in numerous atmospheric and radiative transfer studies since its development. Fiorino et al. compared climatological data to a standard atmosphere for worldwide ladar performance and found that standard atmosphere based predictions were overly optimistic in performance estimates. Additionally, it was found that at high ocean latitudes larger aerosol concentrations and size distributions are present and result in significant differences in transmittance calculations when compared to standard atmosphere conditions. Results were closer for ocean mid-latitudes, but were still not consistent. Signal to noise values were also significantly lower using climatological data from HELEEOS for these northern and southern ocean latitudes. In general, land sites were found to be more favorable for the employment of standard atmosphere calculations, yet the differences were significant [8]. Trade space studies were also conducted for both ladar and radar signal-to-noise ratio performance. Again, aerosols were found to be the primary attenuator of energy for all systems considered; thus suggesting that system performance is highly dependent on location and season [7].

Recently, a unique method for characterizing the boundary layer within the HELEEOS and the HELEEOS derived Laser Environmental Effects Definition and Reference (LEEDR) models in real-time was developed and analyzed by Randall et al. [21]. By utilizing ground observations of temperature, pressure, and relative humidity or dew point, an atmospheric profile is generated using Equation 1, Equation 2, and Equation 3. Above the boundary layer, the standard calculations based on the ExPERT database are still maintained. By analyzing actual vertical profiles for the

Wright-Patterson Air Force Base site, significant improvement in temperature and dew point accuracy within the boundary layer was demonstrated [21]. The operational impact has yet to be shown.

HELEEOS has been used to demonstrate both a need for a HELTDA as well a potential solution. Echeverria performed an effectiveness assessment of tactical engagement scenarios in the lower atmosphere and found significant differences in fluence-on-target values with variations in seasons, location, time-of-day, and atmospheric conditions [10]. The significant variability observed emphasized the importance of mission planning for potential HEL engagements. In a separate study, Fiorino et al. examined the accuracy of HELEEOS assessments and predictions with respect to numerical weather reanalysis data, or numerical weather model data generated from historical weather observations. Analysis indicated significant variations in atmospheric conditions exist over localized areas which could be exploited to obtain an operational advantage in employing HEL weapons. Furthermore, by demonstrating the capability to ingest reanalysis data into HELEEOS, the capability to inject forecast data was also demonstrated as both data sets are of the same format, yet no analysis has been performed to date on forecasted data [12].

III. Methodology

Chapter Overview

The purpose of this chapter is to outline the research methodology used for data collection and analysis. The general approach and reasoning are described in detail followed by a description of the experiment. Data sets and derived products are identified and explained prior to use. The methods for utilization of these products are described in respective simulation descriptions. Setup details and input parameter specifications are given so that results and analysis can be fully understood in context.

Considerations

In order to demonstrate the tactical advantage gained by using a HELTDA, relevant engagement scenarios must be developed. Currently no fielded laser weapon system exists; therefore typical engagement scenarios are undefined. However, by identifying potential users of the envisioned systems, soliciting their inputs, as well as using the tactics and methods currently employed for missions which are similar in nature, it is possible to develop relevant simulations. As these systems are further developed, further analysis will undoubtedly be required. Current operational requirements and warfighter needs, along with prior investments, point to the adoption of HEL weapons by the special operations community. Therefore, this research is tailored for the unique requirements of special operations air to ground engagements. Coordination with the AFSOC's Technology Demonstration Branch was the catalyst for the special operations forces (SOF) focus. Much of the analysis applies to other scenarios but is specifically relevant to low level tactical engagements in or through the boundary layer.

Joint Publication 3-09.3 describes in detail the joint doctrine for planning and

executing close air support (CAS), a fundamental capability for Air Force special operations forces [29]. Close air support is an element of joint fire support and defined as an action by fixed wing and rotary wing aircraft against hostile targets in close proximity to friendly forces. It is recognized as often being the best means to exploit tactical opportunities in both the offense and defense. Doctrine explicitly calls out environmental conditions as a key consideration in the planning and execution of CAS missions, and it specifically states that before operations are undertaken, minimum weather conditions must be considered. Weather conditions can affect things such as visibility and target acquisition, as well as aircraft attack profiles employed in combat. For example, one of the chief concerns of planners today is thermal crossover which occurs when the target and background are the same temperature and imaging infrared systems have the potential to be severely affected. Planners must consider the effects of weather and geography, among other things, on mission objectives and they rely on tactical decision aids such as target acquisition weather software, night vision device planning software, IR target/scene simulation software, and integrated weather analysis aid to do so. One of the many responsibilities of a CAS planner is to access and monitor the capabilities of fires support systems, including aircraft. Doctrine explicitly states that weapon system selection criteria should be effects driven [29].

Similarly, many of the same principles apply to interdiction, a second fundamental capability of special operations. Interdiction, governed by Joint publication 3-03, refers to actions to divert, disrupt, delay, or destroy an enemy's surface capabilities before they can be used against friendly forces or to achieve military objectives [28]. Proper and detailed weapon planning and employment are critical to the success of both mission types and discussions with current SOF mission planner, weather officers, pilots, and weaponeers confirmed this critical role. HEL weapons operate in a distinctly unique domain that differs in many respects from that of conventional

weapons. Therefore, a tactical decision aid is critical to understanding, monitoring, and exploiting their capabilities. The clandestine and often unconventional nature of special operations dictates that planning is even more critical to mission success. Identification and verification of operational advantages must be demonstrated.

Approach

Vertical profile data were collected for multiple land sites corresponding to HELTDA ExPERT sites. These data included both radiosonde data from daily weather balloon launches which measured atmospheric parameters in-situ, and are thus referred to as the control, as well as numerical weather forecast data for multiple time periods. Additionally, profiles derived from climatological data were also generated. Profiles were compared against the control data for various locations, seasons, and times and also provided the inputs into the HELTDA software for mission effectiveness analysis. Multiple relevant engagement scenarios were defined for the purpose of operational effectiveness analyses and simulations were conducted to assess the predictive capability of the various profiles.

Geographic Locations

Three separate geographic locations were chosen for analysis based on operational considerations and data availability. Several sites representing direct threats or areas of concern for the United States were initially considered, but were found to not make climatological information openly available, and data sets that are available are incomplete in nature. Therefore, sites were chosen for their climactic nature as well as their proximity to strategic areas of interest. Wright-Patterson Air Force Base (WPAFB) is representative of a mid-latitude site and is located at 39.83N 84.05W as seen in Figure 11. WPAFB does not routinely launch weather balloons so all analysis

was conducted for the National Weather Service (NWS) site located in Wilmington, OH (ILN) at 39.41N 83.81W. WPAFB ExPERT data were used for climatological comparisons as it is the closest ExPERT site. It was chosen to validate the results reported by Randall et al. and is referred to as *WPAFB* throughout this research [21]. Kuwait International Airport, located at 29.22N and 47.98E as seen in Figure 12, is

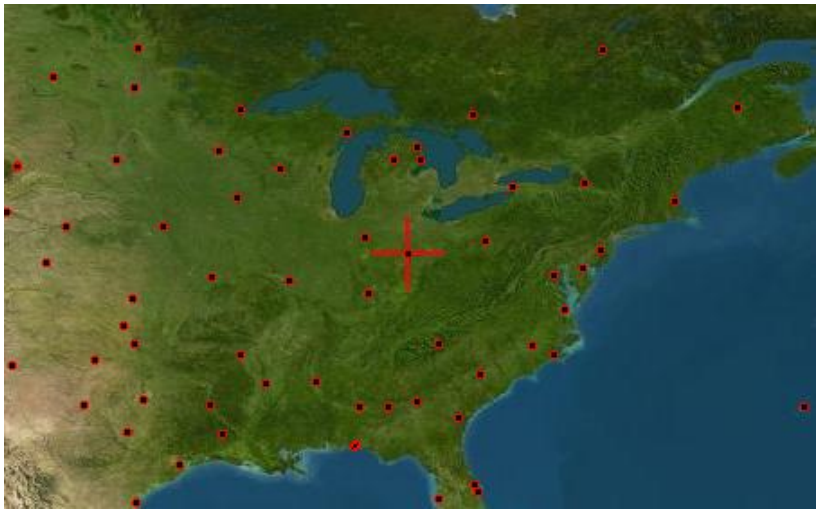

Figure 11. Location of WPAFB ExPERT site and sounding station at 39.83N and 84.05W.

representative of a desert climate and was chosen over other Mid-East sites due to the complete data sets available and correlated ExPERT site. This site is referred to as *Kuwait* throughout this research. Brunei Airport, located at 4.93N and 114.93E as seen in Figure 13, is representative of a equatorial tropical climate and was also chosen for its complete data sets and the correlated ExPERT site. This site is referred to as *Brunei* throughout this research. Radiosondes are routinely launched at all selected sites providing complete control data.

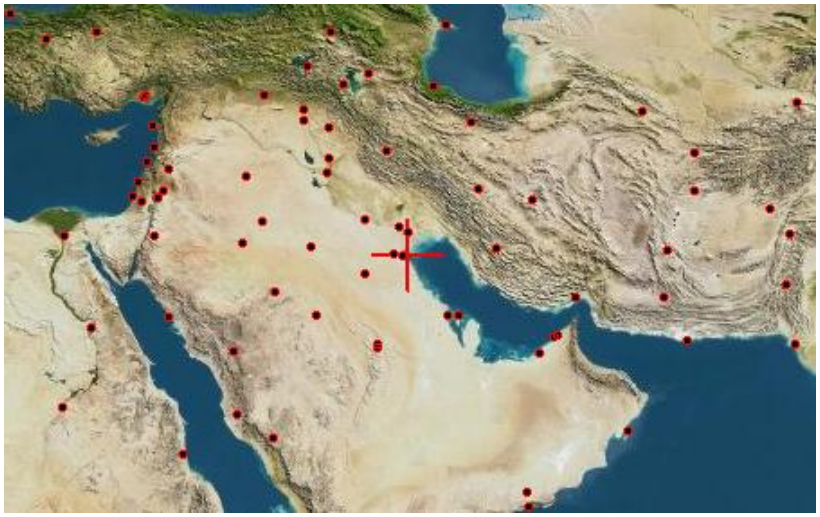

Figure 12. Location of Kuwait ExPERT site and sounding station at 29.22N and 47.98E.

Figure 13. Location of Brunei ExPERT site and sounding station at 4.93N and 114.93E.

Data Sets

Several different data sets were used to acquire actual, forecasted, climatological, and standard atmospheres. The sections below present the details on each of these data sets and their roles in simulation and analysis.

Sounding Data.

Radiosonde data were collected for all locations for both summer and winter seasons, and was used as a control for the atmospheric vertical profiles. Radiosondes are launched by weather balloons globally twice daily on a regular basis for the purpose of upper air observation and data collection. Data are used for multiple purposes, including initialization and validation of numerical weather models. The summer season of this research spanned a period between June and August 2010 while the winter season spanned a period between December 2010 and the first week of March 2011. 25 days were selected for 00z and 12z for both winter and summer at each location for a total of 100 atmospheres at each location. Local times for all three location can be seen in Table 1.

Table 1. Local times for 00z and 12z soundings.

Time/Season	WPAFB	Kuwait	Brunei
Summer 00z	2000	0300	0800
Winter 00z	1900	0300	0800
Summer 12z	0800	1500	2000
Winter 12z	0700	1500	2000

Dates were selected on the criteria that sky observations provided a reasonable chance of a cloud free line of sight for potential laser engagements. Historical surface

METAR reports were used to identify dates for each season and time period for which these conditions were met. This ruled out all time periods with significant weather events and sky cover that was characterized as broken at any level below 27,000 ft. For the 12z summer Brunei data set, only 20 dates matching the specified criteria were available for analysis. Vertical soundings were downloaded from the University of Wyoming's Department of Atmospheric Sciences archive located on the university's web site [1]. Each sounding was converted to match HELTDA input parameters, which include changing units on temperature and wind speed, and converting altitude to above ground values vs above sea level values. Because these data were used as a control, it is important to note the uncertainty associated with the measured/observed values. Randall et al. list radiosonde tolerances as seen in Table 2 [21]. The relative humidity tolerance represented as a percentage suggests that its actual value will vary depending on the observed temperature and that it also affects the known dew point temperature tolerance value. Consequently an approximate tolerance value for the dew point is +/- 1.5 C. Scripts used for the automatic download and conversion of radiosonde data into HELTDA form can be obtained from AFIT/CDE.

Table 2. Specific instrument tolerances for radiosondes

Sensor	Instrument Tolerance	Instrument Response Time
Relative Humidity	+/- 5%	in seconds
Temperature	+/- 0.3 C	< 4 seconds
Pressure	+/- 0.5 millibars	< 1 second

Forecast Data.

Forecast data were collected for the same dates and times corresponding to radiosonde data collects. The Global Forecast System (GFS) numerical weather prediction model was chosen due to the global coverage of the system. The model was originally implemented at the National Meteorological Center in 1981 and has continually been modified as computing capabilities have increased. Currently the GFS is run four times daily at 00z, 06z, 12z, and 18z for a period of 384 hours and grid spacing is set at $0.5^\circ \times 0.5^\circ$ globally for forecasts out to eight days. Beyond eight days resolution is reduced. It is a spectral type model with sigma-pressure hybrid vertical coordinates with a vertical resolution of 64 layers [27]. Forecasts were collected from the National Oceanic and Atmospheric Administration (NOAA) National Operational Model Archive and Distribution System (NOMADS) and included 48, 24, and 12 forecasts for 00z and 12z [3]. Data were collected in the *.grib2 format standard for meteorological data. This is the WMO's second version of their standard for distributing gridded data sets. The data were then probed using the National Digital Forecast Database (NDFD) driver *degrib* (also known as the NDFD GRIB2 decoder) to obtain all GFS outputs for a particular latitude and longitude. When the specific point of interest did not lie at a grid point, a bi-linear interpolation method was employed using the four closest grid points to obtain the interpolated value [26]. Relevant meteorological data were extracted and converted to match the vertical profiles associated with HELTDA inputs parameters and the vertical soundings described above. Scripts created for the automated conversion of forecast data into HELTDA form and can be obtained from AFIT/CDE.

Climatological Data.

Climatological atmospheric profiles are generated in the HELTDA software by obtaining climatological values for the percentile of interest from the ExPERT database and employing Equation 1, Equation 2, and Equation 3. The same method was employed to generate vertical profiles that could be imported directly into the software during batch runs. Atmospheric parameter values were interpolated to sounding levels for direct comparisons. Additionally, climatological wind speeds and directions were used to define the wind profile. The 50th percentile was used as the baseline climatological conditions for the purpose of this study. This profile is referred to as the *50th percentile climatological* or *50%* profile. In some instances, other percentiles are used to illustrate extreme conditions. It is important to note that actual and forecasted conditions may vary significantly from the 50% climatological data.

Ground Tab Data.

The ground tab option in the HELTDA software enables the user to input surface observations for temperature, pressure, relative humidity and/or dew point, and pressure. This allows the user to account for variations from the climatological values. Within the boundary layer, Equation 1, Equation 2, and Equation 3 are used to define the vertical profile. Above the boundary layer values revert back to the upper-air ExPERT percentile values as described in [9]. Climatological winds were used for all levels. For this research, the ground level sounding values were used as the ground level observations and a vertical profile was generated in the same manner enabling import for batch runs. Vertical levels in the profile were interpolated to sounding levels for direct comparison. This profile is referred to as the *ground tab* profile.

Standard Atmosphere Data.

The 1976 U.S. Standard Atmosphere is a default user option. It is independent of location, season, or time of day and representative of a mid-latitude annual atmosphere [18]. A single vertical profile was generated using the HELTDA software, to include climatological wind speed and direction, and then imported for batch runs where required. Vertical levels in the profile were interpolated to the sounding levels for direct comparison. It is referred to as the *1976 U.S. Standard Atmosphere* profile throughout this research.

HELTDA Modifications

Several modifications were made to the HELTDA code to complete this research. While most consisted of standard changes required to implement previously developed functions within the HELTDA framework, some were significant modifications adding new capabilities to the software. One such modification was the addition of a circular orbit geometry. Previous stable versions of the software implemented only straight line geometry for the platform and was only slightly more sophisticated in the addition of ballistic trajectories for the targets. One drawback of this implementation is the lack of support for orbital engagements often employed by special forces. In these scenarios, the slant range remains relatively constant in a circular orbit while required laser dwell time an vary significantly depending on initial heading and length of the engagement. For the purpose of this research, circular orbits were assumed, although multiple engagement geometries including racetrack and figure-eight geometries orbits are also possible in an operational environment [29]. Scripts developed for the automatic generation of complex engagement geometries can be obtained from AFIT/CDE and are planned inclusions in later releases of the HELTDA software.

Several bugs in previously developed software were identified throughout the

course of this research. Of note was the modification of the atmospheric profile import function. HELTDA previously possessed the capability to import an atmospheric vertical profile and utilize those values for engagement calculations. However, it was soon discovered that these profiles were loaded to the wrong geographic location and therefore the aerosol distributions were not consistent with the intended scenario. A simple modification to the code corrected the issue and now all imported vertical profiles default to the correct geographic location, thus eliminating the unnecessary error due to incorrect parameters in the engagement calculation.

Simulations

Multiple simulations were conducted to provide a complete picture of various actual and modeled atmospheres and their characteristics for analysis. The following sections describe the experimental setup for each of these simulations. The results, analysis, and discussions regarding each one can be found in the next chapter. All simulations were based on the prototype ELLA specifications unless otherwise noted. These include a laser wavelength of 1.045 μm, an output power of 150 kW, an output aperture size f 0.4 m, a beam quality of $m^2 = 2.9$, and a platform airspeed of 150 m/s. For all simulations GADS aerosol distributions and a HV 5/7 optical turbulence profile are assumed as aerosol and optical turbulence distributions are not available in real time in operational products. Without the use of certain climatological inputs, the predictive capabilities of all characterization methods are severely limited.

Vertical Profile Validation.

For this simulation, vertical profiles were generated for all forecast data as previously described. Vertical profiles were also generated for the climatology data as well as for a 1976 U.S. Standard Atmosphere. In this simulation, temperature, dew

point, wind speed, and wind direction for each vertical profile were compared to the sounding profile, referred to as the *control*. When using the HELTDA software, a atmospheric boundary layer height is assumed based on the season and time of day as seen in Table 3. Boundary layer height is best estimated using vertical profiles for actual conditions. Since the operational user is unable to asses actual boundary layer height prior to engagement, the boundary layer height is assumed based on Table 3. It is possible that a more accurate estimation prior to engagement may yield more favorable performance, however those estimates are not addressed in this research.

Table 3. Overland Boundary Layer Height (in meters) as a function of season and time of day.

Time of Day (Local)	Summer	Winter
0000-0259	500	500
0300-0559	500	500
0600-0859	1000	500
0900-1159	1524	1000
1200-1459	1524	1524
1500-1759	1524	1524
1800-2059	1524	1000
2100-2359	1000	500

Simulations were conducted for both the portion of the profile within this altitude range (surface to boundary layer height), as well as for the entire profile (surface to approximately 30,000 m). Interpolation was necessary to produce temperature, dew point, wind speed, and wind direction values at the same altitudes as in the control data. This was accomplished using a linear interpolation method and facilitated the calculation of RMSE.

Predicted Dwell Time.

To fully understand the impact of the vertical profile in an operational environment required dwell time was used as a metric to evaluate predicted performance for the various methods of atmospheric characterization. For this simulation, a standard circular orbit geometry was assumed as seen in Figure 14.

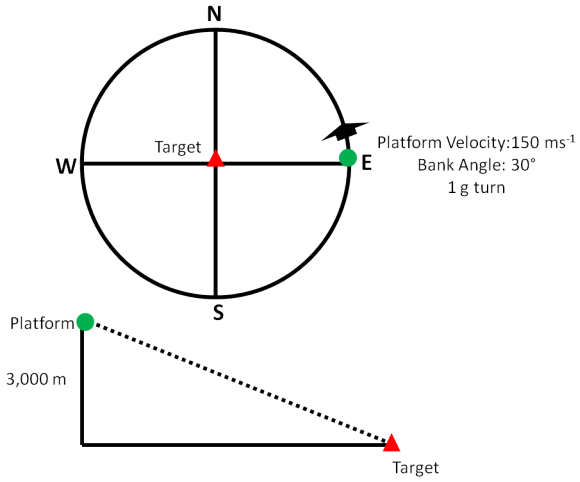

Figure 14. Engagement geometry for predicted dwell time simulations: top view (top), side view (bottom). Initial heading is 0° for a one g turn with a 30° bank angle at 150 ms^{-1}. The target is located 1 m above the ground and at the center of the circular orbit. Altitude is set at 3000 m, except for boundary layer engagements, in which case, the altitude is defined by Table 3. Ground range is approximately 3,977 m.

The platform travels at an initial heading of 0° in a circular orbit around a stationary target located 1 m off of the ground at a velocity of 150 ms^{-1} from a starting location due east of the target. The circular orbit is defined by a 30° bank angle and at constant gravity, or a 1 g turn. This is to capture the effects of the various atmospheric characterization methods at a constant slant range and to account for the differences in wind directions between each atmospheric profile. A constant slant range ensures variations are not a result of changing geometry. Simulations were done for the 3,000 m altitude scenario as well as for altitudes that matched the

boundary layer conditions as seen in Table 3. The target damage threshold for this simulation was set at 1×10^5 J/cm^2 for a 5×5 cm^2 susceptible region or *bucket*. This is considered an extremely hard target and represents the stressing limits of expected targets in an operational environment as seen in Figure 15. It was chosen for the purpose of extending dwell times for the sake of analysis.

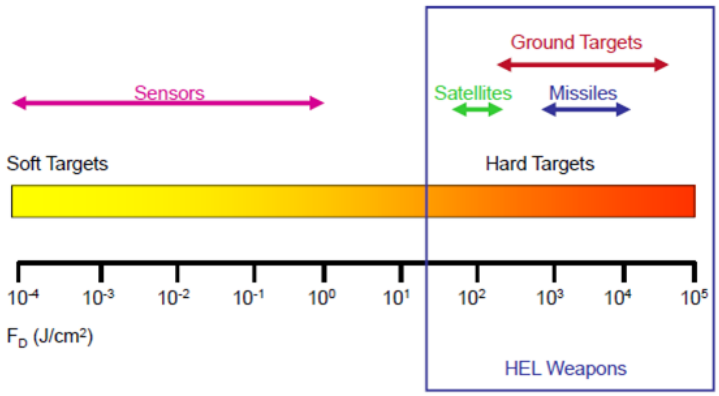

Figure 15. Typical lethal fluences for classes of military targets [19].

Altitude vs Dwell Time.

To simulate the effects of altitude on dwell time requirements, two separate geometry configurations were used in simulations. The first can be seen in Figure 16. In this case, the target position remains fixed while the platform altitude is varied from 500 m to 6,000 m by increments of 250 m. Effectively, as the altitude is varied, the slant range and *look angle* θ are changed for every engagement while the ground range remains constant at approximately 3,977 m. All other engagement parameters remained unchanged from the scenario described in the Forecasted Dwell Time simulation.

To better understand the effects within the boundary layer, a second method of examining dwell time vs altitude was devised. Rather than simply varying platform altitude and slant range, both platform and target altitude were varied simultaneously

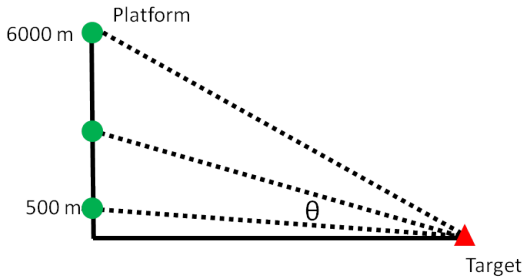

Figure 16. Engagement geometry for altitude vs dwell time simulations with varying slant range. Initial heading is 0° for a one g turn with a 30° bank angle at 150 ms^{-1}. The target is located 1 m above the ground and at the center of the circular orbit. Altitude is varied from 500m to 6000m while the target position remains fixed. Ground range is approximately 3,977 m.

as depicted in Figure 17. This has the effect of maintaining a constant slant range and a constant *look angle* θ. Platform altitude was initially set at 3,000 m and target altitude at 1 m and both were varied by 250 m increments. All other engagement parameters remained unchanged.

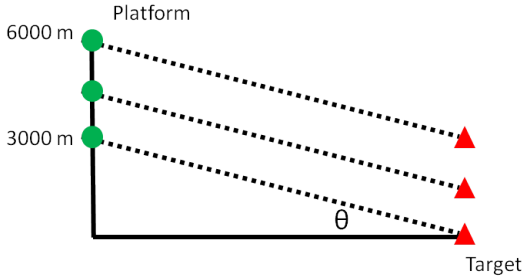

Figure 17. Engagement geometry for altitude vs dwell time simulations with constant slant range. Initial heading is 0° for a one g turn with a 30° bank angle at 150 ms^{-1}. The target is located 1 m above the ground and at the center of the circular orbit and platform is initially located at 3000 m. Altitude is varied for both platform and target in 250 m increments. Ground range is approximately 3,977 m.

Dwell Time vs Heading.

Another scenario of interest is dwell time vs heading. For this case, the same geometry was used as in the predicted dwell time simulation in Figure 14. The initial

heading was varied from 0° to 360° in increments of 5°. This allows for the analysis of thermal blooming effects due to wind speed and wind direction differences while maintaining a constant slant range and altitude. All other engagement parameters remain consistent with previously described simulations.

Mission Planning Scenario.

To demonstrate the effectiveness of the HELTDA for operational mission planning a hypothetical mission planning scenario is described. While the mission profile, target, and platform parameters are hypothetical, the atmospheric data used are actual collected data for the specified location and time. The hypothetical mission scenario is optimized through mission planning and a temporal and spatial operational advantage is demonstrated using in-situ observations as the control for analysis. The results from this case study demonstrate the utility of an operational HELTDA mission planning tool as well as the current process and procedures involved in utilizing such a tool.

IV. Results and Analysis

Chapter Overview

This chapter presents results and analysis obtained throughout the course of the research effort. Results of the vertical profile validation simulations are presented first and are critical to understanding the accuracy and utility of the HELTDA. Next, forecasted dwell times for a hypothetical engagement based on ELLA parameters are analyzed for multiple realistic atmospheres. The results of these simulations necessitated that COIL wavelengths also be studied for the same mission profiles as the original hypothesis was not supported. The results indicate a wavelength dependence for relative performance between the atmospheric characterization methods studied. Altitude optimization for mission planning is addressed by analyzing multiple atmospheres at multiple locations with varying mission profiles. The same approach is also used to understand the effect of platform heading and thermal blooming for air-to-ground engagements. Finally, a mission planning scenario is described and analyzed in order to demonstrate the potential operational advantages gained through the use of the HELTDA for HEL tactical engagements in actual and simulated atmospheres.

The purpose of this research is to quantify the operational advantage gained by using realistic atmospheres for mission planning and execution in operationally relevant metrics. Therefore, results are generally presented in dwell times and probability of kill for relevant engagement scenarios. For direct comparisons, the Root Mean Squared Error (RMSE) was chosen as the method to quantify differences between models and observed data. The absolute mean difference is generally smaller than the RMSE and depending on the operational impact and significance of extreme outliers, may be a better indicator of error. However, for the purposes of this research, the RMSE values are reported.

It is important to note that these results are only valid for the conditions, configurations, and parameters stated. The analysis does not consider all atmospheric or weather conditions possible for a HEL engagement, nor does it imply that the results are valid for all location or condition sets. While certain effects may be correlated to specific parameter conditions, the assumptions can not be made without further research.

Vertical Profile Validation

Vertical profiles were generated based on climatological data in the form of the ExPERT database, the ground tab function within HELTDA (which relies on an in-situ ground observation of temperature, pressure, relative humidity, and/or dew point), a 1976 U.S. Standard Atmosphere, and GFS forecast data. It was initially hypothesized that the forecasted profile would outperform all others in an operational assessment by predicting dwell time with greater accuracy and lower RMSE, and that the ground tab generated profile would outperform the standard and climatological atmospheres. The first step in confirming this hypothesis is to examine the errors or differences in the vertical profiles themselves. The accuracy of the atmospheric vertical profiles is characterized by the RMSE between the profile and the vertical sounding observations previously described as the control data.

The GFS model output includes relative humidity and temperature, but not dew point specifically. Since the HELTDA accepts temperature and dewpoint as atmospheric inputs and makes internal transformations to relative humidity, the same scheme was used in this research. Relative humidity is given by the equation

$$\mathrm{RH} = \frac{e_w}{e^*_w} \times 100\% \tag{20}$$

where e_w is the partial pressure of water vapor and ${e^*}_w$ is the saturated vapor pressure of water at a prescribed temperature. The saturated vapor pressure of water can be estimated using the empirical Goff-Gratch equation

$$\begin{aligned}\text{Log10}\left[{e^*}_w\right] = &-7.90298 * \left(\frac{T_s}{T} - 1\right) + 5.02808. * \text{Log10}\left[\frac{T_s}{T}\right] - 1.3816 \times 10^{-7} \\ &* \left(10^{11.344\left(1-\frac{T}{T_s}\right)} - 1\right) + 8.1328 \times 10^{-3}\left(10^{-3.49149 * \frac{T_s}{T} - 1} - 1\right) \\ &+ \text{Log10}[e_{st}] \end{aligned} \tag{21}$$

where T_s is the steam point and is equal to 373.15 K, T is the temperature in K, and e_s is the steam point pressure equal to 101324.6 Pa. By constructing a table for all dew points between 200 and 350 K at 0.1 K intervals, the partial pressure of water corresponding to each dew point can be calculated from Equation 21. This table is then used as a *lookup table* for dew points where the value of interest is found by using Equation 20 and solving for the partial pressure of water. Values are linearly interpolated between *lookup table* values.

RMSE analysis of the atmospheric profiles was accomplished by interpolating the profile values for temperature, dew point, wind speed, and wind direction to the pressure levels specified in the control profile. A linear interpolation method was employed and extrapolation beyond the endpoints was utilized when necessary. The RMSE quantizes the error in each vertical profile meteorological parameter for a particular atmosphere. Each season (summer and winter) and time of day (00z and 12z) contained multiple cases for which the RMSE in the vertical atmosphere was evaluated. The results are reported by season and time of day and the overall quality of atmospheres examined is reported in the mean RMSE for each data set. Tabular data are included in Appendix A in Table 4 through Table 9.

WPAFB.

Figure 18 shows the vertical temperature, dew point, and relative humidity profile mean RMSE for WPAFB through the boundary layer (surface to boundary layer height as defined in Table 3) for each time and season. Temperature, dew point, and relative humidity profiles are all better predicted by the GFS forecasts than the 50th percentile ExPERT data and the HELTDA ground tab for all seasons and times of day. The 12 hour forecast performs the best of the three forecasts, however, the relative improvement from the 48 and 24 hour forecast is relatively small as the difference in values is smaller than the uncertainty associated with the measurement instruments for almost all cases. The ground tab outperforms the climatology data in terms of relative humidity and temperature profiles for all but the summer 12z times. This is likely because the boundary layer during this time period is set at 500 m coupled with low relative humidity during the summer season. The 1976 U.S. Standard Atmosphere also outperforms the ExPERT climatology and the ground tab in relative humidity for the same time and season yet under performs both in terms of temperature and dew point for all cases. Surprisingly, the 1976 U.S. Standard Atmosphere outperforms all other atmospheres including forecasts in terms of relative humidity prediction for the winter 00z case. In general, errors for many summer atmospheres are lower than corresponding winter times. For all but the 12z time ground tab profiles, the dew point mean RMSE is larger than the temperature mean RMSE. This again is most likely due to the shallow nature of the BL during this time period.

Figure 19 depicts the vertical wind speed and wind direction profile mean RMSE through the boundary layer. The 1976 U.S. Standard Atmosphere, 50th percentile ExPERT profile, and the ground tab profile do not contain wind profiles. Therefore, climatological values are used and are equivalent for all three characterizations. The forecast predictions outperform the climatological values for all seasons and times of

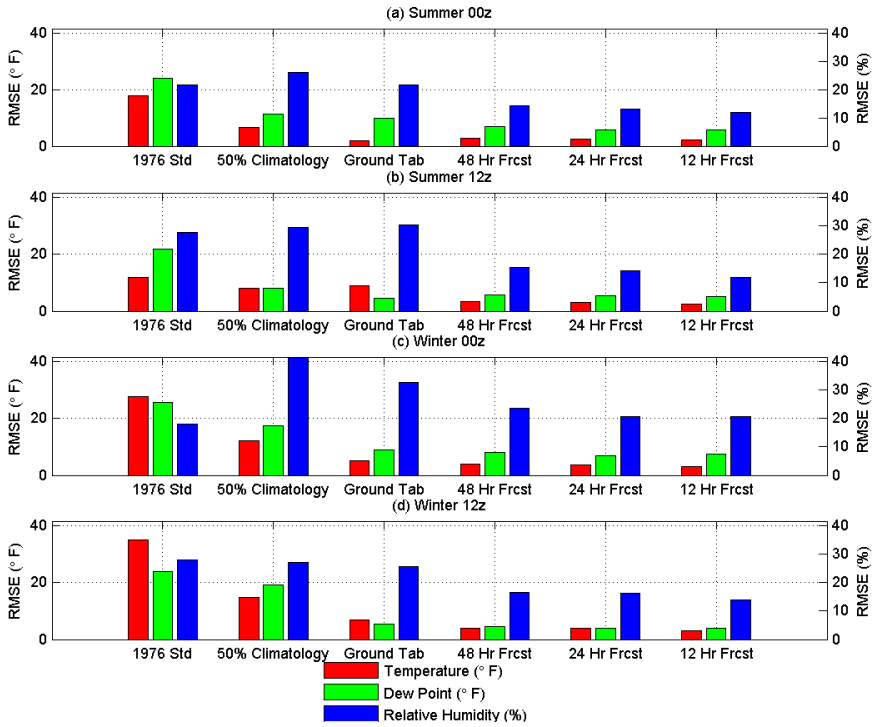

Figure 18. WPAFB temperature, dew point, and relative humidity vertical profile mean RMSE in the boundary layer for (a) Summer 00z, (b) Summer 12z, (c) Winter 00z, and (d) Winter 12z. Atmospheres considered include the 1976 U.S. Standard Atmosphere, 50th percentile ExPERT climatology, HELTDA ground tab, and 48, 24, and 12 hour GFS forecast derived atmospheres.

day, but the difference between the three forecasts is relatively small. Wind speed errors are shown to be higher in the summer for the climatological wind profiles and relatively equal for the forecast profiles. In the winter, wind direction is more accurately predicted at 00z rather than 12z. This is true for the climatological values in the winter, but does not hold true for the GFS forecasts.

When the same analysis is applied to the atmosphere from the surface to approximately 30,000 m (to include the boundary layer) mean RMSE values vary significantly from boundary layer values as seen in Figure 20. The most noticeable differences are in dew point values. Dew point RMSE values are significantly higher for the full atmosphere for all but the standard profile. This suggests that dew point prediction is more difficult than temperature prediction, regardless of the atmospheric character-

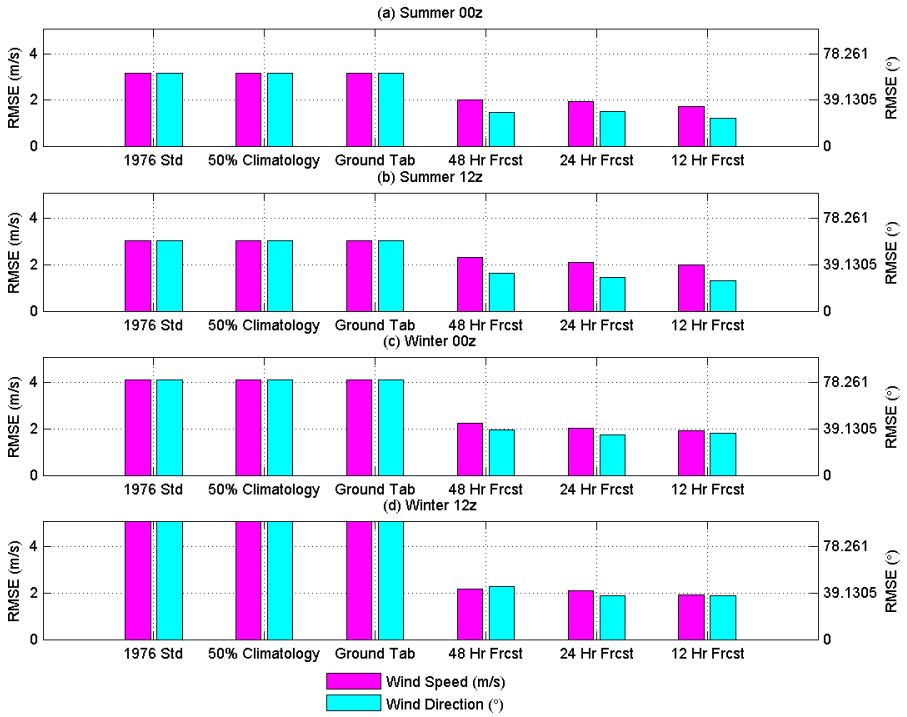

Figure 19. WPAFB wind speed and wind direction vertical profile mean RMSE in the boundary layer for (a) Summer 00z, (b) Summer 12z, (c) Winter 00z, and (d) Winter 12z. Atmospheres considered include the 1976 U.S. Standard Atmosphere, 50th percentile ExPERT climatology, HELTDA ground tab, and 48, 24, and 12 hour GFS forecast derived atmospheres.

ization method employed. Temperature mean RMSE values are also higher for the ExPERT climatology and the ground tab profiles. GFS temperature values show an increase over the boundary layer characterization, but the relative magnitude change is small. Consistent with the boundary layer analysis, the forecasts outperform all other characterization methods.

Vertical wind speed and direction mean RMSE values are shown in Figure 21. Both wind speed and wind direction errors are greater than those in only the boundary layer as is expected. Forecast profiles continue to provide the best predictive capability with little distinguishing between the 48, 24, and 12 hour forecasts.

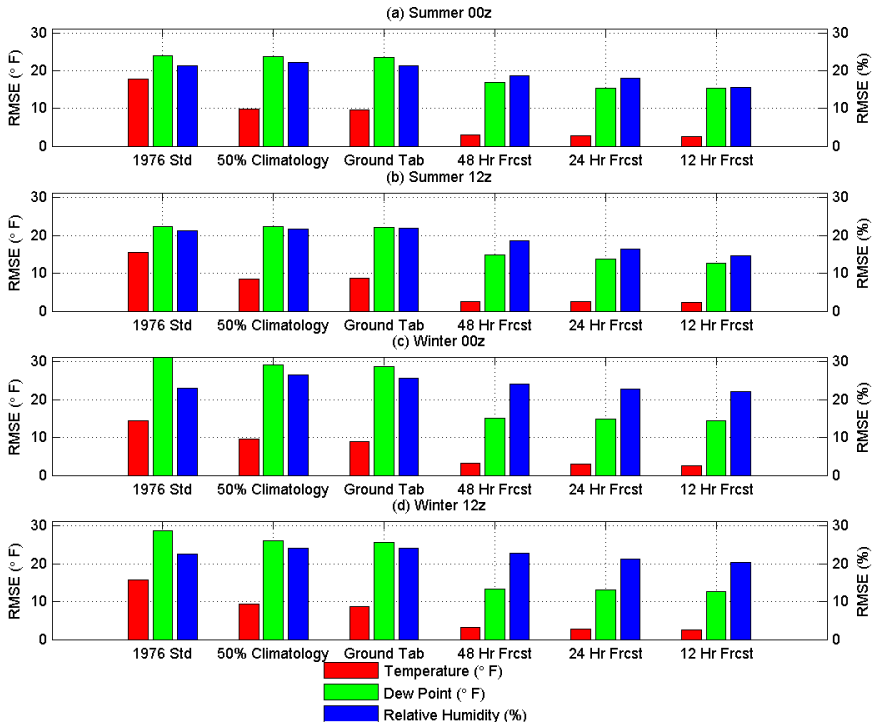

Figure 20. WPAFB temperature, dew point, and relative humidity vertical profile mean RMSE from 0 to approximately 30,000 m for (a) Summer 00z, (b) Summer 12z, (c) Winter 00z, and (d) Winter 12z. Atmospheres considered include the 1976 U.S. Standard Atmosphere, 50th percentile ExPERT climatology, HELTDA ground tab, and 48, 24, and 12 hour GFS forecast derived atmospheres.

Kuwait.

Figure 22 and Figure 23 depict the boundary layer mean RMSE for Kuwait. Significant differences in characterization performance are evident when compared to the WPAFB results.

For all seasons and times of day, except summer 00z, the 24 and 12 hour forecast profiles outperform the climatology and ground tab profiles for temperature, dew point, and relative humidity. The same is true for the 48 hour profile during the winter. The 1976 U.S. Standard Atmosphere has a better predictive capability in the winter season and outperforms climatology, but it is significantly worse than all other atmospheric characterizations. The relatively consistent error values between

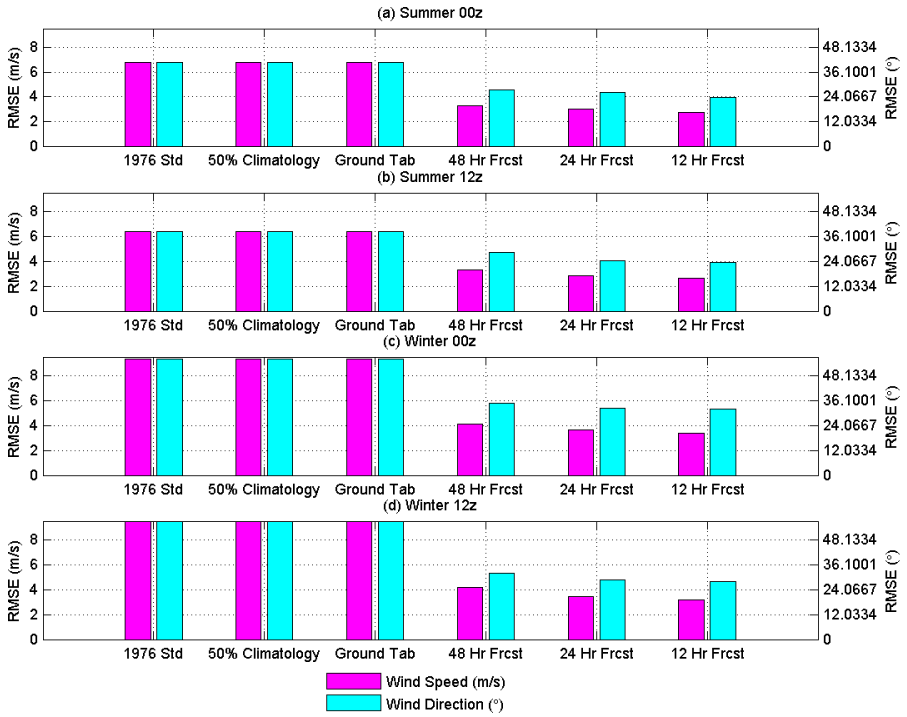

Figure 21. WPAFB wind speed and wind direction vertical profile mean RMSE from 0 to approximately 30,000 m for (a) Summer 00z, (b) Summer 12z, (c) Winter 00z, and (d) Winter 12z. Atmospheres considered include the 1976 U.S. Standard Atmosphere, 50th percentile ExPERT climatology, HELTDA ground tab, and 48, 24, and 12 hour GFS forecast derived atmospheres.

all other atmospheres suggests that this region's boundary layer is well mixed and characterized using climatology and the HELTDA ground tab. The ground tab errors for temperature, dew point, and relative humidity are smaller than climatology for all cases. Dew point is consistently more difficult to predict except for the 00z cases which can be explained by the short boundary layer due to time of day. Relative humidity error is far greater in the winter. This is expected due to highly variable conditions during the winter months in Kuwait. In comparison, summer months are typically hot and dry with little variation.

Wind speed errors are fairly consistent for all cases. Wind direction error is maximized for climatology in the winter, but minimized for GFS forecasts. GFS forecast advantage is evident in the winter months, but less so during the summer.

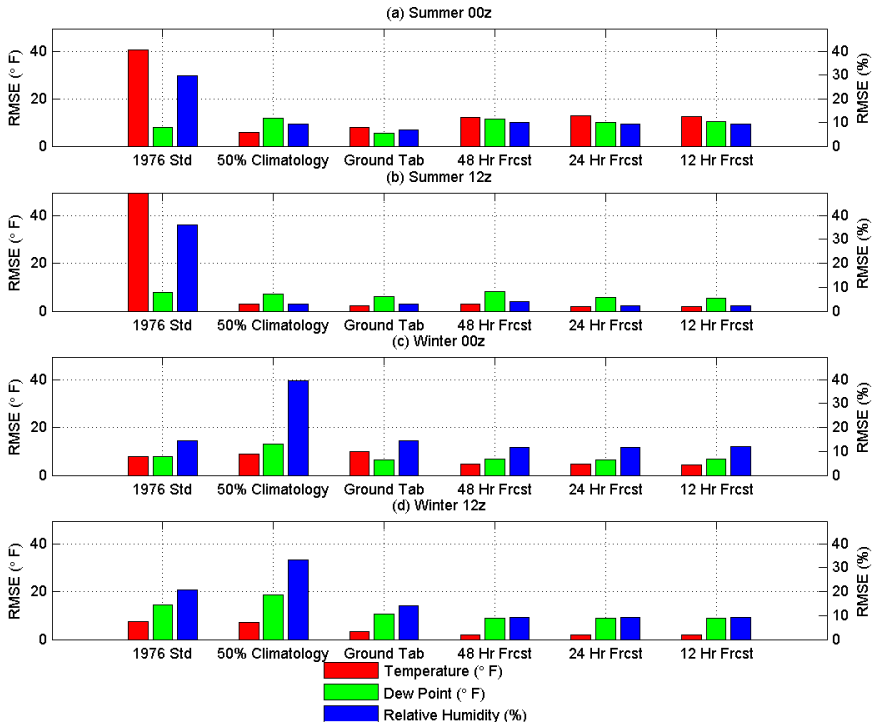

Figure 22. Kuwait temperature, dew point, and relative humidity vertical profile mean RMSE in the boundary layer for (a) Summer 00z, (b) Summer 12z, (c) Winter 00z, and (d) Winter 12z. Atmospheres considered include the 1976 U.S. Standard Atmosphere, 50th percentile ExPERT climatology, HELTDA ground tab, and 48, 24, and 12 hour GFS forecast derived atmospheres.

Figure 24 and Figure 25 depict the full atmosphere error for Kuwait. Figure 24 clearly demonstrates the advantage of the GFS forecasts regarding error in temperature, dew point and relative humidity. For climatology and ground tab profiles, temperature error is greater than dew point error, while the opposite is true for forecasted profiles. The standard atmosphere outperforms climatology and the ground tab for all seasons and times of day, but does not outperform any of the forecasts. This indicates that the standard atmosphere provides more accurate estimates at higher altitudes. For wind speed and wind direction GFS forecasts results in less error than climatological and standard profiles.

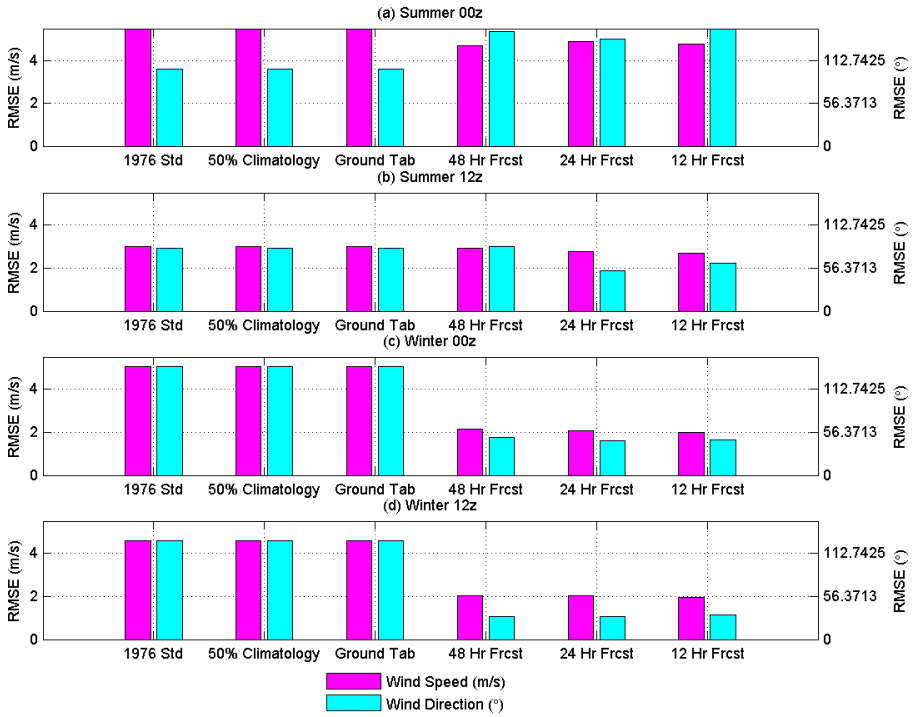

Figure 23. Kuwait wind speed and wind direction vertical profile mean RMSE in the boundary layer for (a) Summer 00z, (b) Summer 12z, (c) Winter 00z, and (d) Winter 12z. Atmospheres considered include the 1976 U.S. Standard Atmosphere, 50th percentile ExPERT climatology, HELTDA ground tab, and 48, 24, and 12 hour GFS forecast derived atmospheres.

Brunei.

Brunei's boundary layer atmosphere characterization is depicted in Figure 26 and Figure 27. The relative performance of the 1976 U.S. Standard Atmosphere is much worse than other atmospheres. Additionally, the difference is far more pronounced than WPAFB or Kuwait. For all profiles, error is greater in the summer as compared to winter. This is to be expected considering the tropical climate. Error in all three parameters is slightly reduced in the winter. There is little difference in values between 12 and 48 hour forecasts for all cases, although 12 hour forecasts have slightly less error. The ground tab profiles do not outperform the climatology profiles, but are approximately equal. This is due to the stable and consistent nature of the tropical

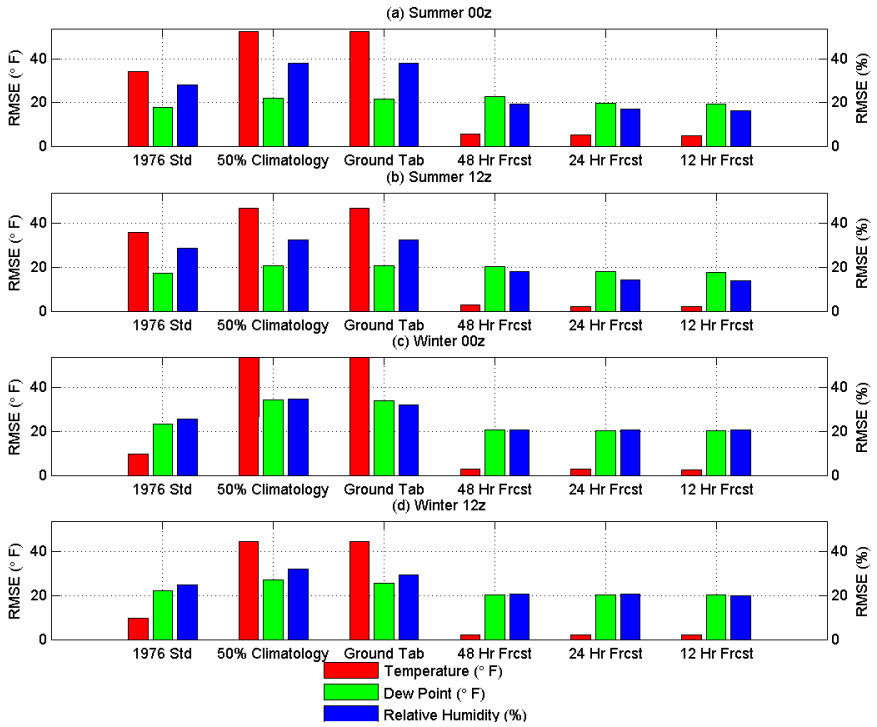

Figure 24. Kuwait temperature, dew point, and relative humidity vertical profile mean RMSE from 0 to approximately 30,000 m for (a) Summer 00z, (b) Summer 12z, (c) Winter 00z, and (d) Winter 12z. Atmospheres considered include the 1976 U.S. Standard Atmosphere, 50th percentile ExPERT climatology, HELTDA ground tab, and 48, 24, and 12 hour GFS forecast derived atmospheres.

climate on fair weather days. Wind speed errors in the boundary layer are nearly equal for all atmospheric characterization methods for all times and seasons as seen in Figure 27. Wind speed direction is better predicted in the winter and GFS forecasts do a far better job of making such predictions.

Considering the full atmosphere, all errors except for the 1976 U.S. Standard Atmosphere are increased as expected. In some cases, relative humidity error is greater for the forecasts compared to the climatology and ground tab as is seen in the 00z cases. In these instances, the ground tab characterization outperforms the forecasts in relative humidity error estimation. Magnitudes of wind speed and wind direction error increase, yet the forecasts continue to provide better predictive capability.

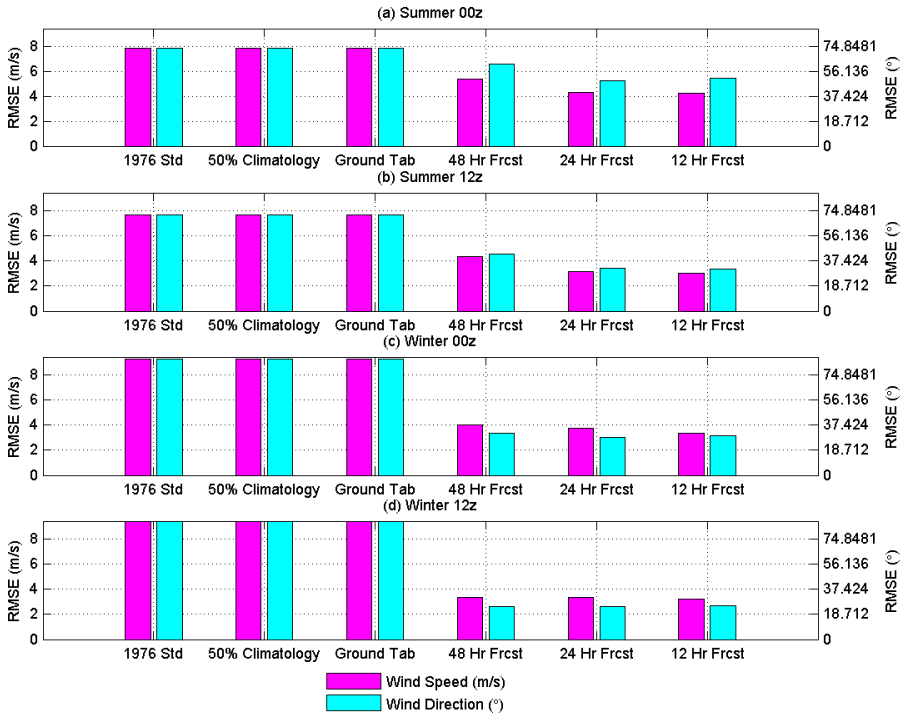

Figure 25. Kuwait wind speed and wind direction vertical profile mean RMSE from 0 to approximately 30,000 m for (a) Summer 00z, (b) Summer 12z, (c) Winter 00z, and (d) Winter 12z. Atmospheres considered include the 1976 U.S. Standard Atmosphere, 50th percentile ExPERT climatology, HELTDA ground tab, and 48, 24, and 12 hour GFS forecast derived atmospheres.

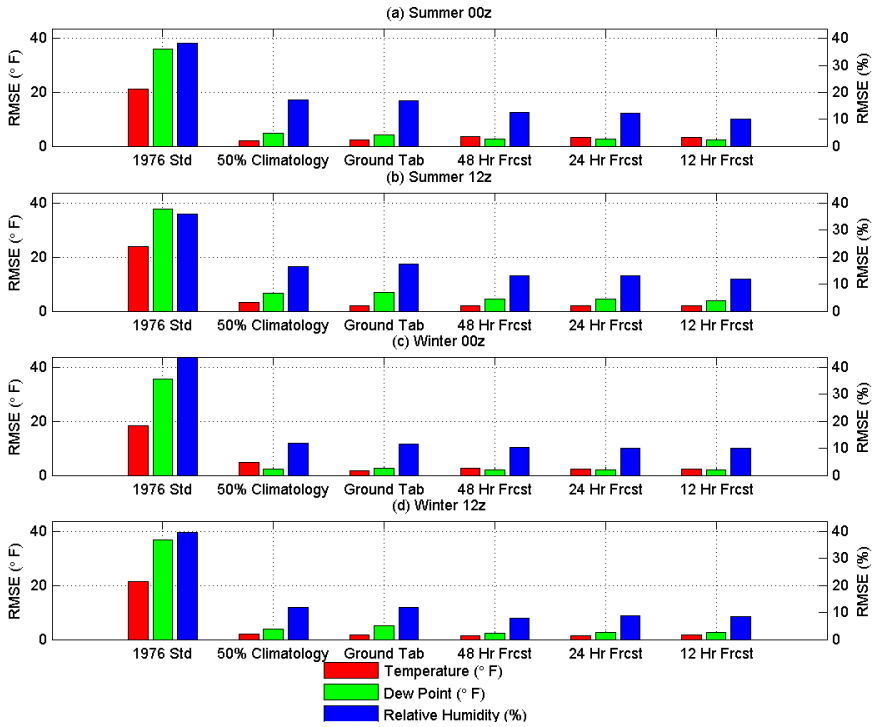

Figure 26. Brunei temperature, dew point, and relative humidity vertical profile mean RMSE in the boundary layer for (a) Summer 00z, (b) Summer 12z, (c) Winter 00z, and (d) Winter 12z. Atmospheres considered include the 1976 U.S. Standard Atmosphere, 50th percentile ExPERT climatology, HELTDA ground tab, and 48, 24, and 12 hour GFS forecast derived atmospheres.

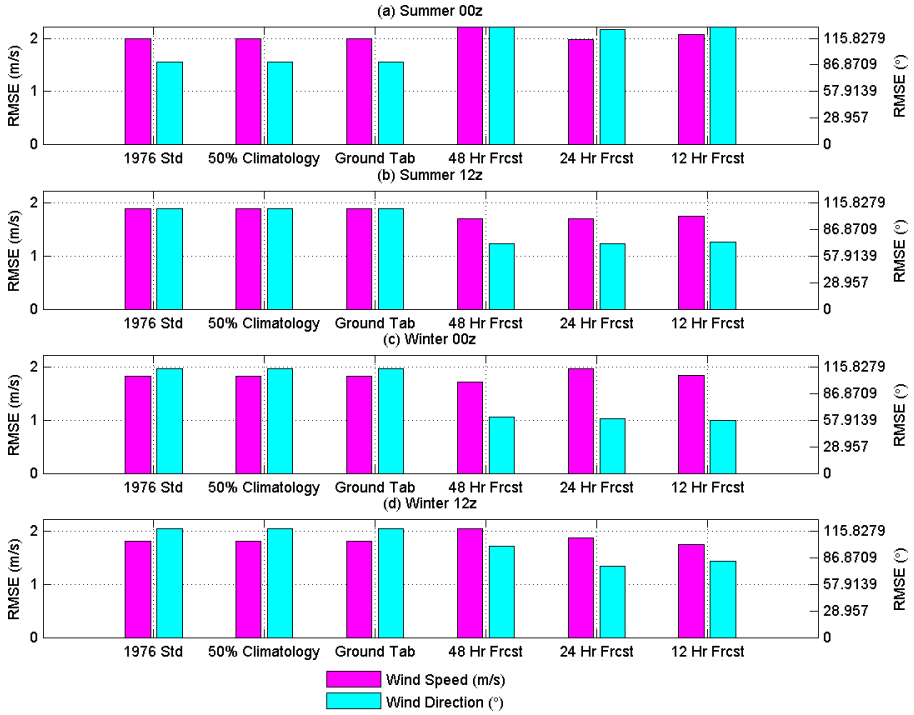

Figure 27. Brunei wind speed and wind direction vertical profile mean RMSE in the boundary layer for (a) Summer 00z, (b) Summer 12z, (c) Winter 00z, and (d) Winter 12z. Atmospheres considered include the 1976 U.S. Standard Atmosphere, 50th percentile ExPERT climatology, HELTDA ground tab, and 48, 24, and 12 hour GFS forecast derived atmospheres.

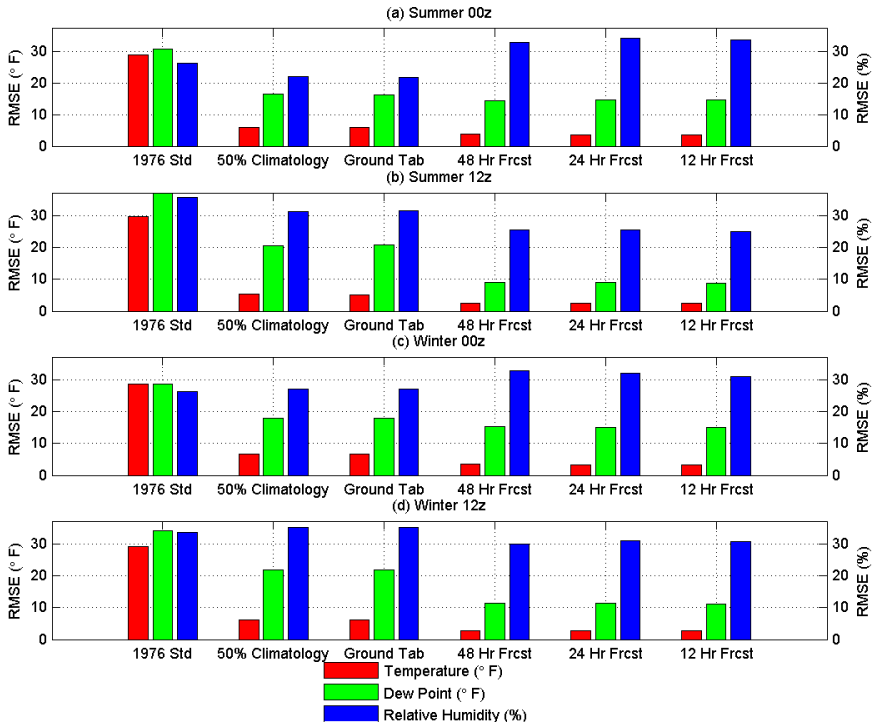

Figure 28. Brunei temperature, dew point, and relative humidity vertical profile mean RMSE from 0 to approximately 30,000 m for (a) Summer 00z, (b) Summer 12z, (c) Winter 00z, and (d) Winter 12z. Atmospheres considered include the 1976 U.S. Standard Atmosphere, 50th percentile ExPERT climatology, HELTDA ground tab, and 48, 24, and 12 hour GFS forecast derived atmospheres.

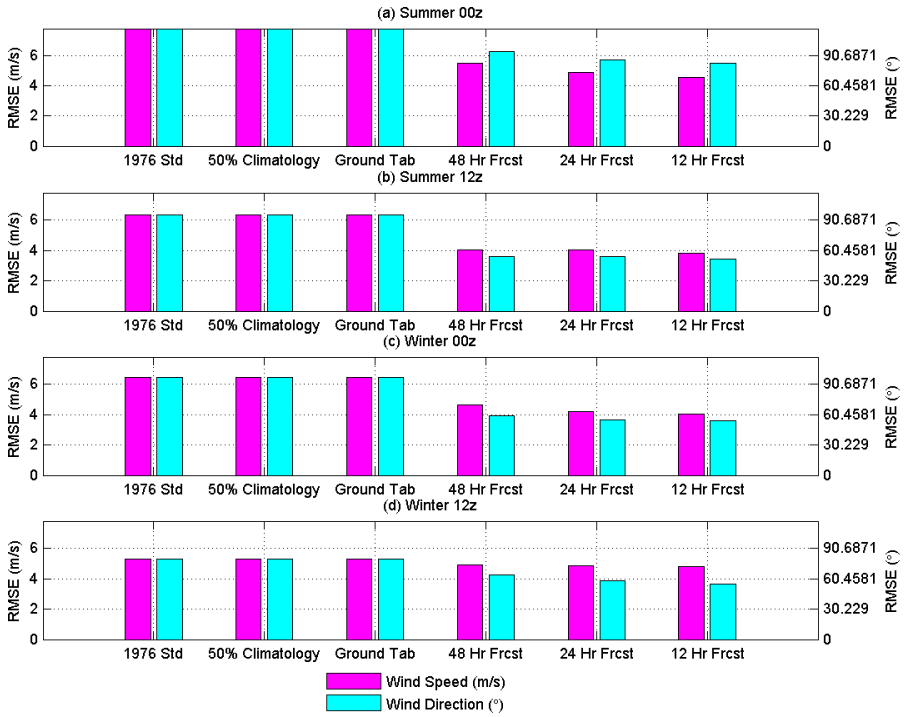

Figure 29. Brunei wind speed and wind direction vertical profile mean RMSE from 0 to approximately 30,000 m for (a) Summer 00z, (b) Summer 12z, (c) Winter 00z, and (d) Winter 12z. Atmospheres considered include the 1976 U.S. Standard Atmosphere, 50th percentile ExPERT climatology, HELTDA ground tab, and 48, 24, and 12 hour GFS forecast derived atmospheres.

Predicted Dwell Time

Operational scenarios were simulated to gain an understanding of the effects of the various atmospheric characterization methods on predicted engagement dwell time. Previously described atmospheric soundings were used as the control data for quantifying error. For operational users, required laser dwell time is the most relevant measure of weapon system performance. HELTDA incorporates multiple attenuation mechanisms along the integrated beam path and utilizes PDF's: thus providing outputs that are correlated with a probability. Typically, a 90% P_k or P_e is considered the standard success criteria for planning purposes. For this research, a 90% threshold was employed for all simulations and all reported dwell times are in reference to this level. Both 1.045 μm and 1.31525 μm wavelengths were considered to demonstrate the effect of wavelength on relative performance between characterization methods. The 1.045 μm wavelength is representative of the proposed ELLA laser system and is directly relevant to the user and mission engagement planning. The results from this simulation contained significant deviations from the hypothesis; therefore the simulation was repeated with a 1.31525 μm wavelength, corresponding to a COIL laser system. The target hardness was reduced from 1×10^5 J/cm^2 for a 5×5 cm^2 susceptible region or *bucket* to 1×10^4 J/cm^2 due to the extended computational simulation time (associated with increased absorption attenuation effects and an extremely hard target) required to use the higher value and beam quality was changed to $m^2 = 1$ as appropriate for a COIL laser. Therefore, it is important to note that dwell time between wavelengths can not be directly compared.

The ELLA engagement is likely to be more relevant and applicable to future weapons systems users; however, the 1.31525 μm wavelength results are still of significant importance. While current laser system development is primarily focused on the *clean* SSL wavelength that minimize molecular absorption due to water as seen

in Figure 6, current and legacy systems operate at 1.31525 μm specifically, as well as at other wavelengths with similar properties. Additionally, COIL systems produce the best possible beam quality currently available and beam quality has been shown to be a significant factor in the design of many different systems. While strategic planning focuses on using technology currently in development, these systems represent the current state of laser weapons systems. Furthermore, even though attenuation due to aerosol absorption is typically at least an order or magnitude less than aerosol scattering effects, the optical properties and loss mechanism are not well understood or characterized. It is feasible that aerosols absorb in a similar manner as atmospheric gases. Thus the similarities and differences between the two can serve to confirm the operational need for innovation in laser system development as well as the need to gain a better understanding of the fundamental loss mechanisms in play.

RMSE analysis of the various atmospheric profiles was accomplished by comparing the predicted dwell time to the control data. The RMSE quantizes the error in each characterization method. Each season (summer and winter) and time of day (00z and 12z) contained multiple cases for which the RMSE in the dwell time was evaluated. The results are reported by season and time of day for each location.

Inherently, some uncertainty is introduced into the results due to the interpolation schemes used to create the vertical profiles in the software. In an effort to achieve consistent results despite the uncertainty due to interpolation, the climatological and ground tab profiles were generated externally from the HELTDA software and then interpolated to the control sounding levels for each case. When calculated internally in the software, the profile is generated for the altitude levels specific to the target-to-platform geometry. The number of levels is fixed and does not pose an issue unless the different target-to-platform geometries are compared. By reading in a vertical profile generated by the same method and equations but for different

altitude levels (consistent with sounding profiles), the fixed number of altitude levels forces a less dense altitude vector between the target and platform. Consequently, the vertical profile must be interpolated to the more dense vector created by the software. Through linear interpolation, slightly different profiles are generated for the resultant profile. By using externally generated profiles for all calculations the results remain consistent with each other and are sufficiently satisfactory for the verification nature of this research. A software validation effort would necessitate these methods be reevaluated. Tabular data are included in Appendix A in Table 10 through Table 15.

WPAFB.

Dwell time RMSE for the ELLA and COIL engagement scenarios in the boundary layer at WPAFB are depicted in Figure 30. It was hypothesized that atmospheric characterization methods corresponding to improved prediction with smaller RMSE of vertical profile meteorological parameters (temperature, dew point, relative humidity, wind speed, and wind direction) would yield improved dwell time predictions. The left column of Figure 30 shows that in some cases, the exact opposite is true at the 1.045 μm wavelength. The 1976 U.S. Standard Atmosphere yields a wide range of dwell time errors depending on season and time of day. This is expected as the same trend was visible in the vertical profile simulations due to the rigid characterization methods of the standard atmosphere that only vary with altitude and not location, time, or season. Despite a better average characterization of all atmospheric parameters in the vertical profile, the ground tab profile fails to outperform the climatology profile for all but the winter 00z case. Note the large increase in errors between the summer 00z and summer 12z case. This is most likely due to the shorter boundary layer for the 12z time coupled with vertical motion caused by a warming atmosphere.

The GFS forecasts outperform the 1976 U.S. Standard Atmosphere as well as the

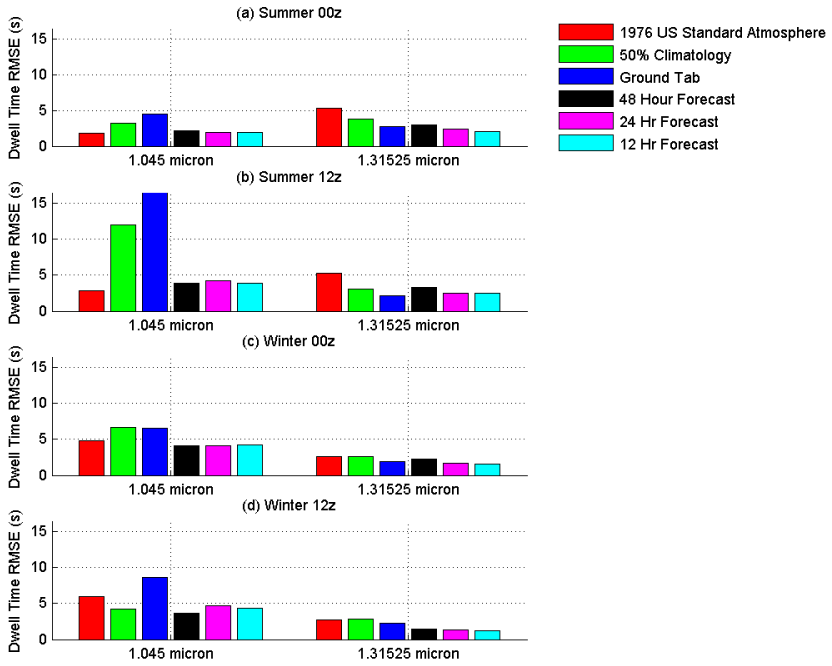

Figure 30. WPAFB dwell time RMSE for a 1.045 μm (left) and 1.31525 μm (right) engagement from top of the boundary layer to the surface for (a) Summer 00z, (b) Summer 12z, (c) Winter 00z, and (d) Winter 12z. Atmospheres considered include the 1976 U.S. Standard Atmosphere, 50th percentile ExPERT climatology, HELTDA ground tab, and 48, 24, and 12 hour GFS forecast derived atmospheres. Note target hardness differs for the two wavelength simulations.

climatology and the ground tab for all seasons and time of day. The improvement between the 48 and 24 hour forecast is minimal for all cases and the 48 hour forecast even performs a tenth of a second better for the 12z time. The forecast advantage over climatology ranges from 0.6 to 8.2 seconds. This suggests that atmospheric characterization through the use of forecast data can on average provide a better prediction of dwell time requirements. Depending on the weapons system parameters, this can make a significant difference in the number of targets engaged, as well as in the methods and tactics employed in such an engagement. Note that the specific dwell times are dependent on scenario.

The primary attenuation factor at 1.045 μm wavelength is aerosol scattering.

Molecular absorption in the atmosphere is primarily attributed to water and the 1.045 μm line is considered a *clean* line with minimal molecular effects. Aerosol scattering is modeled as a function of aerosol size. As noted in Chapter 2, HELTDA assumes Mie scattering for aerosols and the extinction coefficient is a non-linear function of wavelength and aerosol size. Aerosol size distributions in this simulation are taken from the GADS database and modified for varying relative humidity with height in a non-linear manner as seen by

$$\mathrm{Log}r\left(a_w\right) = \pm\left[-\ln\left(\frac{\partial N}{\partial(\mathrm{Log}r)}\sqrt{2\pi}\mathrm{Log}\sigma\right) * 2(\mathrm{Log}\sigma)^2\right]^{1/2} + \mathrm{Log}r_M \qquad (22)$$

where $r(a_w)$ is the humidity altered radius, σ is the standard deviation of the dry aerosols distribution, r_M is the modal radius for the aerosol distribution at the relative humidity of interest, and r is the dry aerosol radius [9]. Obtaining relative humidity is accomplished through a non-linear process as well. While dew point is a direct measure of the amount of water vapor in the atmosphere, relative humidity is dependent on temperature and saturation vapor pressure as seen in Equation 20 and Equation 21.

The unexpected results for the climatology and ground tab profiles at this wavelength can be explained by the combination of these non-linear processes in a multivariable problem. While each atmospheric parameter examined in the vertical profile was shown to have less error for the ground tab profiles, the non-linear combination results in an larger dwell time error. For lasers that operate at high water absorption lines, such as 1.31525 μm, these factors do not have nearly as significant an influence. It is important to note that the control data for this simulation do not include any aerosol size data. All atmospheres are simulated assuming the GADS database for aerosol distributions. While this provides a realistic estimate of aerosols number densities and size distributions, it does not represent actual conditions. The inclusion of these data acquired in-situ would most likely change the control results to some degree.

While these data were not available for analysis, inclusion could prove significant in performance assessments.

For the COIL engagements seen on the right side of Figure 30, the non-linear effects do not affect the dwell time errors in the same manner. This is due to the molecular absorption at 1.31525 μm. Aerosol extinction continues to be larger in magnitude in comparison to molecular absorption; however, molecular absorption induces thermal blooming which produces a larger effect in dwell time. The effects are quantized in the thermal blooming distortion number according to Equation 10. Thermal blooming is directly affected by the amount of water vapor in the atmosphere which is directly measured by dew point; therefore a better prediction of water vapor leads to a better prediction in dwell time when thermal blooming is the dominate attenuation mechanism. For WPAFB, the ground tab outperforms the climatology for all times and seasons in dew point prediction and dwell time prediction for the COIL scenario. Note that during the summer the standard atmosphere is the worst characterization but in the winter it is nearly equivalent to the climatology.

Figure 31 shows the dwell time results for both ELLA and COIL scenarios with the platform altitude set at 3,000 m. Dwell time RMSE of the various atmospheric characterizations maintain the same relationships between each other in terms of relative performance. It is not intuitive, yet the overall dwell time error in the climatology and ground tab atmospheres for all times and seasons decrease as altitude is increased from the boundary layer to 3000 m. This is attributed to the fact that the aerosol size increases with relative humidity and relative humidity increases with height in both of the profiles in accordance with the temperature and dew point lapse rates used in HELTDA calculations. Since scattering is the dominant attenuation factor for the 1.045 μm wavelength, increased aerosol size results in greater scattering effects. These effects increase with altitude to the top of the boundary layer, effectively

create a spike in attenuation effects near the top of the layer. The boundary layer engagement scenario propagates through the boundary layer at more shallow angles than the 3,000 m scenario, thus increasing the scattering effects for the integrated beam path since a larger portion of the beam passes through this spike. Dwell time error decreases for forecast characterizations for all cases except summer 00z. This is likely due to the inability of the forecast model to predict rapid changes in relative humidity in the boundary layer. It may also be due to small scale thunderstorms and vertical convective motion. These local systems, which most often occur in the late afternoon, can drastically change vertical profiles and account for worse performance for the GFS model when compared to other times and seasons.

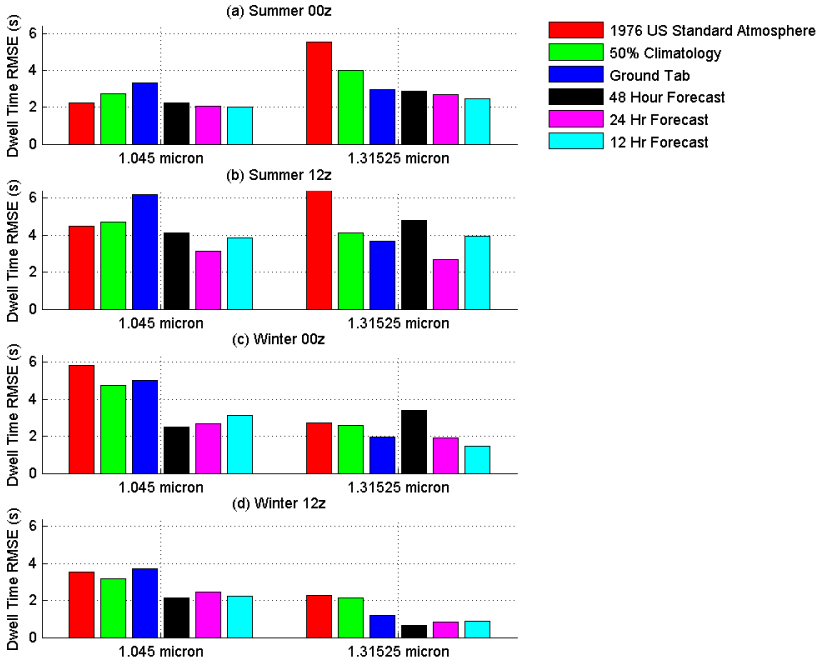

Figure 31. WPAFB dwell time RMSE for a 1.045 μm (left) and 1.31525 μm (right) engagement from 3,000 m to the surface for (a) Summer 00z, (b) Summer 12z, (c) Winter 00z, and (d) Winter 12z. Atmospheres considered include the 1976 U.S. Standard Atmosphere, 50th percentile ExPERT climatology, HELTDA ground tab, and 48, 24, and 12 hour GFS forecast derived atmospheres. Note target hardness differs for the two wavelength simulations.

For COIL engagements, the dwell time errors generally increase with increasing altitude above the boundary layer. This is due to the increased path length of a laser engagement with attenuation primarily a consequence of thermal blooming, opposed to aerosol scattering. Note that the forecast values vary significantly. While the ground tab outperforms climatology for all times and seasons, it also outperforms forecast data for numerous scenarios. For COIL air-to-ground engagemments initiated above the boundary layer, season and time of day dictate forecast characterization method performance and utility to the warfighter.

Kuwait.

Figure 32 shows the results for the boundary layer dwell time simulation in Kuwait. The results are similar to the WPAFB results in terms of relative performance between each characterization method. The 1976 U.S. Standard Atmosphere's performance is varied as expected, but far more consistent for the COIL engagement. For winter 00z it outperforms the climatology. Note that for the ELLA engagement, the GFS forecast are more accurate during the 12z time periods. For both wavelengths, the 48 hour forecast performs worse than climatology and the ground tab in the summer. This is most noticeable in the 00z time period, which is most likely due to shallow nature of the boundary in the early morning hours. The ELLA scenario shows a nearly equal RMSE for climatology and the ground tab for all cases except winter 00z, where the ground tab outperforms the climatology. This was not the case for WPAFB, and is most likely due to minimal variance in the weather for this region, effectively generating the same profiles for climatology and the ground tab a majority of the time. For the COIL wavelength, the ground tab outperforms the climatology for all seasons and times but the gain in predictive performance is minimal due to the relatively small amount of water vapor in the atmosphere. This results in reduced

thermal blooming and effectively negates much of the potential ground tab advantage.

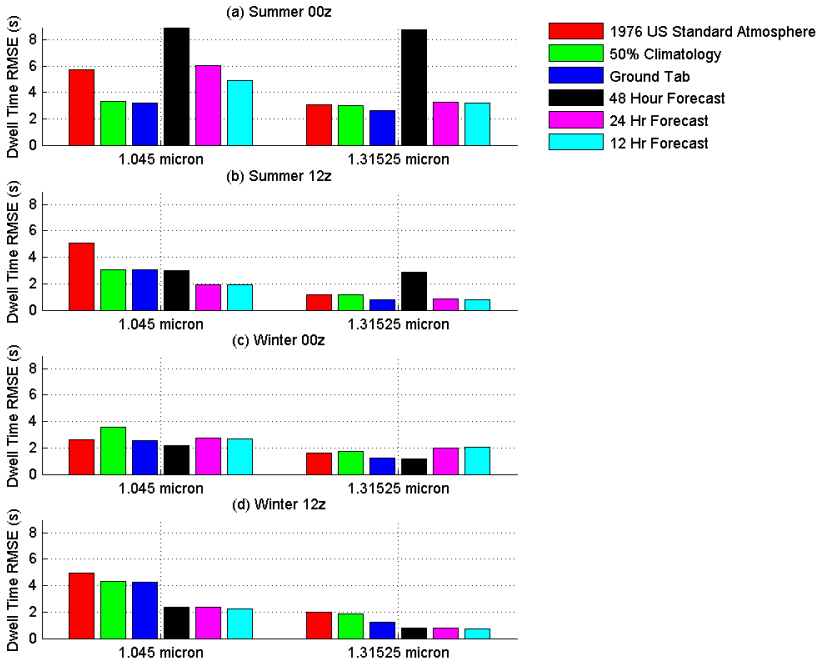

Figure 32. Kuwait dwell time RMSE for a 1.045 μm (left) and 1.31525 μm (right) engagement from top of the boundary layer to the surface for (a) Summer 00z, (b) Summer 12z, (c) Winter 00z, and (d) Winter 12z. Atmospheres considered include the 1976 U.S. Standard Atmosphere, 50th percentile ExPERT climatology, HELTDA ground tab, and 48, 24, and 12 hour GFS forecast derived atmospheres. Note target hardness differs for the two wavelength simulations.

Figure 33 depicts the results from the 3,000 m altitude scenario for Kuwait. At the ELLA wavelength for the 12z times, the forecasts perform better than climatology and ground tab profiles at this altitude, unlike their relative performance in the boundary layer. The difference between climatology and ground tab profiles becomes even smaller due to the minimal variation in aerosol sizes. For all ELLA cases the RMSE in climatology and ground tab profiles is reduced, similar to the effect seen at WPAFB, due to a more vertical slant path. Consistent with WPAFB results, COIL wavelength dwell time errors for climatology and the ground tab generally increase with altitude.

For all cases at both wavelengths, the often high RMSE in the 48 hour forecast in the boundary layer is reduced for the higher altitude engagement.

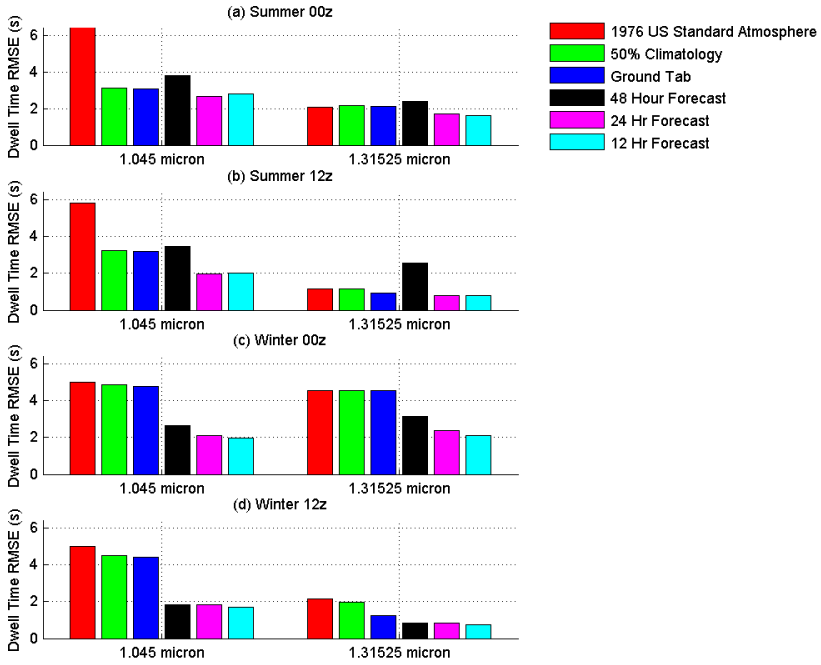

Figure 33. Kuwait dwell time RMSE for a 1.045 μm (left) and 1.31525 μm (right) engagement from 3,000 m to the surface for (a) Summer 00z, (b) Summer 12z, (c) Winter 00z, and (d) Winter 12z. Atmospheres considered include the 1976 U.S. Standard Atmosphere, 50th percentile ExPERT climatology, HELTDA ground tab, and 48, 24, and 12 hour GFS forecast derived atmospheres. Note target hardness differs for the two wavelength simulations.

Brunei.

Dwell time results for Brunei, seen in Figure 34, depict a significant advantage in using GFS forecasts for all seasons and times of day for an ELLA engagement scenario in the boundary layer. While forecasts provide a clear cut operational advantage, the ground tab characterization only provides an advantage over climatology in the summer 00z case. Similar to WPAFB scenario, the ground tab profile's prediction error is worse for all other cases. Due to the high relative humidity of the equatorial tropical

environment, aerosol sizes grow relatively little with increasing altitude, contrary to what is predicted using the surface values.

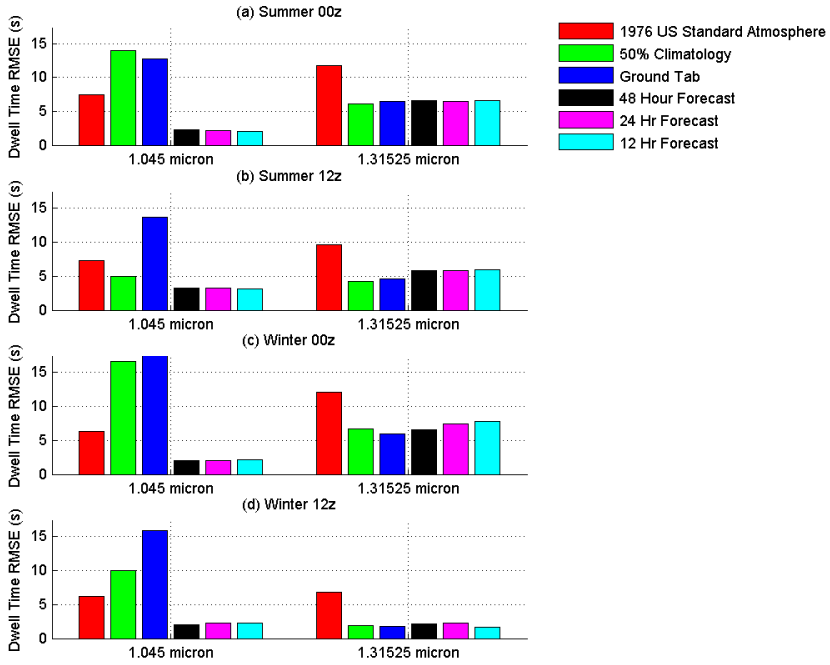

Figure 34. Brunei dwell time RMSE for a 1.045 μm (left) and 1.31525 μm (right) engagement from top of the boundary layer to the surface for (a) Summer 00z, (b) Summer 12z, (c) Winter 00z, and (d) Winter 12z. Atmospheres considered include the 1976 U.S. Standard Atmosphere, 50th percentile ExPERT climatology, HELTDA ground tab, and 48, 24, and 12 hour GFS forecast derived atmospheres. Note target hardness differs for the two wavelength simulations.

It is interesting to note that for all times and seasons, the error associated with the GFS forecasts is greater than the ground tab for the COIL scenario. This is not unexpected as the dew point characterization in the vertical profile was not significantly improved for the GFS forecasts. At 1.31525 μm there is a clear operational advantage to using the ground tab or climatology versus other methods. Consistent with WPAFB and Kuwait locations, there is little difference in RMSE values between the 48, 24, and 12, hour GFS forecasts for either wavelength. For COIL engagements, dwell time

errors remain consistent between morning and evening for the summer season, most likely due to relatively constant amounts of water vapor attributed to the equatorial tropical climate.

Figure 35 shows the dwell time RMSE for Brunei dwell time simulations at altitude. It is interesting to note the increased error in the 1976 U.S. Standard Atmosphere error between the boundary layer and altitude engagement for the 1.045 μm wavelength opposed to the relatively small change for the 1.31525 μm wavelength. For the COIL engagements in the boundary layer, the GFS forecast did not outperform the climatology or ground tab. At altitude, the forecasts do outperform climatology and the ground tab for the winter season.

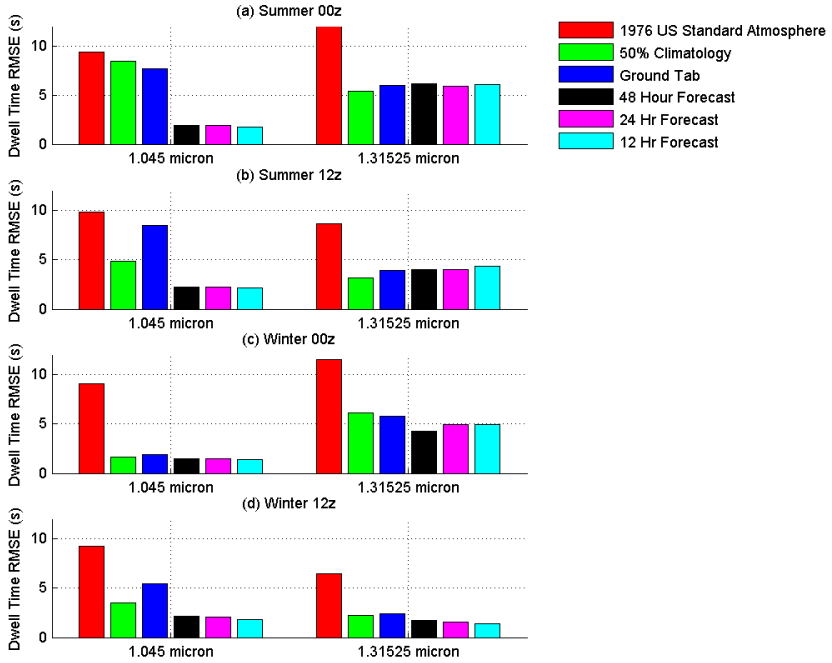

Figure 35. Brunei dwell time RMSE for a 1.045 μm (left) and 1.31525 μm (right) engagement from 3,000 m to the surface for (a) Summer 00z, (b) Summer 12z, (c) Winter 00z, and (d) Winter 12z. Atmospheres considered include the 1976 U.S. Standard Atmosphere, 50th percentile ExPERT climatology, HELTDA ground tab, and 48, 24, and 12 hour GFS forecast derived atmospheres. Note target hardness differs for the two wavelength simulations.

In regards to the ELLA scenario, the ground tab performance at altitude is greatly enhanced relative to the boundary layer engagement for all times and seasons. This is particularly obvious in the winter months, and is most likely due to aerosol sizes increasing with height during these times. Thus, the engagement at altitude traverses larger aerosol size distributions inducing increased scattering effects and the result is better predicted by the ground tab. This is supported by the relative performance between atmospheric characterizations at the COIL wavelength, similar to mid-latitude sites such as WPAFB.

Altitude vs Dwell Time

Potential HEL weapons operators have repeatedly stressed the need to optimize engagement altitude for various air to ground missions prior to target prosecution. The ability to understand the potential impact to a mission when engaging a target at or from various altitudes enables the warfighter to weigh the risks, benefits, and trades involved with flying different flight profiles. While the impact in terms of dwell time required often appears minimal, the operational impacts can be tremendous.

Increasing Slant Path.

As engagement slant range is increased, as seen in Figure 16, dwell time is expected to increase, consistent with a longer platform to target geometry. In general, this trend is true as seen in Figure 36, an engagement at WPAFB on January 5, 2011 at 00z as described in Chapter 3. As altitude increases towards a 6,000 m slant range, dwell time increases approximately 20-25 seconds for all atmospheric profiles studied. Yet, there is a distinct trend seen in the sounding and forecast profiles. As altitude increases dwell time decreases initially at altitude levels below the boundary layer despite the increased range between platform and target. The boundary layer for this

particular case is approximately 1200 m. Above the boundary layer, the dwell time increases as expected. This is attributed to the varying nature of the boundary layer with respect to altitude. The increased scattering effects which occur in the upper portion of the boundary layer due to increased aerosol size resulting from increased relative humidity in the boundary layer are modulated by the angle at which the laser propagates through the boundary layer. At more vertical angles, less of the total beam length propagates through the upper boundary layer and the attenuation effects are mitigated relative to a horizontal engagement. The trade-off between the increased path length and the reduced scattering effects create a *knee* in the curve which corresponds to the optimal altitude to reduce dwell time.

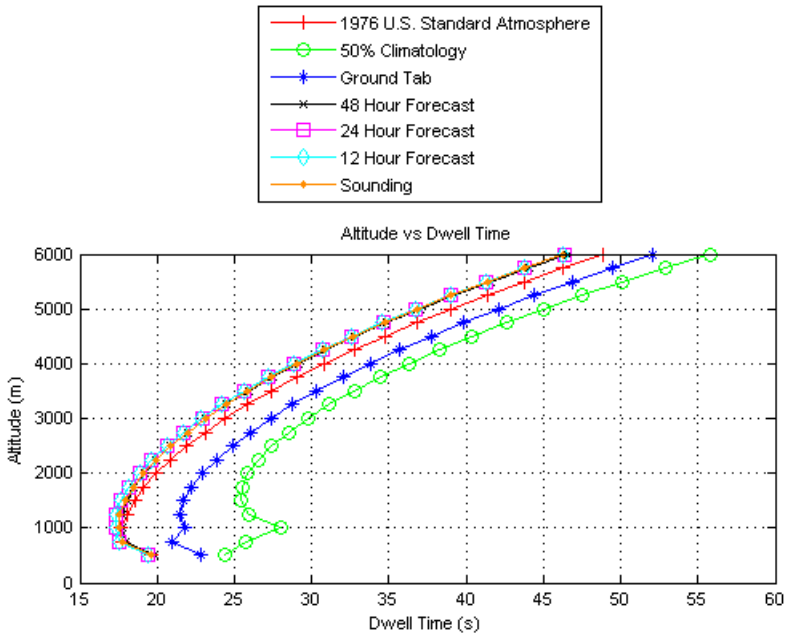

Figure 36. Altitude vs dwell time for a 1.045 μm engagement with a varying slant path for WPAFB on 5 January, 2011 at 00z. Platform altitude is varied from 500 m to 6,000 m in 250 m increments. Target altitude remains fixed at 1 m. Atmospheres considered include the 1976 U.S. Standard Atmosphere, 50th percentile ExPERT climatology, HELTDA ground tab, and 48, 24, and 12 hour GFS forecast derived atmospheres.

The significant differences between the climatology and sounding results can be

explained by significant differences in dew point and relative humidity values in the boundary layer. The large discontinuity in dwell times at 1,000 m is explained by the HELTDA's switch in climatological databases between the boundary layer and the upper atmosphere which occurs at 1,000 m for Winter evening conditions. The same effect is seen in the ground tab profile, but to a lesser extent due to a better characterization of surface values for temperature, dew point, and pressure. It is clear from Figure 36 that the ground tab outperforms the climatology for all levels on 5 January, 2011. However, the forecast profiles provide the greatest operational advantage as they allow the user the greatest accuracy in evaluating performance as a function of altitude. For this case, the standard atmosphere provides an accurate assessment, especially in the boundary layer. This is not true for all cases, particularly at locations outside the United States. If mission altitude is not dictated, a clear advantage can be gained by operating at levels as close to the top of the boundary layer as possible. In situ aerosol distribution data may serve to modify the extent of this advantage or remove it completely. Determining actual boundary layer height is best determined by using forecast data. With charts such as Figure 36, the user can evaluate the operational trades involved with varying altitudes and plan their mission accordingly considering both risk and dwell time factors.

Constant Slant Path.

Figure 37 illustrates the effects of altitude on dwell time for a constant slant path scenario as described in Chapter 3 and seen in Figure 17 for 00z at WPAFB on January 5, 2011. Platform and target altitude were initially set at 3,000 m and 1 m respectively and increased by 125 m increments over a 3,000 m range. If the atmosphere was uniform throughout, one would expect a constant dwell time at all altitudes. One would expect a constant decrease in dwell time if atmospheric effects

decreased linearly with height. Neither of these trends is depicted in Figure 37.

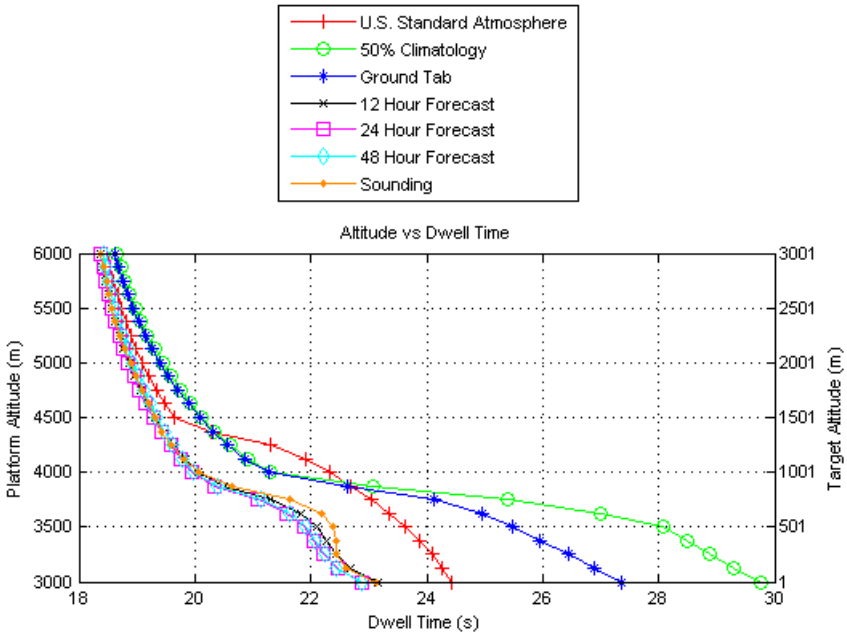

Figure 37. Altitude vs dwell time for a 1.045 μm engagement with a constant slant path for WPAFB on 5 January, 2011 at 00z. Initial platform and target altitudes are set at 3,000 m and 1 m respectively. Platform and target are raised together in 125 m increments. Atmospheres considered include the 1976 U.S. Standard Atmosphere, 50th percentile ExPERT climatology, HELTDA ground tab, and 48, 24, and 12 hour GFS forecast derived atmospheres.

For WPAFB at 00z, the boundary layer at WPAFB is predicted and set by the HELTDA at 1,000 m. As the slant path is incrementally raised through the boundary layer by simultaneously raising platform and target altitude, dwell time decreases at a non-uniform rate for all atmospheric characterizations. The rate of change in dwell time with respect to altitude, increases as the target nears the top of the boundary layer. This is clearly evident in the climatology profile and indicates the non-uniform nature of the boundary layer effects. At lower levels, the beam travels through the entirety of the previously described spike in the vertical aerosol size distribution, thus experiencing a large scattering effect. As the target moves towards the top of

the boundary layer, the beam path travels through less of the upper portion of the atmosphere and the net scattering effect is reduced, thus reducing dwell time. The incremental change in altitude is constant while the dwell time rate of change is not, indicating an exponential effect. Note that the sounding profile predicts the same trend in performance, yet the shape and rate of change is different due to actual temperature and dew point inputs and a boundary layer height that does not match the HELTDA assumed 1,000 m. It is closer to 1,200 m as estimated by the temperature and dew point profile seen in Figure 38. If it were possible to determine the boundary layer height prior to employing the weapon system, one would expected increased performance from the climatology and ground tab profile without temperature and dew point inputs from every level. Unfortunately, it is impossible to determine the actual boundary layer height without some type of in-situ measurement or observation; thus forecasts remain the best characterization method for predictions.

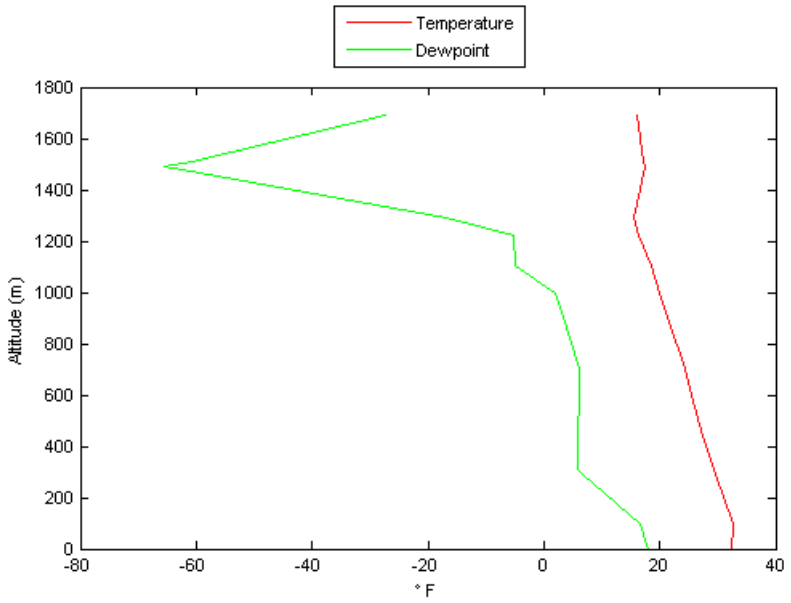

Figure 38. WPAFB boundary layer temperature and dew point profile for 5 January, 2011 at 00z.

The results depicted in Figure 37 have potential operational significance. The increased dwell times noted below the top of the boundary layer affect mission planning for offensive purposes in addition to mission planning for possible defensive countermeasures. Targets near the surface require the longest dwell time as expected. However, targets located below the upper portion of the boundary layer require a significant increase in dwell time in comparison to those located only a few hundred meters above. Additionally, as the vertical angle of the slant path is increased, the corresponding dwell time decreases due to the reduced scattering effects of a more vertical engagement as seen in Figure 36. Thus, for a target being engaged from above, required dwell time for failure is increased by locating the target just below the top of the boundary layer and by creating a more horizontal engagement geometry. These effects can be exploited to create aircraft protection countermeasures in the form of flight profiles. By creating a flight profile below the boundary layer and with a sufficient horizontal standoff distance from the target, the atmosphere itself is employed to decrease the effects of a HEL engagement. Furthermore, when considering an engagement from the surface-to-air, the same atmospheric effects are at work. Therefore, for platforms such as unmanned aerial vehicles (UAV), the optimal altitude for inherent laser protection is a function of boundary layer height. By flying completely above the top of the boundary layer and maintaining an extreme angle from platform to target, the effects of a ground based system are potentially limited, particularly in an aerosol rich environment in which relative humidity increases with altitude.

The standard atmosphere predicts a more accurate required dwell time than climatology and the ground tab in the lower atmosphere and the upper atmosphere, but not in between. This is unlike the predictions from all other characterizations whose relative performance remains constant regardless of altitude. While this appears

favorable for mission planning engagements in the boundary layer, it is important to note that this is due to the fact that the actual conditions happened to match a static characterization. This does not hold true for all scenarios and is even less likely to succeed in different geographic locations. The differences between the ground tab and climatology dwell time values are the result of different temperature, dew point, pressure, and relative humidity. Above the boundary layer, these values are equal for both profiles, thus the equivalent dwell time predictions. The forecast profiles produce simulations much closer to the sounding profile, consistent with the results of the dwell time study. The relative performance of the ground tab and climatology are also consistent with those results. One feature of note in Figure 38 is the slight temperature inversion at the surface. The ground tab is unable to pick up this very small feature, yet it is possible that if a *ground observation* from a slightly higher altitude were used, the ground tab profile may yield more favorable results. At high altitudes, the dwell time differences between profiles are severely limited, confirming that high altitude engagements are far less susceptible to atmospheric variations. Overall, the forecast profiles provide a much more accurate prediction of boundary layer effects which not only aid in offensive mission planning, but provide a natural countermeasure to enemy combatant HEL weapons when exploited correctly.

Figure 39 depicts the same scenario as Figure 37 where wind is eliminated as a variable through the use of climatological winds for all atmospheres. The relative performances of the standard, climatology, and ground tab atmospheres are all significantly altered. The climatology and ground tab perform much better compared to Figure 37 and the standard atmosphere performs slightly worse, but under predicts rather than over predicting dwell time. This highlights the importance of characterizing wind profiles in addition to temperature, dew point, and relative humidity for accurate engagement assessments, particularly in the boundary layer with a high power laser

(150 kW).

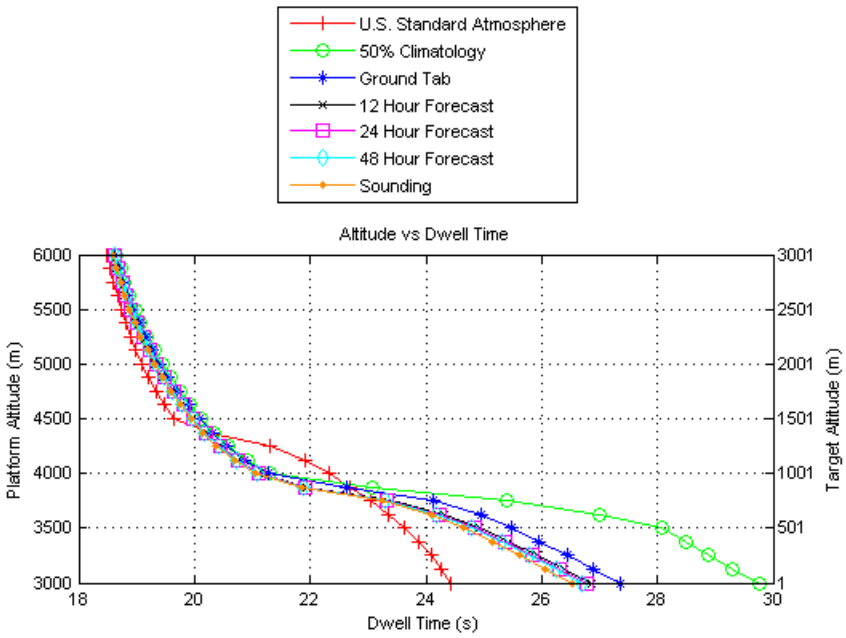

Figure 39. Altitude vs dwell time for a 1.045 μm engagement with a constant slant path for WPAFB on 5 January, 2011 at 00z. All atmospheres are characterized with climatological winds. Initial platform and target altitudes are set at 3,000 m and 1 m respectively. Platform and target are raised together in 125 m increments. Atmospheres considered include the 1976 U.S. Standard Atmosphere, 50th percentile ExPERT climatology, HELTDA ground tab, and 48, 24, and 12 hour GFS forecast derived atmospheres.

Figure 40 depicts the effects attributed to urban environments, the same engagement scenario is used, only with urban aerosols opposed to those defined by the GADS database and target hardness reduced to 1×10^3 J/cm^2 due to extended model run times as the result of an extremely hard target. Wind profiles have not been altered. By specifying urban aerosol composition, aerosols are primarily defined as soot particles which are generally hygroscopic and tend to absorb in the same manner as the molecular absorption at the 1.31525 μm wavelength. In this simulation, the ground tab profile predicts dwell time values much closer relative to the sounding and forecast profiles than in Figure 37. This is consistent with the dwell time results for

the 1.31525 μm wavelength previously discussed. This further confirms the utility of the ground tab characterization method at absorbing wavelengths and illustrates the potential complications for missions in urban environments where factors such as heavy soot or urban aerosols can dramatically alter the attenuation effects over a small region. The HELTDA provides a means to both predict and optimize these varying conditions to ensure success on the battlefield.

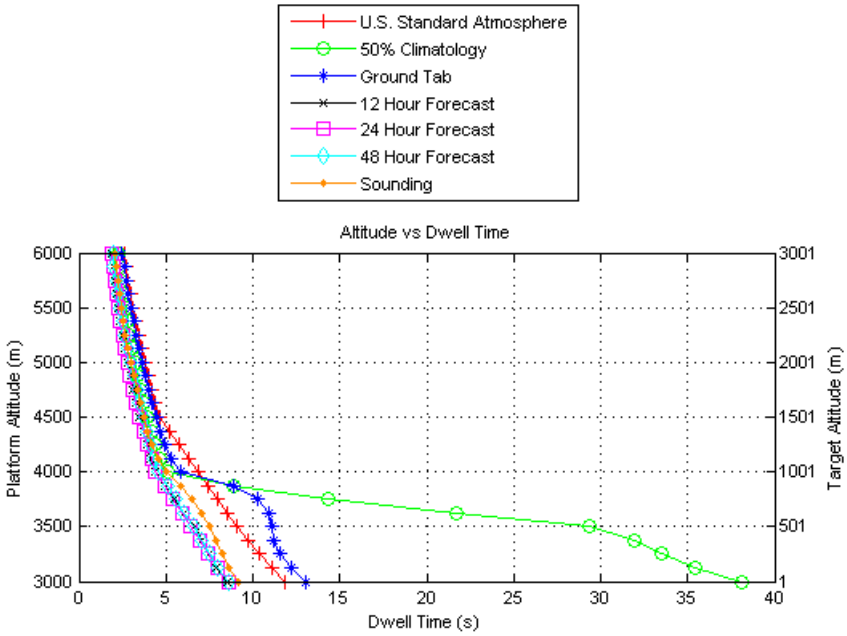

Figure 40. Altitude vs dwell time for a 1.045 μm engagement with a constant slant path for WPAFB on 5 January, 2011 at 00z. Aerosols are defined as urban aerosols primarily composed of soot. Initial platform and target altitudes are set at 3,000 m and 1 m respectively. Platform and target are raised together in 125 m increments. Atmospheres considered include the 1976 U.S. Standard Atmosphere, 50th percentile ExPERT climatology, HELTDA ground tab, and 48, 24, and 12 hour GFS forecast derived atmospheres. Note that target hardness is set at 1×10^3 J/cm^2 for this scenario.

Dwell Time vs Heading

Aside from altitude, a second mission parameter that can significantly affect performance is the relative direction of engagement between platform and target.

Fortunately, this is often times a mission parameter that can be controlled by the weapon system user. While battlefield conditions often limit the engagement profile options, the ability to access mission performance with respect to relative heading provides the operator an opportunity to optimize performance and minimize risk. Figure 41 depicts a 12z engagement at Kuwait on 3 December, 2010 in terms of dwell time vs initial heading as described in Chapter 3. Platform and target altitudes are set at 3,000 m and 1 m respectively, and the platform flight profile is a circular orbit at a constant 1 g turn.

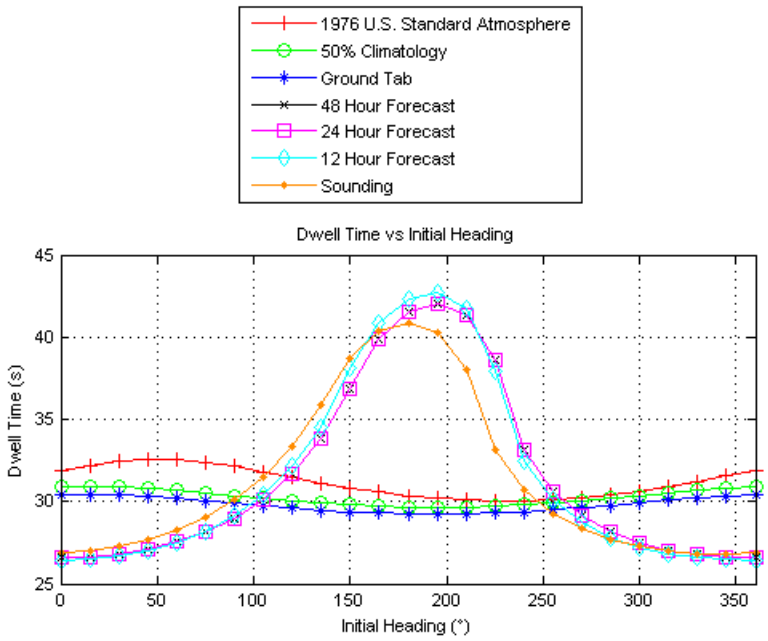

Figure 41. Dwell time vs initial heading for a 1.045 μm engagement for Kuwait on 3 December, 2010 at 12z. Platform and target altitudes are set at 3,000 m and 1 m respectively. Atmospheres considered include the 1976 U.S. Standard Atmosphere, 50th percentile ExPERT climatology, HELTDA ground tab, and 48, 24, and 12 hour GFS forecast derived atmospheres.

Climatological wind profiles predict relatively constant direction and wind speed for Kuwait during the Winter 12Z time period as evidenced by near constant dwell time vs heading curves for the climatology and ground tab profiles. On 3 December

however, there was over a 70° RMSE in wind direction and over a 20 m/s RMSE in wind speed. The resulting difference in wind speed and wind direction had a significant impact on the required dwell time for different headings. This is primarily due to the thermal blooming effects experienced along the propagation bath and the mitigating effect that winds can have on such attenuation. The laser beam itself is essentially moving through the air in the same direction as the platform heading. This movement replaces the column of air in the beam's path with new air molecules, thus reducing the effects of thermal blooming. When the heading of the platform (direction in which the beam is moving or equivalently the opposite of the direction of the effective wind due to platform motion) matches the natural wind direction (direction from which the natural wind is blowing), the platform experiences an effective headwind, and the previously lased air molecules are blown out of the path. When the platform heading is opposite of the wind direction by 180° the platform experiences a tailwind and the previously lased air molecules are maintained in the beam path, contributing to further thermal blooming effects. Since wind speed varies with altitude, this magnitude of this effect is different for every incremental portion of the laser beam. The integrated effect over the entire beam length throughout the engagement period has the cumulative effect seen in Figure 41.

For 3 December, 2010 in Kuwait, by optimizing initial heading, an approximate 14 second advantage, or 34% decrease in dwell time, could be obtained. Figure 42 depicts the error associated with the various atmospheric characterization methods as a function of initial heading. It is important to note that while all methods result in error, the maximum errors from forecasted profiles are half of the maximum error derived from climatological profiles. The error associated with the standard atmosphere is similar to that of the climatology and ground tab since climatological winds are used for this characterization.

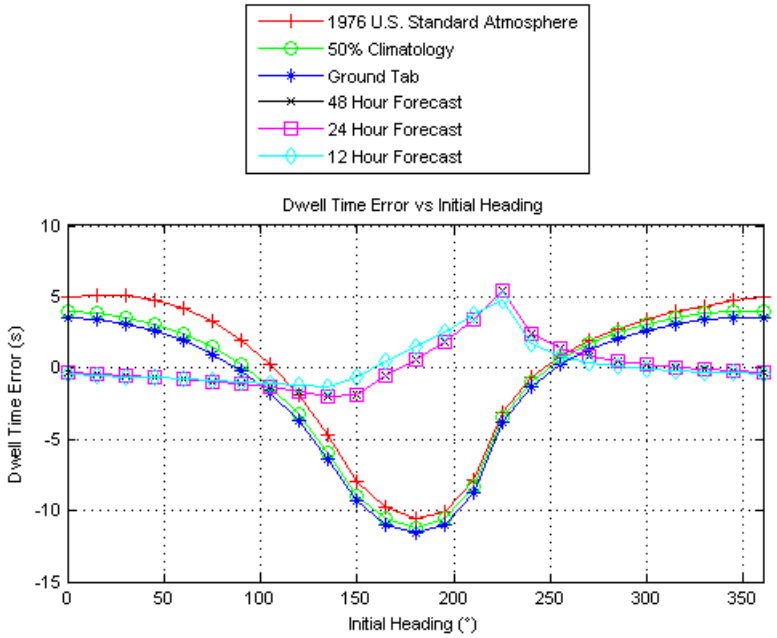

Figure 42. Dwell time error vs initial heading for a 1.045 μm engagement for Kuwait on 3 December, 2010 at 12z. Platform and target altitudes are set at 3,000 m and 1 m respectively. Atmospheres considered include the 1976 U.S. Standard Atmosphere, 50th percentile ExPERT climatology, HELTDA ground tab, and 48, 24, and 12 hour GFS forecast derived atmospheres.

Mission Planning Scenario

The current HELTDA allows an operational user to evaluate the potential battlespace environment and optimize their engagement temporally based on climatological and standard atmospheres. Probability of kill is evaluated with respect to required dwell time for 8 different 3 hour periods throughout the day, providing the user with the ability to adjust engagement durations based on confidence levels required to define mission success. The ability to input various atmospheric conditions and system/target parameters allows nearly any operational scenario to be modeled and analyzed for mission planning purposes. However, the nature of the climatic data and standard models limits the potential advantages. The addition of forecasts allows for both long term planning using climatic data and real-time mission planning based on forecasted conditions. Figure 43 depicts the HELTDA output for a full day analysis

on 25 August, 2010 at WPAFB. The engagement is consistent with the dwell time prediction simulations as defined in Chapter 3 and Figure 14.

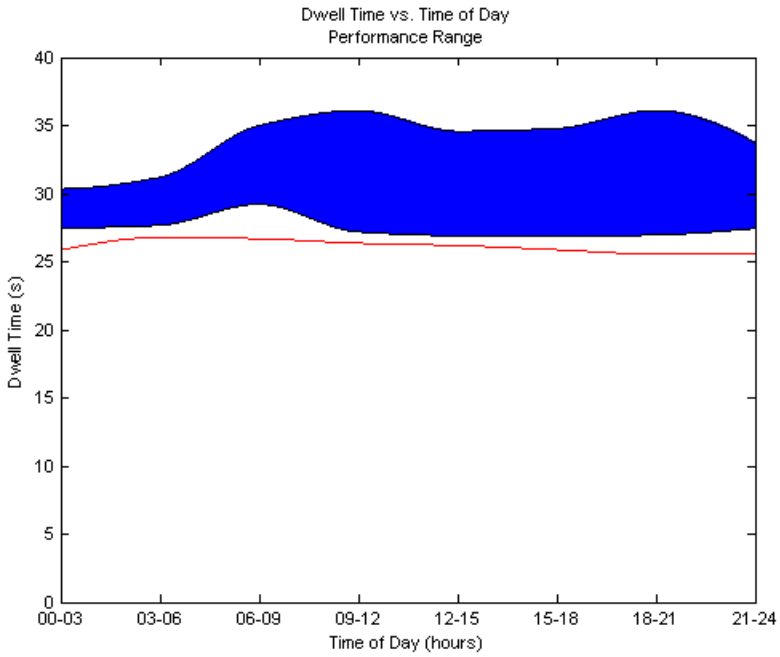

Figure 43. Dwell time vs time of day performance range for 25 August, 2010 at WPAFB for a 150 kW 1.045 μm engagement on a target with a 1×10^5 J/cm^2 hardness. Platform and target altitudes are set at 3,000 m and 1 m respectively. Aerosols are characterized via the GADS database. Blue regions represent the 5% and 95% relative humidity percentiles while the red line represents the 12-24 hour GFS forecast.

The blue lines and shaded region represent the 95th (upper) and 5th (lower) percentile calculations for dwell time required to reach a 90% P_k. The red line represents the same calculation based on the 12-24 hour GFS forecast conditions. One would expected the forecasted conditions to lie withiing the uncertainty levels established by the 5th and 95th percentile conditions, however there are several reasons why this is not necessarily true. First, the forecast includes wind direction and speed values which may vary significantly from the climatological values; this can significantly alter required dwell time values. Second, the values forecasted may be

conditions that have never been observed and that fall outside the databases limits. This is highly unlikely, but possible. Third, the magnitude of various attenuation mechanisms is wavelength dependent. As was the case with the predicted dwell time results for the 1.045 μm wavelength, the combination of non-linear processes leads to unexpected results. Just as the dwell time errors were unexpectedly higher for the ground tab in comparison to climatology, climatology dwell time errors were higher than the forecast error. Therefore it is conceivable that the error shifts the lower boundary established by the 5th percentile upwards throughout the full day analysis.

Figure 44 depicts the dwell time error for the 5th, 50th, 95th, and forecasts for 25 August, 2010. Note that these errors imply the forecast is a better tool for planning actual mission scenarios. While the climatological data provides a reasonable range of values for long term planning purposes in the absence of accurate forecast model outputs, in the near term forecast data are desirable.

Figure 45 depicts the same output for a COIL engagement with a target hardness altered to 1×10^4 J/cm^2 for run time considerations. At the 1.31525 μm wavelength, attenuation due to the induced thermal blooming is far more significant than the aerosol extinction or the lesser molecular absorption. Since the magnitude of this effect is determined from direct measures of atmospheric water content, less error is propagated in the dwell time calculations. Consequently, the forecasted dwell time is far more likely to fall within the climatological bounds as seen in Figure 45.

For absorbing wavelengths, the climatological bounds portray a more accurate representation of realistic limits as opposed to non-absorbing wavelengths such as 1.045 μm. The operational user must keep this in mind when considering the limits predicted by climatological data. Additionally, some situations present conditions where absorption occurs at a typically non absorbing wavelength due to the nature of the aerosols. For example, urban soot aerosols are hygroscopic and tend to absorb in

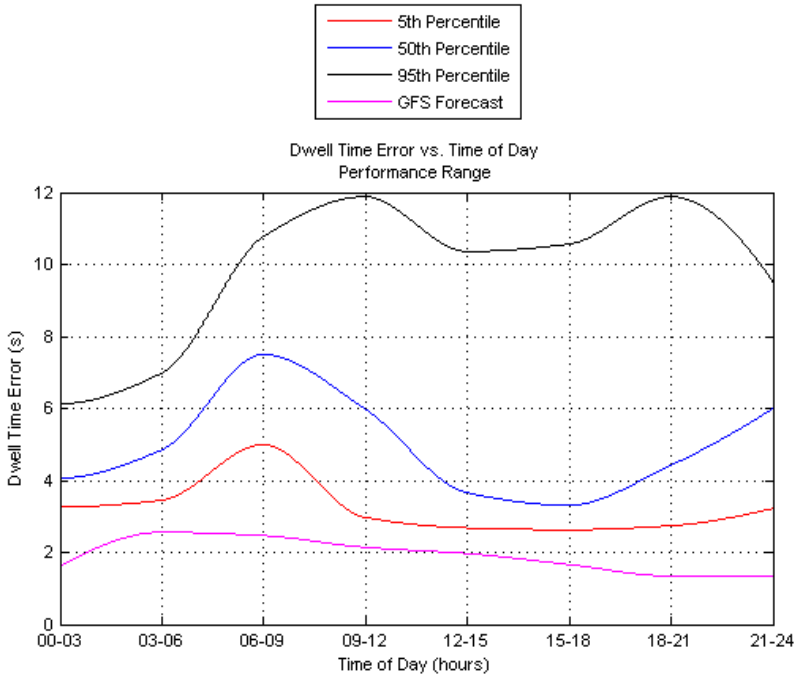

Figure 44. Dwell time error vs time of day performance range for 25 August, 2010 at WPAFB for a 150 kW 1.045 μm engagement on a target with a 1×10^5 J/cm^2 hardness. Platform and target altitudes are set at 3,000 m and 1 m respectively. Aerosols are characterized via the GADS database.

the same manner as molecular absorption at 1.31525 μm. This is depicted in Figure 46 where target hardness is set to 1×10^3 J/cm^2 for run time considerations.

Figure 46 illustrates one of the potential concerns that must be considered when using climatological data. The 5th and 95th percentile results overlap each other and produce unrealistic predictions when considered in relation to each other. This is primarily due to the fact that the relative humidities for both percentiles are nearly equal and the correlation of atmospheric parameters with relative humidity results in different densities and absorption rates. Lower percentiles are typically associated with colder temperatures and thus larger densities. A finite volume of air will contain more molecules in colder temperatures. This leads to increases in the absorption effects, and thus increased dwell time predictions. Coupled with interpolation errors, which tend to be more pronounced for smaller dwell times, these conditions produce

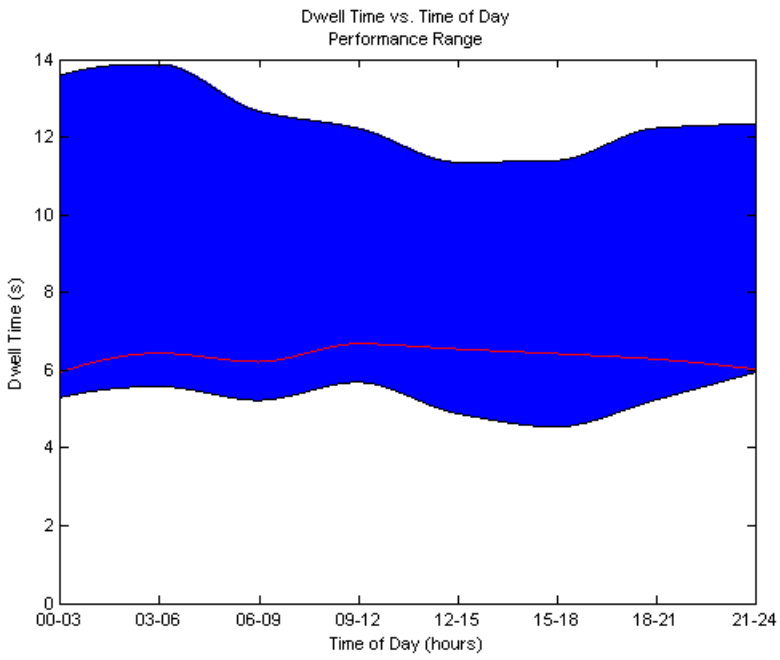

Figure 45. Dwell time vs time of day performance range for 25 August, 2010 at WPAFB for a 150 kW 1.31525 μm engagement on a target with a 1×10^4 J/cm^2 hardness. Platform and target altitudes are set at 3,000 m and 1 m respectively. Aerosols are characterized via the GADS database. Blue regions represent the 5% and 95% relative humidity percentiles while the red line represents the 12-24 hour GFS forecast.

results such as those seen in Figure 46.

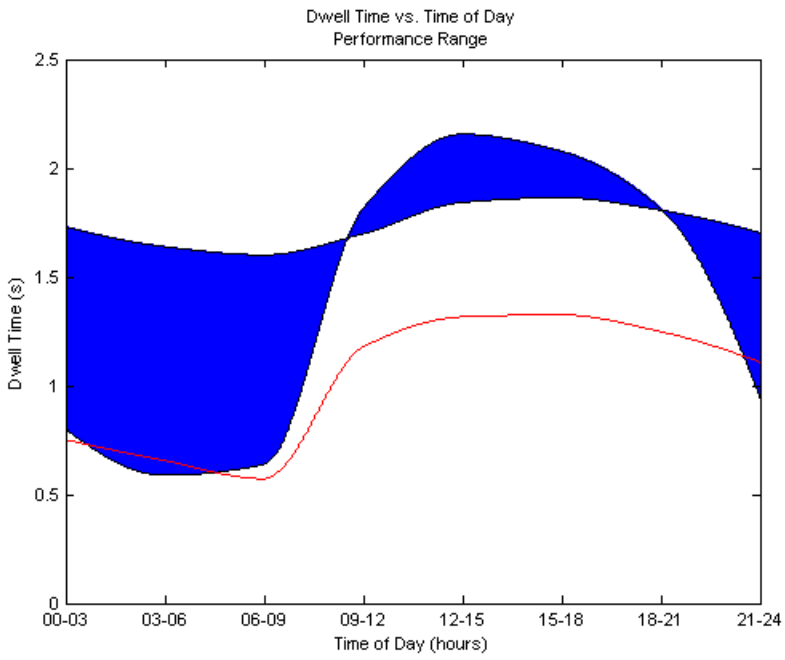

Figure 46. Dwell time vs time of day performance range for 25 August, 2010 at WPAFB for a 150 kW 1.045 μm engagement on a target with a 1×10^3 J/cm^2 hardness. Platform and target altitudes are set at 3,000 m and 1 m respectively. Aerosols are characterized via the GADS database and set to the urban (soot) constituent. Blue regions represent the 5% and 95% relative humidity percentiles while the red line represents the 12-24 hour GFS forecast.

V. Conclusions

Conclusions

This research effort attempted to demonstrate the operational advantages of using a HELTDA for relevant, low-altitude, tactical HEL engagement scenarios. Multiple atmospheric characterization methods (atmospheres) were assessed and compared in terms of temperature, dew point, relative humidity, wind speed, and wind direction in the vertical profile for multiple diverse geographic locations. Relative performance and dwell time prediction error were successfully characterized and indicated several potential advantages obtained through the use of a HELTDA mission planning tool.

When assessing advantages in terms of atmospheric characterization of meteorological parameters, geographic location is a significant factor in determining prediction accuracy. The performance of numerical forecast derived atmospheres consistently out performs other methods. For other methods, relative performance is highly variable. The 1976 U.S. Standard Atmosphere displays the most variance in performance, yet performs exceedingly well in some cases. The variability is expected due to the static nature of the characterization method, and the accurate performance in certain situations emphasizes the fortunate outcome possible without sophisticated prediction methods. However, there is little confidence in the repeatability of these exceptional performances in a dynamic environment and the high costs of mission failure necessitate the use of other characterization methods.

The accuracy of the meteorological predictions varies depending on the extent of the atmosphere considered. Within the boundary layer, climatology and ground tab profiles perform better on average opposed to profiles extending to approximately 30,000 m. For both profiles, the GFS forecast atmospheres consistently outperform standard, climatology, and ground tab derived atmospheres in all measures and

for all locations studied. For the full atmosphere profile, this was always true for the locations under consideration. Within the boundary layer, this is a highly probable result, yet deviations were observed, particularly during the morning hours in the tropical locations. For the tactical engagements described in this research, GFS atmospheres were expected to perform better at higher altitudes than lower altitudes. Within the boundary layer they were expected to outperform all other methods but deviations were observed. The ground tab atmosphere consistently outperformed climatology within the boundary layer. Above the boundary layer the two atmospheres are identical; thus overall performance differences are decreased as more of the atmosphere is taken into consideration. Consequently, the ground tab provides a valuable alternative for atmospheric characterization, particularly in or near the boundary layer, when numerical forecasts are not available. In forecast atmospheres, temperature is characterized more accurately than dew point for all locations, seasons, and times, suggesting that dew point characterization is not as robust as preferred. Overall, the desert location is characterized more accurately for all methods, yet this result is far from guaranteed. Consequently, it is impossible to conclusively determine a superior characterization method for any single parameter without specifying a geographic location.

Advantages in atmospheric characterization must translate to performance advantages in the operational environment in order to have a significant impact on operations. For relevant engagement scenarios, dwell time errors differed significantly from the hypothesized results. Variability in the standard atmosphere's meteorological performance translated to variability in dwell time error. In some cases, standard atmospheres continued to provided accurate results, yet the confidence in reported dwell times would be extremely limited in a real-world engagement scenario. However, based on vertical profile validation results, it was hypothesized that HEL engagement

dwell times would be better predicted by ground tab atmospheres versus climatology for most locations, seasons, and times. This was not true for the ELLA 1.045 μm wavelength, indicating a wavelength dependence for the performance prediction results. Despite the fact that most meteorological parameters were better characterized by the ground tab versus climatology, the overall results were worse. For the COIL 1.31525 μm wavelength the ground tab consistently outperformed climatology as hypothesized. This discrepancy is credited to the increased non-linear effects of thermal blooming at the COIL wavelength due to molecular absorption (which is not nearly as significant at 1.045 μm) and the multivariate nature of the total dwell time calculation.

Despite individual meteorological parameter performance, the complex physical process results in an increased dwell time error for the ground tab at the ELLA wavelength. Thermal blooming is directly proportional to the amount of water vapor present in the atmosphere while scattering effects are primarily determined by relative humidity and aerosol distributions. Water vapor is directly correlated to the dew point measurement while relative humidity is empirically derived from dew point, temperature, and pressure measurements. As a result, a better prediction of dew point corresponds to a more accurate ground tab dwell time estimate for wavelengths where thermal blooming is a dominate attenuation mechanism. At wavelengths where scattering is the primary attenuation mechanism, better predictions of dew point, temperature, relative humidity, wind speed, and wind direction do not necessarily correspond to better dwell time predictions and are not a direct measure of the loss mechanism. This can have significant impacts on the way in which mission planning is accomplished depending on the type of system being employed. Additionally, it indicates that further research into the physical processes of aerosol absorption should be pursued. Operationally, this research demonstrates that the movement to solid state lasers reduces the impact of a dynamic atmosphere on HEL engagements and

quantifies the results in terms of required dwell time.

In general, the GFS forecast atmospheres outperformed all other atmospheres in dwell time predictions for the 1.045 μm wavelength. This was also true for the 1.31525 μm wavelength except in the tropical location. The relative advantage gained by using a 12 hour forecast as opposed to a 24 or 48 hour forecast is negligible in most cases, thus indicating the limits of the forecast system. In general, seasonal and time of day advantages can be gained through proper planning, but conditions for such engagements are location dependent. Depending on the conditions, climatology may outperform the ground tab or vice versa.

It was demonstrated that higher altitudes tend to diminish the attenuating effects for engagements with all other non atmospheric parameters being equal, supporting the notion that a decision aid is less useful for high altitude engagements far above the boundary layer. Near the boundary layer, there is an optimal altitude for air-to-ground engagements that minimizes required dwell time indicating a potential trade between increasing altitude and scattering effects due to slant path angle through the boundary layer. GFS forecasts predicted this optimal value best and allow the user to optimize flight profiles for mission needs. Furthermore, altitude assessments for constant path lengths indicate operating near the top of the boundary layer requires the longest dwell times. This has significant implications for both offensive and defensive operations as the engagement can be optimized for prosecuting targets or conversely, the atmosphere can be utilized as a natural countermeasure. The HELTDA provides a means to analyze and optimize both types of engagements.

The wind direction and wind speed parameters were found to have a significant impact on required dwell times as well. Climatological wind profiles may provide a measure of reality, but their predictive capability is severely lacking. There exists a relatively large operational advantage when optimizing heading to factor in wind

speed and direction deviations from climatology and the attenuation effects primarily due to thermal blooming.

Forecast derived atmospheres proved to consistently provide the most accurate dwell time predictions for all locations, seasons, and times of day. While climatological values provide an excellent baseline for performance and trade studies, the operational user would be well served utilizing numerical weather prediction models when planning tactical HEL engagements. When unavailable, the utility of the ground tab atmospheric characterization is dependent on wavelength and aerosol types and distributions.

Recommendations and Future Work

The results of this research support the use of a HELTDA for mission planning and optimization functions. However, to better serve the warfighter, there are several factors that should be considered for implementation in an operational HELTDA software package. First and foremost, the wavelength dependent results on dwell times must be fully understood. A greater understanding of the physical processes leading to unexpected attenuation levels will profit the scientific community as well as the operational user. It is suggested that a design of experiments type analysis be conducted to evaluate the impact of different meteorological parameters and their associated errors on the overall dwell time results. A greater understanding of the relevant parameters will facilitate a more accurate boundary layer model for fast characterization and operational employment optimizations when forecasted data are not readily available or computationally accessible.

Current research utilized the GFS forecast model for all analyzed forecast data. While this model provides global coverage, other models exist with greater resolution for specific geographic areas. Increased resolution has the potential to generate

forecasts that take small scale disturbances and weather phenomena into consideration. These models should be evaluated and compared to the GFS in order to gage the relative performance. Additionally, all forecast data used throughout this research was collected from the NWS repositories. It was not gathered in real-time. These data are currently available to the public in near real-time but it is not a DOD product. The potential impact of losing access to these data for any reason necessitates the investigation of acquiring data through DOD channels for operational employment. Air Force weather data should be coordinated and employed directly within the HELTDA.

Other potential incorporations include the use of actual aerosol distribution data in the control data set. All aerosol distributions for the current research were modeled with the GADS database. While more accurate than assuming aerosol distributions, this database does not provide an accurate estimate of actual aerosol conditions. Utilizing a light detection and ranging (LIDAR) system or other methods to determine real-time aerosol size distributions would provided valuable information in determining the attenuation effects most significant to a particular mission scenario. Additionally, radiosonde sampling within the boundary layer is sparse. The limited number of data collections at these levels due to the rapid rise of the balloon may result in the non detection of significant variations in parameters over a small vertical extent. While balloon launched radiosonde data are the primary data set used to characterize the atmosphere in the meteorological community, the disproportional effects resulting from boundary layer interactions may necessitate that other methods be employed to collect control data. One possible method would employ the use of UAVs to collect atmospheric data at specified levels. The ability to make multiple measurements at a single level over an extended period of time may provide a better estimate of actual atmospheric conditions. A more accurate and time specific control data set

ensures that the analyzed atmosphere most accurately represents actual conditions and facilitates the study of wavelength dependent performance measures.

The engagements studied in this research were specific to proposed ELLA parameters and specifications and were limited in scope. While these represented some of the more stressing conditions, the results can not be interpreted as accurate for missions with varying parameters. As HEL weapon systems continue to be developed, additional research should mirror the technology in development and continue in unison to ensure that a viable weapon system is fielded. Specifically, engagement scenarios for other targets should be considered to verify the utility of the HELTDA. While wind speed and direction were observed to have significant impacts on this particular scenario, the overall impact is undetermined for targets with varying hardness as well as varying laser power. The missions sensitivity to individual parameters such as wind speed or relative humidity will undoubtedly dictate weapon system employment.

In conjunction with system parameter impact studies, the potential countermeasure effects obtained through the clever use of boundary layer attenuation should be closely examined. The offensive and defensive advantage gained can be optimized by our own forces, or by those of our enemies. By fully understanding the tactics for taking advantage of this layer of protecting, we can better prepare for actual combat situations. Additionally, the utility of a HELTDA mission planning tool should be examined in relation to predictive avoidance considerations. The operational advantages for a weapon system operator discussed in this research are undoubtedly correlated to optimization opportunities in the field of predictive avoidance. Rather than basing policies and time critical decisions on worst case scenarios, a HELTDA would enable real-time realistic assessments. Several new windows of opportunity may be available when realistic atmospheric conditions are taken into account.

The HELTDA is a capable software package that clearly gives the warfighter

an opportunity to exploit an operational advantage when employing HEL weapons. The dynamic nature of the atmosphere and its severe attenuating effects necessitate accurate prediction and characterization for reliable mission success. The HELTDA is a viable option for mission planning, and with continued support, HEL weapon employment will be introduced with unparalleled efficiency.

Appendix A.

Table 4. WPAFB mean RMSE values for temperature, dew point, relative humidity, wind speed, and wind direction in the boundary layer for Summer 00z, Summer 12z, Winter 00z, and Winter 12z. Atmospheres considered include the 1976 U.S. Standard Atmosphere, 50th percentile ExPERT climatology, HELTDA ground tab, and 48, 24, and 12 hour GFS forecast derived atmospheres.

Time/Season	Profile	Temperature (°F)	Dew Point (°F)	Wind Speed (m/s)	Wind Direction (°)	Relative Humidity (%)
Summer 00z	1976 US Standard	17.9	24.1	3.2	83.5	21.6
	50% Climatology	6.8	11.2	3.2	83.5	26.1
	Ground Tab	2.0	9.8	3.2	83.5	21.6
	48 Hr GFS Frcst	2.8	6.9	2.0	38.9	14.3
	24 Hr GFS Frcst	2.5	5.7	1.9	39.7	13.1
	12 Hr GFS Frcst	2.1	5.6	1.7	32.2	12.0
Summer 12z	1976 US Standard	12.0	21.8	3.0	99.8	27.6
	50% Climatology	8.1	8.1	3.0	99.8	29.3
	Ground Tab	9.0	4.5	3.0	99.8	30.3
	48 Hr GFS Frcst	3.2	5.8	2.3	53.5	15.3
	24 Hr GFS Frcst	3.1	5.3	2.1	48.0	14.1
	12 Hr GFS Frcst	2.4	5.2	2.0	42.4	11.7
Winter 00z	1976 US Standard	27.7	25.6	4.1	59.5	17.9
	50% Climatology	12.3	17.5	4.1	59.5	41.6
	Ground Tab	5.1	8.9	4.1	59.5	32.8
	48 Hr GFS Frcst	3.8	8.0	2.2	28.6	23.5
	24 Hr GFS Frcst	3.6	7.0	2.0	25.3	20.6
	12 Hr GFS Frcst	3.0	7.6	1.9	26.6	20.7
Winter 12z	1976 US Standard	35.1	23.9	5.1	63.1	28.1
	50% Climatology	14.8	19.0	5.1	63.1	27.2
	Ground Tab	6.8	5.5	5.1	63.1	25.5
	48 Hr GFS Frcst	3.9	4.5	2.2	28.0	16.6
	24 Hr GFS Frcst	3.8	3.9	2.1	23.4	16.1
	12 Hr GFS Frcst	3.0	3.8	1.9	23.3	14.0

Table 5. WPAFB mean RMSE values for temperature, dew point, relative humidity, wind speed, and wind direction from 0 to approximately 30,000 m for Summer 00z, Summer 12z, Winter 00z, and Winter 12z. Atmospheres considered include the 1976 U.S. Standard Atmosphere, 50th percentile ExPERT climatology, HELTDA ground tab, and 48, 24, and 12 hour GFS forecast derived atmospheres.

Time/Season	Profile	Temperature (°F)	Dew Point (°F)	Wind Speed (m/s)	Wind Direction (°)	Relative Humidity (%)
Summer 00z	1976 US Standard	17.9	24.1	6.8	56.3	21.4
	50% Climatology	9.9	23.8	6.8	56.3	22.2
	Ground Tab	9.6	23.7	6.8	56.3	21.5
	48 Hr GFS Frcst	3.1	17.0	3.3	38.1	18.8
	24 Hr GFS Frcst	2.9	15.4	3.0	36.5	18.0
	12 Hr GFS Frcst	2.6	15.4	2.7	32.9	15.7
Summer 12z	1976 US Standard	15.6	22.3	6.4	57.2	21.3
	50% Climatology	8.6	22.3	6.4	57.2	21.8
	Ground Tab	8.6	22.2	6.4	57.2	21.9
	48 Hr GFS Frcst	2.6	14.9	3.3	42.3	18.6
	24 Hr GFS Frcst	2.4	13.7	2.8	36.2	16.5
	12 Hr GFS Frcst	2.2	12.7	2.6	35.2	14.6
Winter 00z	1976 US Standard	14.3	31.2	9.3	35.0	22.9
	50% Climatology	9.5	29.1	9.3	35.0	26.5
	Ground Tab	8.9	28.8	9.3	35.0	25.6
	48 Hr GFS Frcst	3.1	15.1	4.1	21.7	24.1
	24 Hr GFS Frcst	2.9	14.9	3.6	20.2	22.9
	12 Hr GFS Frcst	2.6	14.4	3.4	20.1	22.2
Winter 12z	1976 US Standard	15.8	28.7	9.5	36.8	22.6
	50% Climatology	9.4	26.1	9.5	36.8	24.2
	Ground Tab	8.8	25.6	9.5	36.8	24.1
	48 Hr GFS Frcst	3.2	13.4	4.2	20.7	22.8
	24 Hr GFS Frcst	2.8	13.0	3.5	18.5	21.3
	12 Hr GFS Frcst	2.6	12.7	3.2	18.1	20.4

Table 6. Kuwait mean RMSE values for temperature, dew point, relative humidity, wind speed, and wind direction in the boundary layer for Summer 00z, Summer 12z, Winter 00z, and Winter 12z. Atmospheres considered include the 1976 U.S. Standard Atmosphere, 50th percentile ExPERT climatology, HELTDA ground tab, and 48, 24, and 12 hour GFS forecast derived atmospheres.

Time/Season	Profile	Temperature (°F)	Dew Point (°F)	Wind Speed (m/s)	Wind Direction (°)	Relative Humidity (%)
Summer 00z	1976 US Standard	40.5	7.8	5.5	49.7	29.8
	50% Climatology	5.9	11.9	5.5	49.7	9.3
	Ground Tab	8.0	5.4	5.5	49.7	6.9
	48 Hr GFS Frcst	12.3	11.4	4.7	73.6	9.9
	24 Hr GFS Frcst	12.8	10.1	4.9	68.6	9.3
	12 Hr GFS Frcst	12.5	10.4	4.8	75.4	9.2
Summer 12z	1976 US Standard	49.5	7.9	3.0	55.9	36.1
	50% Climatology	3.0	7.2	3.0	55.9	3.0
	Ground Tab	2.2	6.1	3.0	55.9	3.1
	48 Hr GFS Frcst	3.0	8.3	2.9	57.5	4.2
	24 Hr GFS Frcst	2.0	5.7	2.8	36.2	2.3
	12 Hr GFS Frcst	1.8	5.5	2.7	42.6	2.1
Winter 00z	1976 US Standard	7.8	7.8	5.1	129.6	14.6
	50% Climatology	8.8	13.2	5.1	129.6	39.5
	Ground Tab	9.8	6.3	5.1	129.6	14.4
	48 Hr GFS Frcst	4.7	6.6	2.2	44.9	11.8
	24 Hr GFS Frcst	4.5	6.5	2.1	41.2	11.6
	12 Hr GFS Frcst	4.5	6.7	2.0	41.8	12.0
Winter 12z	1976 US Standard	7.4	14.5	4.6	104.8	20.7
	50% Climatology	7.0	18.5	4.6	104.8	33.1
	Ground Tab	3.2	10.6	4.6	104.8	14.1
	48 Hr GFS Frcst	2.0	8.9	2.0	24.5	9.3
	24 Hr GFS Frcst	2.0	8.9	2.0	24.5	9.3
	12 Hr GFS Frcst	1.8	8.9	1.9	25.8	9.2

Table 7. Kuwait mean RMSE values for temperature, dew point, relative humidity, wind speed, and wind direction from 0 to approximately 30,000 m for Summer 00z, Summer 12z, Winter 00z, and Winter 12z. Atmospheres considered include the 1976 U.S. Standard Atmosphere, 50th percentile ExPERT climatology, HELTDA ground tab, and 48, 24, and 12 hour GFS forecast derived atmospheres.

Time/Season	Profile	Temperature (°F)	Dew Point (°F)	Wind Speed (m/s)	Wind Direction (°)	Relative Humidity (%)
Summer 00z	1976 US Standard	34.2	17.8	7.8	82.2	28.1
	50% Climatology	52.7	22.1	7.8	82.2	38.2
	Ground Tab	52.7	21.8	7.8	82.2	38.2
	48 Hr GFS Frcst	5.5	22.7	5.4	68.8	19.5
	24 Hr GFS Frcst	5.0	19.5	4.3	54.9	17.1
	12 Hr GFS Frcst	4.8	19.3	4.2	57.0	16.2
Summer 12z	1976 US Standard	35.8	17.2	7.6	88.1	28.6
	50% Climatology	47.1	20.9	7.6	88.1	32.5
	Ground Tab	47.1	20.9	7.6	88.1	32.5
	48 Hr GFS Frcst	3.0	20.4	4.4	52.6	18.2
	24 Hr GFS Frcst	2.2	17.9	3.2	39.5	14.1
	12 Hr GFS Frcst	2.0	17.6	3.0	38.7	13.9
Winter 00z	1976 US Standard	9.8	23.4	9.2	64.6	25.7
	50% Climatology	54.0	34.4	9.2	64.6	34.8
	Ground Tab	54.0	34.1	9.2	64.6	32.1
	48 Hr GFS Frcst	2.9	20.8	4.0	23.4	20.8
	24 Hr GFS Frcst	2.7	20.3	3.8	21.2	20.7
	12 Hr GFS Frcst	2.6	20.4	3.4	21.9	20.7
Winter 12z	1976 US Standard	9.7	22.2	9.4	57.0	24.8
	50% Climatology	44.6	27.1	9.4	57.0	32.3
	Ground Tab	44.5	25.8	9.4	57.0	29.4
	48 Hr GFS Frcst	2.1	20.2	3.4	15.9	20.8
	24 Hr GFS Frcst	2.1	20.2	3.4	15.9	20.8
	12 Hr GFS Frcst	2.0	20.3	3.2	16.2	20.0

Table 8. Brunei mean RMSE values for temperature, dew point, relative humidity, wind speed, and wind direction in the boundary layer for Summer 00z, Summer 12z, Winter 00z, and Winter 12z. Atmospheres considered include the 1976 U.S. Standard Atmosphere, 50th percentile ExPERT climatology, HELTDA ground tab, and 48, 24, and 12 hour GFS forecast derived atmospheres.

Time/Season	Profile	Temperature (°F)	Dew Point (°F)	Wind Speed (m/s)	Wind Direction (°)	Relative Humidity (%)
Summer 00z	1976 US Standard	21.1	36.0	2.0	68.4	38.2
	50% Climatology	1.9	4.8	2.0	68.4	17.3
	Ground Tab	2.3	4.2	2.0	68.4	16.9
	48 Hr GFS Frcst	3.6	2.7	2.2	97.8	12.4
	24 Hr GFS Frcst	3.4	2.7	2.0	96.2	12.3
	12 Hr GFS Frcst	3.2	2.2	2.1	98.4	10.2
Summer 12z	1976 US Standard	24.0	37.6	1.9	91.2	36.0
	50% Climatology	3.4	6.7	1.9	91.2	16.6
	Ground Tab	2.1	7.0	1.9	91.2	17.3
	48 Hr GFS Frcst	1.9	4.4	1.7	59.3	13.1
	24 Hr GFS Frcst	1.9	4.4	1.7	59.3	13.1
	12 Hr GFS Frcst	1.9	3.9	1.7	60.7	12.0
Winter 00z	1976 US Standard	18.2	35.6	1.8	118.4	43.7
	50% Climatology	4.7	2.4	1.8	118.4	11.8
	Ground Tab	1.8	2.6	1.8	118.4	11.6
	48 Hr GFS Frcst	2.5	2.0	1.7	63.2	10.2
	24 Hr GFS Frcst	2.3	2.0	2.0	61.5	9.9
	12 Hr GFS Frcst	2.3	2.0	1.8	59.6	10.1
Winter 12z	1976 US Standard	21.3	36.8	1.8	60.7	39.4
	50% Climatology	1.9	3.8	1.8	60.7	11.9
	Ground Tab	1.8	5.2	1.8	60.7	11.9
	48 Hr GFS Frcst	1.3	2.4	2.0	50.7	7.8
	24 Hr GFS Frcst	1.5	2.8	1.9	39.7	8.8
	12 Hr GFS Frcst	1.6	2.8	1.7	42.5	8.5

Table 9. Brunei mean RMSE values for temperature, dew point, relative humidity, wind speed, and wind direction from 0 to approximately 30,000 m for Summer 00z, Summer 12z, Winter 00z, and Winter 12z. Atmospheres considered include the 1976 U.S. Standard Atmosphere, 50th percentile ExPERT climatology, HELTDA ground tab, and 48, 24, and 12 hour GFS forecast derived atmospheres.

Time/Season	Profile	Temperature (°F)	Dew Point (°F)	Wind Speed (m/s)	Wind Direction (°)	Relative Humidity (%)
Summer 00z	1976 US Standard	29.0	30.6	7.8	65.0	26.3
	50% Climatology	6.0	16.4	7.8	65.0	21.9
	Ground Tab	6.0	16.3	7.8	65.0	21.9
	48 Hr GFS Frcst	3.9	14.5	5.5	52.5	32.8
	24 Hr GFS Frcst	3.7	14.8	4.9	47.5	34.2
	12 Hr GFS Frcst	3.5	14.6	4.5	45.8	33.6
Summer 12z	1976 US Standard	29.7	37.2	6.4	70.8	35.8
	50% Climatology	5.3	20.7	6.4	70.8	31.4
	Ground Tab	5.0	20.7	6.4	70.8	31.5
	48 Hr GFS Frcst	2.5	9.0	4.0	40.3	25.6
	24 Hr GFS Frcst	2.5	9.0	4.0	40.3	25.6
	12 Hr GFS Frcst	2.4	8.8	3.8	38.2	25.0
Winter 00z	1976 US Standard	28.7	28.6	6.4	80.5	26.4
	50% Climatology	6.7	18.0	6.4	80.5	27.1
	Ground Tab	6.6	18.0	6.4	80.5	27.1
	48 Hr GFS Frcst	3.4	15.3	4.6	49.3	32.9
	24 Hr GFS Frcst	3.4	15.1	4.2	45.9	32.0
	12 Hr GFS Frcst	3.3	15.0	4.0	44.7	31.1
Winter 12z	1976 US Standard	29.2	34.1	5.3	76.3	33.6
	50% Climatology	6.0	21.9	5.3	76.3	35.3
	Ground Tab	6.0	22.0	5.3	76.3	35.3
	48 Hr GFS Frcst	2.8	11.4	4.9	60.9	30.1
	24 Hr GFS Frcst	2.7	11.4	4.9	55.6	30.9
	12 Hr GFS Frcst	2.7	11.2	4.8	52.4	30.8

Table 10. WPAFB dwell time (DT) and RMSE values for 1.045 and 1.31525 μm engagements from the top of the boundary layer to the surface for Summer 00z, Summer 12z, Winter 00z, and Winter 12z. Atmospheres considered include the 1976 U.S. Standard Atmosphere, 50th percentile ExPERT climatology, HELTDA ground tab, and 48, 24, and 12 hour GFS forecast derived atmospheres. Note target hardness differs for the two wavelength simulations.

Time/Season	Profile	1.045 µm DT (s)	1.045 µm DT RMSE (S)	1.31525 µm DT (s)	1.31525 µm DT RMSE (S)
Summer 00z	1976 US Standard	19.6	1.8	3.6	5.4
	50% Climatology	23.2	3.2	7.3	3.8
	Ground Tab	23.4	4.4	8.5	2.7
	48 Hr GFS Frcst	20.0	2.2	6.8	3.0
	24 Hr GFS Frcst	19.7	1.9	6.3	2.5
	12 Hr GFS Frcst	19.8	1.9	6.1	2.1
Summer 12z	1976 US Standard	18.7	2.9	3.6	5.2
	50% Climatology	32.9	12.1	7.3	3.1
	Ground Tab	37.0	16.5	7.0	2.2
	48 Hr GFS Frcst	22.2	3.9	7.5	3.4
	24 Hr GFS Frcst	22.3	4.2	7.3	2.5
	12 Hr GFS Frcst	22.2	3.9	7.3	2.5
Winter 00z	1976 US Standard	17.7	4.8	3.2	2.6
	50% Climatology	27.2	6.7	2.7	2.6
	Ground Tab	24.9	6.5	2.5	1.9
	48 Hr GFS Frcst	22.8	4.1	3.7	2.2
	24 Hr GFS Frcst	22.7	4.1	3.6	1.6
	12 Hr GFS Frcst	22.7	4.2	3.6	1.5
Winter 12z	1976 US Standard	19.6	6.0	3.6	2.8
	50% Climatology	27.2	4.2	3.8	2.8
	Ground Tab	30.3	8.6	2.8	2.2
	48 Hr GFS Frcst	25.8	3.6	3.4	1.4
	24 Hr GFS Frcst	26.5	4.7	3.5	1.3
	12 Hr GFS Frcst	26.0	4.4	3.5	1.3

Table 11. WPAFB dwell time (DT) and RMSE values for 1.045 and 1.31525 μm engagements from 3,000 m to the surface for Summer 00z, Summer 12z, Winter 00z, and Winter 12z. Atmospheres considered include the 1976 U.S. Standard Atmosphere, 50th percentile ExPERT climatology, HELTDA ground tab, and 48, 24, and 12 hour GFS forecast derived atmospheres. Note target hardness differs for the two wavelength simulations.

Time/Season	Profile	1.045 µm DT (s)	1.045 µm DT RMSE (S)	1.31525 µm DT (s)	1.31525 µm DT RMSE (S)
Summer 00z	1976 US Standard	25.5	2.3	4.5	5.6
	50% Climatology	28.5	2.7	8.4	4.0
	Ground Tab	28.6	3.4	9.4	3.0
	48 Hr GFS Frcst	26.0	2.2	7.5	2.9
	24 Hr GFS Frcst	25.6	2.1	7.1	2.7
	12 Hr GFS Frcst	25.7	2.0	6.9	2.5
Summer 12z	1976 US Standard	25.5	4.5	4.5	6.4
	50% Climatology	31.8	4.7	8.6	4.1
	Ground Tab	33.2	6.2	8.2	3.7
	48 Hr GFS Frcst	28.7	4.1	8.6	4.8
	24 Hr GFS Frcst	29.0	3.1	8.5	2.7
	12 Hr GFS Frcst	28.6	3.9	8.1	4.0
Winter 00z	1976 US Standard	24.4	5.8	4.1	2.7
	50% Climatology	29.5	4.8	3.2	2.6
	Ground Tab	28.5	5.0	3.0	2.0
	48 Hr GFS Frcst	27.4	2.5	3.7	3.4
	24 Hr GFS Frcst	27.5	2.7	3.3	1.9
	12 Hr GFS Frcst	27.7	3.1	3.2	1.5
Winter 12z	1976 US Standard	24.4	3.5	4.1	2.3
	50% Climatology	27.8	3.2	4.0	2.1
	Ground Tab	28.6	3.7	2.9	1.2
	48 Hr GFS Frcst	27.3	2.1	2.6	0.6
	24 Hr GFS Frcst	27.4	2.4	2.7	0.8
	12 Hr GFS Frcst	27.2	2.2	2.7	0.9

Table 12. Kuwait dwell time (DT) and RMSE values for 1.045 and 1.31525 μm engagements from the top of the boundary layer to the surface for Summer 00z, Summer 12z, Winter 00z, and Winter 12z. Atmospheres considered include the 1976 U.S. Standard Atmosphere, 50th percentile ExPERT climatology, HELTDA ground tab, and 48, 24, and 12 hour GFS forecast derived atmospheres. Note target hardness differs for the two wavelength simulations.

Time/Season	Profile	1.045 µm DT (s)	1.045 µm DT RMSE (S)	1.31525 µm DT (s)	1.31525 µm DT RMSE (S)
Summer 00z	1976 US Standard	29.8	5.8	3.6	3.1
	50% Climatology	24.0	3.3	3.9	3.0
	Ground Tab	24.1	3.2	3.5	2.6
	48 Hr GFS Frcst	30.0	8.9	5.7	8.8
	24 Hr GFS Frcst	27.1	6.0	2.9	3.3
	12 Hr GFS Frcst	27.1	4.9	2.9	3.2
Summer 12z	1976 US Standard	27.9	5.1	2.9	1.1
	50% Climatology	22.4	3.1	2.0	1.1
	Ground Tab	22.4	3.0	2.5	0.8
	48 Hr GFS Frcst	25.3	3.0	3.6	2.9
	24 Hr GFS Frcst	24.1	1.9	2.3	0.8
	12 Hr GFS Frcst	24.1	1.9	2.5	0.8
Winter 00z	1976 US Standard	27.5	2.6	4.5	1.6
	50% Climatology	28.6	3.5	4.5	1.7
	Ground Tab	27.4	2.5	3.2	1.2
	48 Hr GFS Frcst	24.6	2.1	3.2	1.2
	24 Hr GFS Frcst	24.9	2.7	3.4	2.0
	12 Hr GFS Frcst	24.9	2.7	3.4	2.0
Winter 12z	1976 US Standard	25.7	4.9	3.8	2.0
	50% Climatology	24.3	4.3	3.6	1.9
	Ground Tab	24.1	4.2	2.6	1.2
	48 Hr GFS Frcst	22.7	2.3	2.2	0.8
	24 Hr GFS Frcst	22.7	2.3	2.2	0.8
	12 Hr GFS Frcst	22.7	2.2	2.2	0.7

Table 13. Kuwait dwell time (DT) and RMSE values for 1.045 and 1.31525 μm engagements from 3,000 m to the surface for Summer 00z, Summer 12z, Winter 00z, and Winter 12z. Atmospheres considered include the 1976 U.S. Standard Atmosphere, 50th percentile ExPERT climatology, HELTDA ground tab, and 48, 24, and 12 hour GFS forecast derived atmospheres. Note target hardness differs for the two wavelength simulations.

Time/Season	Profile	1.045 µm DT (s)	1.045 µm DT RMSE (S)	1.31525 µm DT (s)	1.31525 µm DT RMSE (S)
Summer 00z	1976 US Standard	34.2	6.5	3.5	2.1
	50% Climatology	29.3	3.1	2.8	2.2
	Ground Tab	29.3	3.1	2.6	2.1
	48 Hr GFS Frcst	30.9	3.8	3.7	2.4
	24 Hr GFS Frcst	29.8	2.7	2.8	1.7
	12 Hr GFS Frcst	29.7	2.8	2.9	1.6
Summer 12z	1976 US Standard	34.2	5.8	3.5	1.2
	50% Climatology	28.1	3.2	2.3	1.2
	Ground Tab	28.1	3.2	2.8	0.9
	48 Hr GFS Frcst	31.2	3.5	3.9	2.6
	24 Hr GFS Frcst	29.8	2.0	2.8	0.8
	12 Hr GFS Frcst	29.9	2.0	3.0	0.8
Winter 00z	1976 US Standard	31.9	5.0	4.5	4.6
	50% Climatology	31.7	4.9	3.1	4.6
	Ground Tab	31.4	4.8	2.5	4.6
	48 Hr GFS Frcst	28.0	2.7	3.1	3.2
	24 Hr GFS Frcst	28.2	2.1	3.2	2.4
	12 Hr GFS Frcst	28.2	2.0	3.2	2.1
Winter 12z	1976 US Standard	31.9	5.0	4.5	2.2
	50% Climatology	30.9	4.5	4.2	2.0
	Ground Tab	30.7	4.4	3.1	1.2
	48 Hr GFS Frcst	28.9	1.8	2.7	0.9
	24 Hr GFS Frcst	28.9	1.8	2.7	0.9
	12 Hr GFS Frcst	28.9	1.7	2.7	0.7

Table 14. Brunei dwell time (DT) and RMSE values for 1.045 and 1.31525 μm engagements from the top of the boundary layer to the surface for Summer 00z, Summer 12z, Winter 00z, and Winter 12z. Atmospheres considered include the 1976 U.S. Standard Atmosphere, 50th percentile ExPERT climatology, HELTDA ground tab, and 48, 24, and 12 hour GFS forecast derived atmospheres. Note target hardness differs for the two wavelength simulations.

Time/Season	Profile	1.045 µm DT (s)	1.045 µm DT RMSE (S)	1.31525 µm DT (s)	1.31525 µm DT RMSE (S)
Summer 00z	1976 US Standard	26.5	7.4	4.4	11.8
	50% Climatology	33.0	14.0	10.6	6.1
	Ground Tab	31.7	12.8	10.1	6.5
	48 Hr GFS Frcst	17.4	2.3	10.3	6.6
	24 Hr GFS Frcst	17.5	2.1	10.4	6.5
	12 Hr GFS Frcst	17.6	2.0	10.1	6.6
Summer 12z	1976 US Standard	25.6	7.3	4.4	9.6
	50% Climatology	23.0	5.0	14.2	4.2
	Ground Tab	31.0	13.6	13.2	4.5
	48 Hr GFS Frcst	17.2	3.3	11.7	5.8
	24 Hr GFS Frcst	17.2	3.3	11.7	5.8
	12 Hr GFS Frcst	17.3	3.2	11.5	5.9
Winter 00z	1976 US Standard	28.3	6.3	3.7	12.1
	50% Climatology	37.7	16.6	9.5	6.6
	Ground Tab	38.4	17.4	10.3	5.9
	48 Hr GFS Frcst	21.1	2.1	19.0	6.5
	24 Hr GFS Frcst	21.2	2.1	19.5	7.3
	12 Hr GFS Frcst	21.3	2.1	19.9	7.8
Winter 12z	1976 US Standard	25.6	6.2	3.2	6.7
	50% Climatology	29.2	9.9	8.6	1.9
	Ground Tab	34.6	15.9	8.8	1.8
	48 Hr GFS Frcst	18.0	2.0	8.5	2.1
	24 Hr GFS Frcst	17.9	2.3	8.8	2.3
	12 Hr GFS Frcst	17.9	2.3	8.8	1.7

Table 15. Brunei dwell time (DT) and RMSE values for 1.045 and 1.31525 μm engagements from 3,000 m to the surface for Summer 00z, Summer 12z, Winter 00z, and Winter 12z. Atmospheres considered include the 1976 U.S. Standard Atmosphere, 50th percentile ExPERT climatology, HELTDA ground tab, and 48, 24, and 12 hour GFS forecast derived atmospheres. Note target hardness differs for the two wavelength simulations.

Time/Season	Profile	1.045 µm DT (s)	1.045 µm DT RMSE (S)	1.31525 µm DT (s)	1.31525 µm DT RMSE (S)
Summer 00z	1976 US Standard	33.6	9.4	5.4	12.0
	50% Climatology	32.6	8.5	12.6	5.4
	Ground Tab	31.8	7.7	11.9	6.0
	48 Hr GFS Frcst	22.7	1.9	11.9	6.2
	24 Hr GFS Frcst	22.8	1.9	11.9	5.9
	12 Hr GFS Frcst	22.9	1.8	11.6	6.1
Summer 12z	1976 US Standard	33.6	9.8	5.4	8.6
	50% Climatology	28.4	4.9	12.6	3.2
	Ground Tab	31.7	8.5	11.3	3.9
	48 Hr GFS Frcst	22.8	2.2	12.9	4.0
	24 Hr GFS Frcst	22.8	2.2	12.9	4.0
	12 Hr GFS Frcst	22.8	2.2	12.6	4.4
Winter 00z	1976 US Standard	33.7	9.1	3.9	11.5
	50% Climatology	25.7	1.6	9.5	6.2
	Ground Tab	25.8	1.9	10.0	5.8
	48 Hr GFS Frcst	23.9	1.5	16.4	4.2
	24 Hr GFS Frcst	24.0	1.5	16.8	4.9
	12 Hr GFS Frcst	24.1	1.4	17.1	4.9
Winter 12z	1976 US Standard	33.7	9.3	3.9	6.5
	50% Climatology	27.5	3.5	8.6	2.3
	Ground Tab	29.4	5.5	8.4	2.4
	48 Hr GFS Frcst	23.1	2.2	9.9	1.7
	24 Hr GFS Frcst	23.1	2.1	9.9	1.6
	12 Hr GFS Frcst	23.2	1.9	10.2	1.4

Bibliography

1. ''Atmospheric Soundings''. World Wide Web Page. Available at http://weather.uwyo.edu/upperair/sounding.html.

2. ''Maritime Laser Demonstration''. World Wide Web Page. Available at http://www.as.northropgrumman.com/products/maritime_laser/index.html.

3. ''NOAA National Operational Model Archive & Distribution System''. World Wide Web Page. Available at http://nomads.ncdc.noaa.gov/.

4. ''Advanced tactical laser aircraft fires high-power laser in flight''. World Wide Web Page, 2009. Available at http://www.af.mil/news/story.asp?id=123154924.

5. ''Railgun, Laser Weapon Lose Senate Funding, Face Uncertain Future''. World Wide Web Page, 2011. Available at http://www.foxnews.com/scitech/2011/06/20/railgun-laser-weapon-lose-senate-funding-face-uncertain-future/.

6. Echeverria, Francesco J. *Assessment of Weather Sensitivites and Air Force Weather (AFW) Support to Tactical Lasers in the Lower Troposphere*. Master's thesis, Air Force Institute of Technology, 2009.

7. Fiorino, S.T., R.J. Bartell, M.J. Krizo, G. Caylor, K.P. Moore, T.R. Harris, and S.J. Cusumano. ''Worldwide uncertainty assessments of ladar and radar signal-to-noise ratio performance for diverse low altitude atmospheric environments''. *Journal of Applied Remote Sensing*, 4(1):3533, 2010.

8. Fiorino, S.T., R.J. Bartell, M.J. Krizo, D. Fedyk, K. Moore, T. Harris, S.J. Cusumano, R.D. Richmond, and M.J. Gebhardt. ''Worldwide Assessments of Laser Radar Tactical Scenario Performance Variability for Diverse Low Altitude Atmospheric Conditions at 1.0642 microns and 1.557 microns''. *Journal of Applied Remote Sensing*, 3(1):3521, 2009.

9. Fiorino, S.T., R.J. Bartell, G.P. Perram, D.W. Bunch, L.E. Gravley, C.A. Rice, Z.P. Manning, and M.J. Krizo. ''The HELEEOS Atmospheric Effects Package: A Probabilistic Method for Evaluating Uncertainty in Low-Altitude High Energy Laser Effectiveness''. *Journal of Directed Energy*, 1(4):347--360, 2006.

10. Fiorino, S.T., R.M. Randall, F.J. Echeverria, R.J. Bartell, M.J. Krizo, and S.J. Cusumano. ''Effectiveness Assessment of Tactical Laser Engagement Scenarios in the Lower Troposphere''. in review AIAA Journal of Aerospace Computing, Information, and Communication, 2010.

11. Fiorino, Steven T., Richard J. Bartell, Matthew J. Krizo, Kenneth P. Moore, and Salvatore J. Cusumano. ''Validation of a worldwide physics-based, high spectral resolution atmospheric characterization and propagation package for UV to RF wavelengths''. *Proceedings of SPIE*, volume 7090, 70900I. SPIE Optics and Photonics, San Diego, CA, August 2008.

12. Fiorino, Steven T., Richard J. Bartell, Matthew J. Krizo, Glen P. Perram, Daniel J. Fedyk, Kenneth P. Moore, Thomas R. Harris, and Salvatore J. Cusumano. ''Worldwide Mission Planning Tool for Tactical Laser Systems''. *Journal of Aerospace Computing Information and Communication*, 6(8):491--506, 2009.

13. Fiorino, StevenT., Robb.M. Randall, Richard J. Bartell, Adam D. Downs, Peter C. Chu, and C.W. Fan. ''Climate Change: Anticipated Effects on High Energy Laser Weapon Systems in Maritime Environments''. *Journal of Applied Meteorology and Climatology*, 50(1):153--166, 2010.

14. Gravley, Liesebet E. *Comparison of Climatological Optical Turbulence Profiles to Standard, Statistical and Numerical Models Using Heleeos*. Master's thesis, Air Force Institute of Technology, 2006.

15. Jacobson, Mark Z. *Fundamentals of Atmospheric Modeling*. Cambridge Univ Press, 2005.

16. Lefevre, R.J., F.H. Ruggiero, and K. Roe. *Impacts of Numerical Weather Prediction Spatial Resolution On An Atmospheric Decision Aid For Directed Energy Weapon Systems*. Technical report, Air Force Research Lab Space Vehicles Directorate, Hanscomb AFB, MA, 2004.

17. Narcisse, De Leon, Steven T. Fiorino, and Richard J. Bartell. ''Optimizing the Effectiveness of Directed Energy Weapons with Specialized Weather Support''. *Air & Space Power Journal*, XXIII(2):57--66, 2009.

18. National Oceanic and Atmospheric Administration, United States Air Force, National Aeronautics and Space Administration. ''U.S. Standard Atmosphere, 1976''.

19. Perram, Glen P., Salvatore J. Cusumano, Robert L. Hengehold, and Steven T. Fiorino. *An Introduction to Laser Weapons Systems*. Directed Energy Professional Society, 2010.

20. Petty, G.W. *A First Course in Atmospheric Radiation*. Sun Dog Books, 2004.

21. Randall, R.M., S.T. Fiorino, and M.F. Via. ''Validation of Technique to Hyperspectrally Characterize the Lower Atmosphere with Limited Surface Observations''. Linda M. Wasiczko Thomas and Earl J. Spillar (editors), *Atmospheric Propagation VIII, Proceedings of SPIE*, volume 8038. 2011.

22. Rosenberg, Barry. ''DARPA Paves the Way for U.S. Efforts in Ballistic Missile Defense''. *DARPA: 50 Years of Bridging the Gap*, United States. Defense Advanced Research Projects Agency and United States. Dept. of Defense. Office of the Secretary of Defense, 64--73. Faircount LLC, 2009.

23. Squires, M.F., B.A. Beitler, S.T. Fiorino, D.L. Parks, F.W. Youkhana, and H.G. Smith. ''A Method for Creating Regional and Worldwide Datasets of Extreme and Average Values''. *41st Annual Meeting*. 1995.

24. Stull, R.B. *An Introduction to Boundary Layer Meteorology*, volume 13. Springer, 1988.

25. United States Missile Defense Agency. ''Airborne Laser Test Bed Fact Sheet''. World Wide Web Page. Available at http://www.mda.mil/global/documents/pdf/laser.pdf.

26. University Corporation For Atmospheric Research. ''About the NDFD GRIB2 Decoder''. World Wide Web Page. Available at http://slosh.nws.noaa.gov/degrib2/.

27. University Corporation For Atmospheric Research. ''GFS Introduction''. World Wide Web Page. Available at http://www.meted.ucar.edu/nwp/pcu2/avintro.htm.

28. U.S. Joint Chiefs of Staff. *Joint Publication 3-03: Joint Interdiction*. U.S. Joint Chiefs of Staff, 2007.

29. U.S. Joint Chiefs of Staff. *Joint Publication 3-09.3: Close Air Support*. U.S. Joint Chiefs of Staff, 2009.

30. Verdeyen, J.T. *Laser electronics*. Prentice Hall, Englewood Cliffs, NJ, 1989.

31. Vlahos, Kelley. ''Navy Breaks World Record With Futuristic Free-Electron Laser''. World Wide Web Page, 2011. Available at http://www.foxnews.com/scitech/2011/02/18/navy-breaks-world-record-futuristic-laser-getting-real/.

32. Wallace, J.M. and P.V. Hobbs. *Atmospheric Science: An Introductory Survey*. Academic Press, 2006.

33. Wisdom, Brett W. *Assessment of Optical Turbulence Profiles Derived From Probabilistic Climatology*. Master's thesis, Air Force Institute of Technology, 2007.

REPORT DOCUMENTATION PAGE

Form Approved
OMB No. 0704–0188

1. REPORT DATE *(DD–MM–YYYY)*	2. REPORT TYPE	3. DATES COVERED *(From — To)*
22--03--2012	Master's Thesis	Aug 2010 --- Mar 2012

4. TITLE AND SUBTITLE

Comparison of High Energy Laser Expected Dwell Times and Probability of Kill for Mission Planning Scenarios in Actual and Standard Atmospheres

5a. CONTRACT NUMBER

5b. GRANT NUMBER

5c. PROGRAM ELEMENT NUMBER

6. AUTHOR(S)

Burley, Jarred L., Capt, USAF

5d. PROJECT NUMBER

5e. TASK NUMBER

5f. WORK UNIT NUMBER

7. PERFORMING ORGANIZATION NAME(S) AND ADDRESS(ES)

Air Force Institute of Technology
Graduate School of Engineering and Management (AFIT/EN)
2950 Hobson Way
WPAFB OH 45433-7765

8. PERFORMING ORGANIZATION REPORT NUMBER

AFIT/APPLYPHY/ENP/12-M02

9. SPONSORING / MONITORING AGENCY NAME(S) AND ADDRESS(ES)

High Energy Laser Joint Technology Office (Mr. Mark Neice)
901 University Blvd SE
Albuquerque, NM 87106
(505)248-8205, Mark.Neice@jto.hpc.mil

10. SPONSOR/MONITOR'S ACRONYM(S)

HELJTO

11. SPONSOR/MONITOR'S REPORT NUMBER(S)

12. DISTRIBUTION / AVAILABILITY STATEMENT

DISTRIBUTION A: APPROVED FOR PUBLIC RELEASE; DISTRIBUTION UNLIMITED.

13. SUPPLEMENTARY NOTES

14. ABSTRACT

The 1976 U.S. standard atmosphere, a 50th percentile climatological profile, a ground observation based profile, and 48, 24, and 12 hour GFS forecast derived profiles are compared to actual sounding data and characterized for meteorological parameter predictive performance. Predictive HEL engagement performance is analyzed through AFIT/CDEs HELTDA for relevant engagement scenarios for multiple wavelengths. Operational optimization is demonstrated utilizing GFS forecast predictions in nearly all cases. Ground observation-based profiles prove advantageous for certain wavelengths regardless of decisive predictive capability in vertical profile characterization methods revealing wavelength dependence attributed to the multivariate nature of HEL energy propagation. Specific cases are analyzed and demonstrate dwell time optimization and tactical advantages possible with altitude, heading, and flight profile modifications. Results indicate that in a majority of cases, existing conditions may be exploited for an operational advantage in the employment of directed weapons if correctly anticipated and analyzed.

15. SUBJECT TERMS

HEL, high energy laser, tactical decision aid, wavelength, dwell time, probability of kill, probability of effect, model, irradiance, fluence, forecast, climatology, standard atmosphere, GFS, HELTDA

16. SECURITY CLASSIFICATION OF:			17. LIMITATION OF ABSTRACT	18. NUMBER OF PAGES	19a. NAME OF RESPONSIBLE PERSON
a. REPORT	b. ABSTRACT	c. THIS PAGE			Dr. Steven Fiorino
U	U	U	U	131	19b. TELEPHONE NUMBER *(include area code)* (937) 255-3636, x4506; Steven.Fiorino@afit.edu